AFCRL-62-1021

THE UNIVERSITY OF MICHIGAN

COLLEGE OF ENGINEERING
Department of Aeronautical and Astronautical Engineering

Final Report

STUDY OF THE ROCKET-SOUNDING METHODS OF MEASURING THE UPPER ATMOSPHERE

(Some Gas Kinetic Problems Pertaining to the
Upper Atmospheric Measurements)

Prepared for the Project by

V. C. Liu

Project 6690
Task 66904

ORA Project 02885

under contract with:

GEOPHYSICAL RESEARCH DIRECTORATE
AIR FORCE CAMBRIDGE RESEARCH LABORATORIES
OFFICE OF AEROSPACE RESEARCH
CONTRACT NO. AF 19(604)-5477
UNITED STATES AIR FORCE
BEDFORD, MASSACHUSETTS

administered through:

OFFICE OF RESEARCH ADMINISTRATION ANN ARBOR

August 1962

PREFACE

This final report is submitted on the work done under contract No. AF 19 (604)-5477 with Air Force Geophysics Research Directorate for the period from March 1959 to June 1962.

This report is more than a compilation of the progress reports and reprints of published works. It is organized according to subject matter rather than chronologically; it contains some new results and a good deal of analysis and discussions not included in the progress reports; and it attempts to present an over-all picture of the work accomplished and future works needed to be done.

For economy of writing, detail description of works that have been published or prepared to submit for publication are not included; instead they are attached in reprint form and preliminary manuscript form respectively as appendixes to this report.

Preliminary results of some studies, which are still in progress, have also been included.

An attempt has been made to keep the notations used in the equations and formulas self-consistent within each chapter; they are not necessarily consistent from one chapter to another and from one appendix to another; but they are all defined in each case.

THE UNIVERSITY OF MICHIGAN PROJECT PERSONNEL

(Both Full Time and Part Time)

P. B. Hays,	M. S.,	Assistant in Research
G. R. Inger,	PhD,	Assistant in Research
H. Jew,	M. S.,	Assistant Research Engineer
Y. L. Lim,	PhD,	Assistant in Research
V. C. Liu,	PhD,	Project Director and Professor of Aeronautical and Astronautical Engineering

CONTENTS

CONTENTS (Concluded)

ABSTRACT

The present report aims at resolving some rarefied gas dynamical problems pertaining to atmosphere measurements by means of sounding rocket, and satellites. Specific problems treated are the following: Sphere drag in semi-rarefied gas (often called transition flows), electro-hydrodynamic interaction of ionosphere with a moving body, propagation of sound in a rarefied gas under external force field, rarefied gas dynamical considerations of sounding measurements of upper atmosphere. Report also includes several basic problems of possible geophysical interest.

Specific recommendation is made in regard to coordinating the geophysical experiment and gas dynamical studies in the free flight measurements.

I. Introduction

The systematic exploration of the upper atmosphere by direct means started in the late forties when sounding rockets, capable of climbing to an altitude of several hundred kilometers were introduced to probe the upper air. Much of the geophysical measurements, thus conducted, are based on gas dynamical principles. This happens not by choice but by necessity because of the special experimental environment. As one can easily see, the experimental aim of direct-measuring the undisturbed ambient quantity such as density, temperature, or pressure with a probe, carried by a fast-moving rocket which continually generates aerodynamical disturbances, is not feasible. Therefore, some indirect scheme must be made in which measurable aerodynamic quantities are taken as primary data that can be used to derive the ambient quantity of interest. A basic premise for the success of this indirect scheme of measurement is the availability of a satisfactory gas dynamic theory, either mathematical or empirical, that relates uniquely the ambient quantity of interest to the measured (primary) quantities. Such a gas dynamic theory, appropriate for a rarefied gas as the upper atmosphere, is not easily available.

In the earlier works of upper air measurements, such basic difficulty of the experiment was not resolved scientifically. Instead, an experiment was usually planned on the basis of a gas dynamic theory

which is known to be valid only for non-rarefied gas. As a result, the measurements of the rarefied atmosphere were not meaningful. Fortunately, some measurements, such as the pitot tube method in which Rayleigh's theory of supersonic pitot pressure is used, turns out to be reasonable approximations even at moderately high altitude (about 80 Km) according to later study (Liu 1956).

One of the basic works to be done in upper atmospheric research program is a realistic appraisal of the validity of the contemporary methods of measurements in the light of modern rarefied gas dynamics. It is expected that new rational methods, appropriate for high altitude experimental exploration, may be conceived; admittedly the development of rarefied gas dynamics is still in her infant stage.

It is worth noting that one vital reason for the slow advancement of rarefied gas dynamics, especially in the transition flow regime, is the unusual difficulty in generating satisfactory uniform flow condition in the laboratory. As we know, the upper atmosphere provides unlimited uniform medium. It is quite conceivable that appropriately designed experiments of upper air measurements can serve a very useful purpose of advancing the state of art of rarefied gas dynamics.

The above discussion for the measurement of neutral atmosphere would apply, in general, to the ionosphere except that the disturbances induced by the moving body becomes further complicated with the added electrodynamic aspect.

Besides the methodology of measurements, the atmospheric physicists also face with the task of interpreting and predicting phenomena of geophysical interest, e.g., the gravitational diffusive separation of the upper atmosphere, the distribution and escape of the earth's atmosphere, the dynamic equilibrium between the earth's atmosphere, and the interplanetary gas, etc. The advance to the eventual resolution of these problems, which are basic to the physical laws of atmosphere, must rest on gas kinetic approach.

It is for the initial understanding and exploration of all these problems mentioned above that the present report tries to make its modest attempt. The author is fully aware of the fearsome difficulty ahead.

2. Sphere Drag in a Rarefied Atmosphere

2.1 Introduction

The aerodynamic drag of a sphere has been used successfully as a dia-gnostic device in the exploration of the upper atmosphere. This can be done, e.g., by the use of a falling sphere which carries an accelerometer or is tracked with electromagnetic system to provide data for analysis of the sphere trajectory from which the ambient density can be determined. A basic premise of this method of ambient density measurement is that a well-established function of sphere drag coefficient (C_D ≡ drag/dynamic pressure x cross sectional area) in terms of flow parameters such as the free stream Mach number (M_∞) and Reynolds number (Re_∞) is available.

In spite of the great amount of works done on the aerodynamic drag of sphere, there is no general theory available that gives the sphere drag under various flow conditions. In fact the present knowledge of sphere drag has been cumulated mostly through experimental investigations. As to the theory of sphere drag, the success has been limited to the flows of extraordinary nature, e.g., very low Re_∞ and M_∞ (Stokes theory); utmost rarefaction (free molecule flow theory); and extremely high M_∞ in non-rarefied gases (Liu 1957). From the viewpoint of the falling sphere experiments in upper air measurements, the sphere drag of much geophysical interest, which corresponds to an altitude near 100 Km, belongs to aerodynamics of the semi-rarefied gases, a flow regime with characteristics lying between the continuum and the free

molecules. Unfortunately, transition flow regime is the least developed.

It is unrealistic to anticipate that the problem of sphere drag in transition flows can be completely solved in a short and specified time interval. This, however, does not mean to imply that the falling sphere experiments should be withheld until the aerodynamic problem is resolved. On the contrary, a well-planned geophysical experiment of falling spheres can be very valuable to the theoretical study of sphere drag. In other words, the free-flight sphere in the atmosphere, properly programmed in measurements, may serve the causes of both geophysical exploration and rarefied gas dynamics of sphere.

In the present study, we have attempted an integrated effort of theoretical and experimental approach to the sphere drag problem. The experimental investigation with low density wind tunnel facilities was undertaken by the Institute of Aerophysics, University of Toronto; the results of this experimental study had been reported in an earlier scientific report of this project (see Appendix IV). In the following, we shall report the status of the analytical approach to the problem.

2.2 Almost-Free-Molecule-Flow Theory

The theory of gas dynamics deals with the integrated effect of momentum and energy transfers between the gas medium and the submerged moving body. A fast moving object produces gas dynamical disturbances in its neighborhood, the intensity of which decays with

distance from the body. It is the momentum and energy transfers induced by these disturbances that are of primary interest to the gas dynamicists. At distance from the solid surface, in general it is the intermolecular collisions which determine the molecular velocity distribution of the gas. For normal density where the mean free path is extremely small, the effect of the presence of a solid body is transmitted primarily through the intermolecular collisons. The random nature of these collisions tends to create near-Maxwellian distribution for the gas molecules should a true Maxwellian distribution of an equilibrium state not be attained because of the non-vanishing transport fluxes. In other words, beyond an order of a mean free path from the solid boundary the molecular velocity distribution representing the disturbances can be closely approximated by a small perturbation from the local Maxwellian distribution. This intrinsic property of a gas is responsible for the success of Chapman-Enskog's kinetic theory of transport phenomena which laid the molecular foundation of macroscopic gas dynamics.

On the other hand, with a rarefied flow where the mean free path is much longer than the dimension of the body, the effect of these intermolecular collisions is insignificant in the determination of the flow field near the body. Essentially we are saying that the presence of the solid body does not create any significant disturbance to the molecular distribution in the free stream. This is the condition of free-molecule flows, also called Knudsen gas flows. Under this simplified situation the momentum and energy transfer to the body are completely determined by

the two independent streams of molecules incident to and reflected from the solid surface. Eventually, of course, they would collide but only at large distances from the body; hence, the collision effect is spread and thinned out in a large volume of action.

It is obvious that with a less rarefied medium which, of course, has shorter mean free path, there will be higher concentration of the above mentioned collisions in the immediate neighborhood of the body, hence more intense distrubance to the molecular distribution of the free stream. It is based on the single collision consideration that the almost-free-molecule-flow theory is formulated. It represents an attempt to analyze a first order iteration to the problem considering the free-molecule flow approximation as the zeroth order.

In the original formulations of the almost-free-molecule-flow theory (Liu 1957, Liu 1958, Liu 1959), the collision effects were calculated based on physical considerations without regard to the Boltzmann's kinetic equation. An effort has been made to give the physical theory a more rigorous mathematical basis by developing, formally, the first order iteration of collision effect from the Boltzmann's equation.

2.3 Formal Development of the Iteration Process

A rigorous kinetic theory of flows depends on a knowledge of the distribution of molecular velocities throughout the flow field. The distribution function $f(\vec{r}, \vec{v}, t)$ when multiplied by $d\vec{r}\, d\vec{v}$ gives the probable number of gas molecules which, at time t, are located in the region of space

between $\vec{r}$ and $\vec{r} + d\vec{r}$ and have velocities between $\vec{v}$ and $\vec{v} + d\vec{v}$. The above description should suffice for monatomic gases which have translational degrees of freedom only. If there are more than one species of molecules present, each species must have its own distribution function. We assume there is only one kind of monatomic molecule of mass m present which are under the influence of an external force*($\vec{F}$), the distribution function $f(\vec{r}, \vec{v}, t)$ satisfies the Boltzmann equation (Chapman and Cowling 1952)

$$\frac{\partial f}{\partial t} + \vec{v} \cdot \frac{\partial f}{\partial \vec{r}} + \frac{\vec{F}}{m} \cdot \frac{\partial f}{\partial \vec{v}} = J(f, f_1) \equiv \iiint (f' f_1' - f f_1) \left| \vec{v} - \vec{v}_1 \right| b \, db \, d\varepsilon \, d\vec{v}_1 \quad (2.1)$$

Equation (2.1) states that the change of f with time, apart from the streaming molecular motion, and the influence of the external force field, is due to the binary intermolecular collisions in which the velocities of the two encountering molecules before collision are $\vec{v}$ and $\vec{v}_1$; after collision, $\vec{v}'$ and $\vec{v}_1'$. The integration extends over all values of $\vec{v}_1$ and also over all values of the polar coordinates b and ε which specify the relative position, based on the asymptotes of the initial trajectories, of the two encountering molecules. In the collision term $\left[J(f, f_1) \right]$, the prime and the index 1 of the f's refer to the velocity variables alone, e.g., $f_1 \equiv f(\vec{r}, \vec{v}, t)$, etc. The two terms in the collision integral represent the gains due to the restituting

*We have given here a more general form of Boltzmann's kinetic equation than it is necessary for the discussion of sphere drag. This, however, provides the background for later discussions in Chapters 3 and 4.

collisions $(\vec{v}', \vec{v}_1') \longrightarrow (\vec{v}, \vec{v}_1)$ and the losses due to direct collisions $(\vec{v}, \vec{v}_1) \longrightarrow (\vec{v}', \vec{v}_1')$ respectively.

To gain some physical insight into the mathematical formulation, we propose to give a dimensional analysis of equation (2.1). Let us introduce the dimensionless variables defined by:

$$b = \sigma\, b^*, \quad \vec{r} = R\,\vec{r}^*, \quad t = \frac{R}{V_\infty}\, t^*, \quad v = V_\infty\, v^*, \quad f = \frac{N_\infty}{R^3 V_\infty^3}\, f^*, \quad \vec{F} = \frac{m V_\infty^2}{R}\, F^* \qquad (2.2)$$

where R is a characteristic length of the flow field, e.g., the radius of a sphere; V_∞ represents the mean mass velocityof the molecules upstream from the body ; σ, the effective range of the intermolecular force, e.g., the diameter of an elastic sphere; N_∞, number of molecules in volume R^3.

Equation (2.1), in dimensionless variables, becomes

$$\frac{\partial f}{\partial t} + \vec{v}^* \cdot \frac{\partial f}{\partial \vec{r}} + \vec{F}^* \cdot \frac{\partial f}{\partial \vec{v}^*} = \frac{R}{\sqrt{2}\,\pi\lambda} J(f^*, f_1^*) \equiv \frac{R}{\sqrt{2}\,\pi\lambda} \iiint (f^{*\prime} f_1^{*\prime} - f^* f_1^*) \cdot \left| \vec{v}^* - \vec{v}_1^* \right| b^*\, db^*\, d\varepsilon\, d\vec{v}_1^* \qquad (2.3)$$

where $\lambda = R^3/\sqrt{2}\,\pi\sigma^2 N_\infty$ is the mean free path of gas at the free stream density. The Boltzmann equation in the form (2.3) clearly reveals that the molecular collision effects on the rate of change of f^* is of the order R/λ or inverse Knudsen number ($Kn \equiv \lambda/R$). Equation (2.3) is uniformly valid for gases at normal density as well as at rarefied state. In fact, from equation (2.3) one can observe the anticipated difference in mathematical structures of the treatments of flow problems in continuum vs. those in

rarefied state; with the former, terms on the left hand side of equation (2.3) has the weaker influence on f, hence the iteration must start with the Fredholm type integral equation which is what Chapman and Enskog did. With the latter, such as the almost-free-molecule flows, the reverse is true, we have therefore a differential equation in f with the inhomogeneous term provided by the collision integral which is prescribed in terms of f from lower order approximation.

We may further observe that the left hand side of equation (2.3) is the derivative of f in the direction of the vector $(t, \vec{v}, \vec{F})$ in the seven-dimensional space. At each point in this space, this vector points in the direction of the molecular trajectory through that point, which is also the characteristic curve of the equation with collision term omitted. Hence, if s denotes arc length along a trajectory, equation (2.3) becomes:

$$v^* \frac{Df^*}{Ds} = (\sqrt{2}\,\pi\,Kn)^{-1}\; J\,(f^*, f_1^*) \qquad (2.4)$$

where $Kn = \lambda/R$.

To assess formally the order of approximation of the iteration process in treating rarefied flows, we let:

$$f^* = f^{*(0)} + \frac{R}{\lambda} f^{*(1)} + \left(\frac{R}{\lambda}\right)^2 f^{*(2)} + \cdots\cdots \qquad (2.5)$$

The significance of $f^{*(0)}, f^{*(1)}, f^{*(2)} \ldots$ will be clear after equation (2.5) is substituted in (2.5) and coefficients of like powers in R/λ are equated:

$$v^* \frac{Df^{*(0)}}{Ds} = 0 \qquad (2.6)$$

$$v^* \frac{Df^{*(1)}}{Ds} = (\sqrt{2}\,\pi\,Kn)^{-1}\; J\,(f^{*(0)}, f_1^{*(0)}) \qquad (2.7)$$

Equation (2.6) says that $f^{*(0)}$ is constant along a trajectory; in other words, it is the distribution function for the free-molecule flow. We shall see that $f^{*(0)}(\vec{r}, \vec{v})$ for a sphere in free molecule flow does satisfy equation (2.6) except for the points on the solid boundary as expected.

Equation (2.7) which entails collision effect prescribed with the use of free-molecule distribution $f^{*(0)}$ constitutes the formal basis of the almost-free-molecule flow theory discussed in §2.2. Note that a formal solution to equation (2.7), after the boundary condition, $f = f(s_o, v^*)$ at $s = s_o$ is substituted, can be written in the following form:

$$f^{*(1)} = f^{*(0)}(s_o, v^*) + \frac{1}{\sqrt{2}\,\pi\,Kn} \int_{s_o}^{s} J \frac{ds}{v^*} \qquad (2.8)$$

It may be noted that the almost-free-molecule flow analyses made in references (3 , 4 & 5) are essentially some macroscopic moments of equation (2.8), giving the mass and momentum fluxes, etc., after the collision integral J in equation (2.8) has been simplified with physically justifiable assumptions.

Up to now, the development of the iteration is formal and is uniformly valid for rarefied flows. In the following, we attempt to make a first order iteration of the sphere drag.

2.4 Zeroth Order Approximation to the Sphere Drag - Free-Molecule-Flow Theory

In the zeroth order approximation, we neglect the collisions between the streams of molecules incident on and reflected from the sphere, hence the classical free-molecule flow is obtained. It must be noted, however, in the standard works on free molecule flows (see, e.g., Patterson 1956), the molecular distribution function for the entire flow field, namely $f^{(0)}(\vec{r}, \vec{v})$ is usually not of interest unless one wants to map out the flow field around the sphere. In the present study, we must know $f^{(0)}(\vec{r}, \vec{v})$ in order to calculate the distribution of collision frequencies as prescribed in the collision integral $J(f^{(0)}, f_1^{(0)})$ for the first order iteration.

It is noted that the aggregation of molecules at any point $(\vec{r})$ in a free-molecule flow must come from two sources:

(i) Stream inciding on the sphere, f_I: $n_\infty \left(\frac{m}{2\pi k T_\infty}\right)^{\frac{3}{2}} e^{-\frac{m}{2kT}(\vec{v} - \vec{V}_\infty)^2}$ (2.9)

(ii) Stream reflected (assumed diffusely) from the sphere f_R: $n_R \left(\frac{m}{2\pi k T_R}\right)^{\frac{3}{2}} e^{-\frac{m c^2}{2 k T_R}}$ (2.10)

where n_R is a fictitious number density which can be determined by the conservation of the number of molecules during the process of reflection at the solid boundary.

$$n_r = n_\infty \left(\frac{T_\infty}{T_R}\right)^{\frac{1}{2}} \left[e^{-S_v^2} + \sqrt{\pi}\, S_v (1 + \operatorname{erf} S_v)\right] \qquad (2.11)$$

where $S_v = \left(\frac{m}{2 k T_\infty}\right)^{\frac{1}{2}} (\vec{V}_\infty \cdot \vec{n}')$[++] and c is the random molecular speed at T_R.

In general we can write the distribution function at a point $(\vec{r})$ in the following form:

[++] See Fig. 2-1

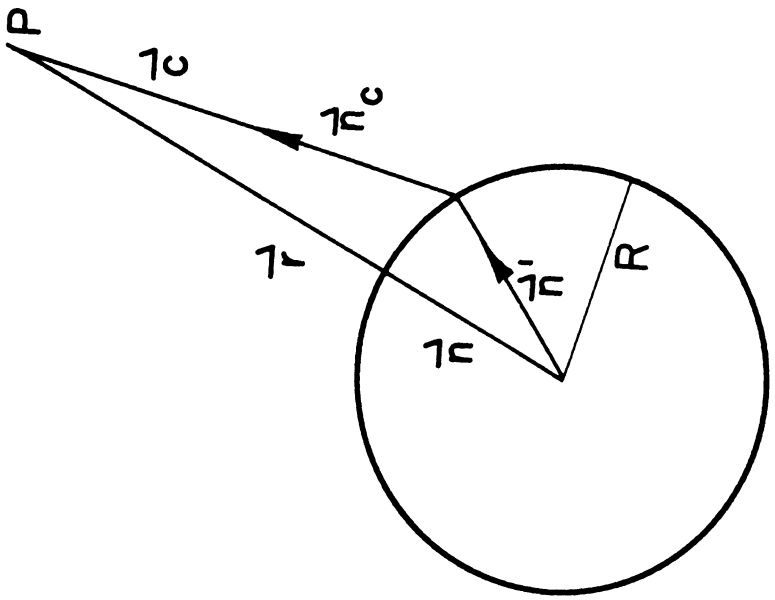

Fig. 2-1

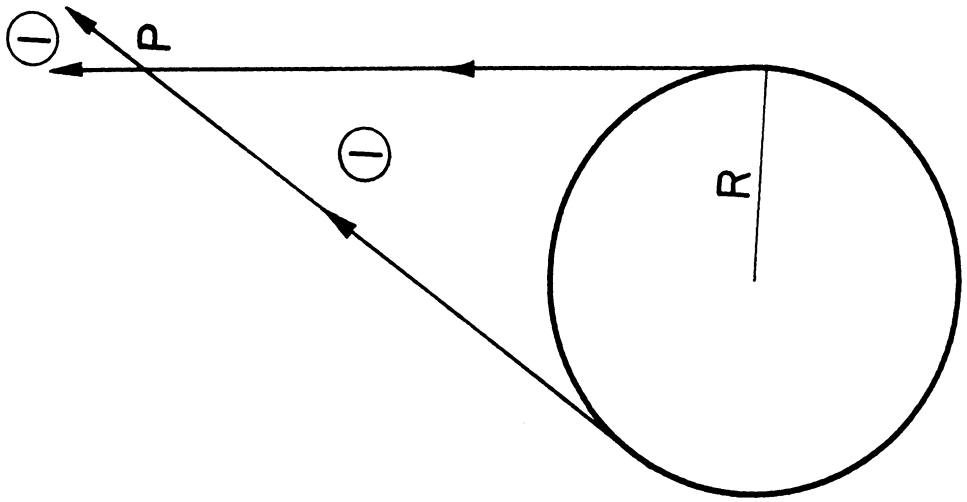

Fig. 2-2

$$f^{(0)}(\vec{r}, \vec{v}) = Z\, f_I + (1 - Z)\, f_R \qquad (2.12)$$

where $Z(\vec{r}, \vec{n}_v)$, n_v being a unit vector in the direction $\vec{v}$ (see Figs. 2-1 and 2-2), is a discontinuous function defined as follows:

It is zero if the molecule with velocity $\vec{v}$ at the point $(\vec{r})$ comes from the sphere (i.e., in zone 1, see Fig. 2-2) and one otherwise. Analytically

$$Z = 0 \text{ if } \vec{n} \cdot \vec{n}_v > 0 \text{ and } r^2 - (\vec{r} \cdot \vec{n}_v)^2 < R^2$$

Hence, we can express Z, after simplification,

$$Z = \frac{1}{2}\left[1 - \operatorname{sgn}(\vec{n} \cdot \vec{n}_v)\right] + \frac{1}{4}\left[1 + \operatorname{sgn}(\vec{n} \cdot \vec{n}_v)\right]\left[1 + \operatorname{sgn}\left(\sqrt{1 - \frac{R^2}{r^2}} - \vec{n} \cdot \vec{n}_v\right)\right] \qquad (2.13)$$

where sgn x ≡ signum (x) = -1 when $x < 0$; 0, when $x = 0$; and +1, when $x > 0$.

It can be shown by simple differentiation that $f^{(0)}$ given by (2.12) satisfies the collisionless Boltzmann equation (2.6) except at the solid boundary r = R, which is, of course, expected. Note that $f^{(0)}$ is equivalent to $f^{*(0)}$ except in dimensional form.

2.5 First Order Approximation to the Sphere Drag - Almost-Free-Molecule Flow Theory

It may well be admitted at this point that formal mathematical deduction with respect to equation (2.7) which involves complicated integration along characteristic directions is not expected to be fruitful. To make any progress we must simplify the collision integral (J) by invoking physically justifiable assumptions for a specific flow problem of interest.

It appears that, for an almost free molecule flow of not very low speed, the restituting collisions near the body which produce molecular distribution of significant drag contribution (positive or negative) is much less frequent than the direct collisions. This statement can be justified by invoking the second law of thermodynamics. Hence, $f^{(0)'} f_1^{(0)'}$ - term in the collision integral (J) in equation (2.7) can be neglected.

It can be shown that under the specific flow condition mentioned above, the contribution to $f^{(0)} f_1^{(0)}$ - term in J of equation (2.7) from $f_R f_R$ and $f_I f_I$ collisions are much less significant than from $f_I f_R$ collisions.#

Even after these simplifications, the mathematical work in solving equation (2.7) for a sphere is still very heavy. An indiscriminate computation without inquiring its physical significance may lead to waste as far as physical interpretation of the flow phenomena is concerned.

Before starting with the computation of the single-collision contribution to the sphere drag (δD) we may take advantage of the result of the dimensional analysis in § 2.3 to see what is likely to be the significant parameters governing δD. It is not difficult to see that $(V_\infty/c_M)(R/\lambda)$

#This can be justified by comparing the numbers of collisions per unit distance for these species.

must be the parameter in question. In other words, for diffuse reflection, the sphere drag is likely to be in the following form:[#]

$$D = \pi R^2 m n_\infty V_\infty^2 \left\{1 + \mathcal{F}\left[(V_\infty/c_M)(R/\lambda)\right]\right\} \tag{2.14}$$

or to a first order effect:

$$D = \pi R^2 m n_\infty V_\infty^2 \left[1 + \alpha\,(V_\infty/c_M)(R/\lambda)\right] \tag{2.15}$$

where α depends on the geometry of the molecular trajectories in the vicinity of the sphere.

We can give an order of magnitude analysis of the single-collision effect on drag based on a simple physical model in order to throw some light on the result of (2.15). Suppose that, to start with, the sphere, by its forward velocity (V_∞) has trapped a molecule against its surface. This trapped molecule, owing to its the thermal speed say, c_M, will in general move out of the region swept by the surface of the sphere within a certain time ($\tau_1 \sim R/c_M$) unless τ_1 be equal to or greater than the time required by the sphere to cover the distance of a mean free path of the molecules ($\tau_2 \sim \lambda_\infty/V_\infty$). In the latter case, other molecules will collect in front of the sphere before the trapped molecule finds time to escape and a concentrated layer begins to form. At this point, we would like to make a remark concerning a general misconception of the criterion for free-molecule flows: should this concentrated layer of trapped gas form around the sphere, the free-molecule flows cannot exist, no matter how large the

---

[#] $c_M = (2kT/m)^{1/2}$ is the most probable value of the random (thermal) speed.

[#] $\mathcal{F}$ denotes an arbitrary function; it should be emphasized that the hypothsis expressed in Eq. (2.14) is based merely on dimensional considerations.

ratio λ_∞/R is! (Note: it is commonly claimed that free-molecule flows exist if $\lambda_\infty/R \gg 1$). Instead, for a free molecule flow to exist, the ratio of the two time constants $(\lambda_\infty/V_\infty) / (R/c_M)$ must be larger than one. Alternatively, one may define a new mean free path $\Lambda = \lambda_\infty c_M/V_\infty$ which can be considered as a mean free path of a reflected molecule moving among the incident molecules assuming that the body is fixed in space and the surface temperature is equal to T_∞ of the gas.

The number of molecules reflected per unit time from the sphere must be of the order $\pi R^2 n_\infty V_\infty$, a fraction of the order $(V_\infty/c_M)(R/\lambda_\infty)$ of which will probably collide with the incoming molecules within a distance of the order R from the sphere. Thus, the number of molecules created in unit time within the region of consideration is of the order , $(V_\infty/c_M)(R/\lambda_\infty)\, \pi R^2 n_\infty V_\infty$. As a gross estimate, the momentum transfer to the sphere per unit time from these colliding molecules is of the order:

$$(V_\infty/c_M)\,(R/\lambda_\infty)\,\pi\, m n_\infty R^2\, V_\infty^2 \qquad (2.16)$$

Note that the sphere drag for a free molecule flow under the assumption of diffuse reflection is:

$$D_{F.M.} = m n \pi R^2 V_\infty^2 \qquad (2.17)$$

combining (2.16) and (2.17) with an unknown coefficient α that depends on detailed geometrical considerations of the collision effects near the sphere, we obtain equation (2.15) for sphere drag considering single collisions. The exact formulation for α will come out of precise analysis.

It is interesting to note that the results of recent measurements of sphere drag in the transition flow regime (see Appendix IV) appear to comply with the present prediction (see Appendix V) although one should be cautious in drawing conclusions on the basis of limited data to a single Mach number (note: only the U T I A test seems to satisfy the almost free molecule flow condition).

2.6 Method of Analysis of the Single-Collision Effect

For the general case of arbitrary Mach number, we have not been successful in our attempts to arrive at a form simple enough to be presented analytically. With a rarefied gas at hypersonic speeds, the mathematical analysis becomes more tractable. This entails the neglect of the thermal velocity component of the incident molecules (f_I) in comparison with the mass velocity component.

The work on sphere drag in a rarefied gas is still in progress. In the following we shall briefly describe one of the schemes that has been used in treating the single collision effect.

Consider the flow past a sphere. Let $J(\vec{r}, \vec{v})\, d\vec{r}\, d\vec{v}$ denote the number of molecular collisions per unit time in the volume element of the phase space bounded by $\vec{r}$, $\vec{r} + d\vec{r}$ and $\vec{v}$, $\vec{v} + d\vec{v}$. Let $\vec{v}$ represent the velocity vector of a molecule which emerges from collision at $P(\vec{r})$ and intersects on a surface element dS of the sphere at Q. From geometrical considerations we have

$$d\vec{v} = v^2\, dv\, \frac{\cos \phi\, dS}{|QP|^2} \qquad (2.18)$$

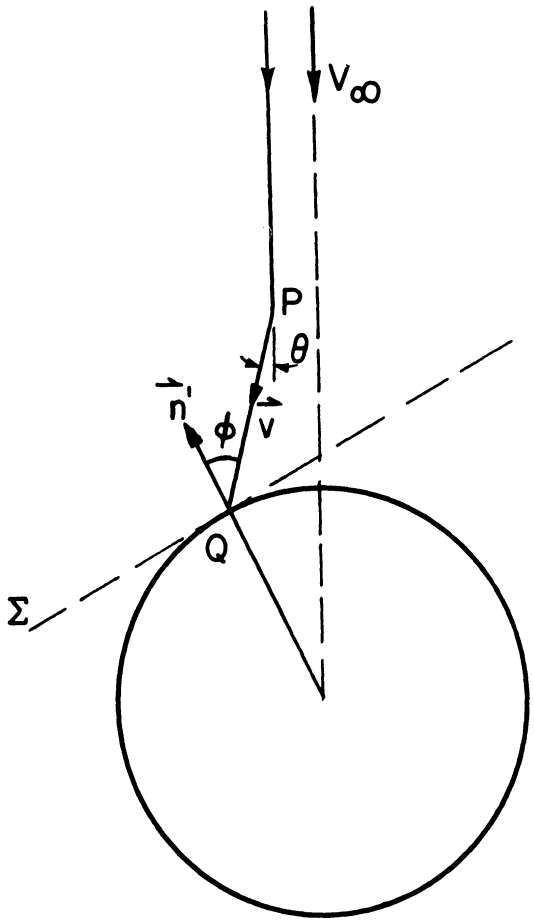

Fig. 2-3

where ϕ is the angle between $\overrightarrow{QP}$ and the normal $\vec{n}'$ to the surface passing through Q (see figure 2-3). Let dH_1 denote the number of molecules which emerges from a collision in $d\vec{r}\, d\vec{v}$ and deposit on dS at Q

$$dH_1 = G_\theta J(\vec{r}, \vec{v})\, d\vec{r}\, \frac{\cos\phi\, v^2\, dv}{|QP|^2} \tag{2.19}$$

where G_θ is the solid angle scattering coefficient. Note that the direction of $\vec{v}$ appearing in (2.19) is related to the direction of $\overrightarrow{QP}$:

$$\vec{v} = v\frac{\overrightarrow{QP}}{|QP|} \tag{2.20}$$

The total contribution to the incident molecular flux by the collision is:

$$H_1(Q) = \int_{\Sigma} d\vec{r} \int_0^\infty G_\theta\, v^2\, J\left(\vec{r}, -v\frac{\overrightarrow{QP}}{|QP|}\right) \frac{\cos\phi}{|QP|^2}\, dv \tag{2.21}$$

where Σ denotes the semi-infinite region bounded by the plane tangent to the sphere at Q (see figure 2-3).

Following the same reasoning, we can calculate the contribution to the momentum flux in the direction of $\vec{V}_\infty$ by the molecules emerged from collisions

$$\vec{H}_2(Q) = \int_{\Sigma} d\vec{r} \int_0^\infty \left(G_\theta \cos\theta + G_{\left(\frac{\pi}{2}-\theta\right)} \sin\theta\right) m\, v^3\, J\left(\vec{r}, -v\frac{\overrightarrow{QP}}{|QP|^2}\right) \frac{\cos\phi}{|QP|^2}\, dv \tag{2.22}$$

To calculate the net change in sphere drag due to collisions relative to its zeroth order approximation, we must consider the loss accounted for those f_I molecules being thrown out by the collisions. The net contribution to drag by single collision effect can be written as:

$$\delta D = \int_S \left[\vec{H}_2(Q) - m\vec{V}_\infty H_1(Q)\right] dS \tag{2.23}$$

The results of the preliminary calculations using the formulation given by (2.23) are not very satisfactory because the values of the two functions in the integrand are very close, thus throwing doubt on the accuracy of the results unless extreme precise calculation is followed. Comparing with results from this preliminary analysis, the drag coefficient given in Baker and Charwat (1958) appears reasonable.

Much improved analysis of the problem is still under investigation.

3. Gas Kintetic Problems of the Neutral Particles in the Upper Atmosphere

3.1 Generally speaking, the upper atmosphere is a multi-component mixture of neutral particles, ions and electrons, the concentrations of which are functions of altitude. A general theory of flow of this mixture with due considerations of the couplings between the various components would be quite untractable. It is often not necessary to face this difficulty because for many problems of the atmosphere, it can be avoided from the use of physical arguments. For instance, at lower altitude where the concentration of charged particles is extremely small, the effect of the ionized particles can be ignored except the cases where charged components play a significant role of the physical phenomena in spite of their minute constituents.

Even for some atmospheric phenomena at very high altitude, the analysis of the kinetics of the neutral atmospheric particles, because of its analytical simplicity and therefore more tenable to solve, can reveal much physical insight into the atmospheric problems. It is under this supposition that we divide the atmospheric problems of interest into two groups: (i) gas kinetics pertaining to neutral particles, (ii) to the ionized particles. In this chapter we shall concentrate on the first group; in the next chapter, on the second group. It goes without saying that the feasibility of this convenient division must be considered with caution in treating a particular atmospheric problem in question.

3.2 Propagation of Sound Disturbances in a Rarefied Atmosphere

The use of sound waves as a diagnostic probe of the atmospheric

temperature distribution dated back half a century ago. It has been applied recently in a modified version to the rocket-borne grenade experiments in which sound is generated by grenade explosions at specified altitudes. In this experiment the ambient temperature distribution is determined from the time taken by the sound waves to travel a specified distance through the atmosphere in question. The basic principle of the experiment is that the velocity of propagation of the sound wave is a simple function of ambient temperature, as given by Laplace for an ideal non-viscous gas, namely $V_o = (\gamma k \frac{T}{m})^{1/2}$. It is natural to raise the question whether Laplace's formula of sound velocity is applicable to the rarefied atmosphere in which the grenade sound experiment is conducted.

In rarefied gas dynamics, the problem of sound absorption and dispersion is of unusual interest because it is a case to which the linearized Boltzmann equation, derived from assuming a small perturbation to the equilibrium distribution function, is known to be valid; furthermore, the solid boundary, a source of difficulty in rarefied gas dynamics is not involved. Another reason is that experiment for checking the theory can be set up without unusual difficulty.

Wang-Chang (1948) give the solution to the sound propagation in a rarefied monatomic gas without external force and found that the change in speed of propagation (ΔV) is[#]

$$\frac{\Delta V}{V_o} = 44.4\,\mu^2 \left(\frac{\omega}{p}\right)^2 \qquad (3.1)$$

where μ is the viscosity in c. g. s. units; ω, sound waves in megacycles

---

[#] $\Delta V = V - V_o$ where V denotes the sound velocity in any gas medium.

per second; and p, in atmosphere. From equation (3. 1) one can easily see that for waves of ultra-high frequencies the change in propagation speed from the Laplace value, V_o, can be significant. This change can become significant also when the ambient pressure (p) is extremely low. Since the physical mechanism of propagation of a sound disturbance is collisions, the process will be disrupted when an appreciable number of molecules cross a wave length without colliding

We have made a study of the sound propagation in a rarefied atmosphere considering the external force, e. g. , gravity, acting on the molecules (see Appendix VI) and found that the effect of gravitational field is not significant until the wave length is comparable with the scale height of the atmosphere. The analysis is, however, valid also for other kind of external force field which may have a much shorter "scale height".

3. 3 Ofifice Flow of a Rarefied Gas

The flow of a rarefied gas through an orifice is a problem fundamental to the pitot tube experiment for the measurement of the upper atmosphere (Liu 1956). We have developed a transition flow theory (see Appendix VII) which appears in agreement with existing measurements in the laboratory.

3. 4 Rarefied Gas Dynamical Considerations in Rocket Sounding Measurements

To carry out low density experiments in the laboratory involves the generation of a uniform flow and the measurements of minute forces under

the most unfavorable conditions concerning forces of interference, both of which are experimental difficulties of the highest order. On the other hand, the upper atmosphere provides an unlimited uniform medium. It is therefore worth considering the possible free flight facilities in geophysical experiment for rarefied gas dynamics study. An effort has been made to discuss this possibility and the comparison of results from the laboratories and free flights (see Appendis X).

3.5 Gravitational Diffusive Separation of the Atmosphere

The atmosphere is a multi-component mixture of gases situated in the earth's gravitational field. Unlike the moon, the earth has sufficient force of attraction that prevents its atmosphere from escape in a catastrophic rate. From kinetic theory of gases one learns that when two gases of unequal molecular masses are mixed, a diffusion flux is set up due to acceleration of the gases* which tends to make the heavier molecules move, relative to the lighter ones, toward the lower altitude. In diffusive equilibrium, an isothermal atmosphere will have for each of its components a separate exponential distribution with altitude, defined by a scale height (kT/mg) of its own.

In the lower atmosphere, the molecular action, exhibited by the diffusion flux mentioned above, is likely to be nullified by the stronger

*An alternate way of saying is that an hydrostatic pressure distribution is set up by the gravitational field. Pressure diffusion flux is developed which tends to make the heavier molecules move to the region of higher pressure.

macroscopic mixing action of the atmosphere--often called atmospheric turbulence. It is therefore the relative strength of these two actions that determines the status of the diffusive separation of the atmosphere (see Appendix XI).

Although measurements of diffusive separation in rocket sounding program carried out at The University of Michigan and U. S. S. R. showed atmospheric separation effect at altitudes as low as 60 Km, our calculation, based on standard atmosphere, shows that this is most unlikely in view of the long time constant for the diffusion and the evidence of atmospheric turbulence shown in meteor trails at altitudes below 80 Km.

4. Gas Kinetic Problems Pertaining to Ionospheric Measurements

4.1 Introduction

Recent interest in the gas dynamics of the ionosphere arises essentially from two groups of technical problems: (i) the anomaly of radar cross section of space vehicles moving through the F-region of the ionosphere; (ii) the interpretation of ionospheric measurements from the use of sounding probes, e.g. Langmuir's ion traps (also called Langmuir Probe), mounted on a sounding rocket. As we shall see later, these two problems mentioned above are actually intimately related phenomena which are originated from the electro-hydrodynamic disturbances created by a moving body in an ionized medium - generally called plasma.

Inasmuch as the problem of plasma interaction with a moving body arises whenever prospective experiments of studying the ionosphere with the aid of satellites and sounding rockets are considered, it becomes important in upper atmospheric research to understand the behavior of a tenuous plasma which interacts with a moving body. Unfortunately, up to now, very little progress has been made in this field. This is caused by the fact that the theoretical analysis is harassed by the complex mathematical nonlinearity encountered and the experimental investigation is rendered helpless by the difficulty of generating satisfactory plasma in the laboratory. It is encouraging to learn that useful results on plasma

can be gained from geophysical experiments in which the procedure is based on various physical phenomena that take place in the vicinity of a satellite or a sounding rocket. In other words, the geophysical exploration of the ionosphere can serve a dual purpose of investigation in basic plasma dynamics as well as diagnostic study of ionospheric phenomena.

4.2 Ionosphere as a Flow Medium

A review of the physical properties of the ionosphere as a gas dynamical medium seems desirable before we start with the discussion of ionospheric gas dynamics.

It is well known that the upper layers of the earth's atmosphere are continually being bombarded by radiations from the sun and from the regions of outer space. Particles present in this bombardment have been identified as to their chemical species and charge. In addition, the role of electromagnetic radiation has been shown to play a very important part for the maintenance of the plasma state in the ionosphere. The production of electrons and ions in the atmosphere is, of course, counter-balanced to some extent by their recombinations which produce neutral atoms or molecules. In any small region of the ionosphere, there must be equal numbers of positive and negative charges. If this were not so, strong electrostatic forces would arise between different parts of the ionosphere. Rapid motion is then anticipated within the

regions to redistirbute the charges. These motions would continue until inequalities between concentrations of charges of opposite signs were smoothed out. It is often (but not always!) necessary to assume as a useful first approximation that the ionosphere is in the state of quasi-thermal equilibrium, thus in the absence of external field, the distribution of particles is Maxwellian for each species.

The ionosphere is a weakly ionized plasma, hence of low conductivity in the lower ionosphere; the degree of ionization, denoted by the ratio of the concentration of the electrons to the neutral particles increases from the order 10^{-8} at 100 Km; 10^{-5} at 200 Km; 10^{-3} at 300 Km; 1 at 1000 Km. At 3000 Km the degree of ionization rises to an order 10^{3}. It should be noted that the increase in the degree of ionization of the ionosphere with altitude is not uniform. The detail structure of the ionosphere is not of our interest here. The above description serves only to show that the plasma through which a satellite or rocket travels varies over a wide range.

4.3 Kinetic Properties of a Plasma

A plasma differs from a gas of neutral particles in certain important respects such as the nature of interaction between neighboring particles. It is well known in the kinetic theory of gases that the collision frequency between particles in a gas is determined by the force of interaction between the encountering particles, among other factors. For a

gas of neutral particles this interaction force is short-ranged, that is to say, the effective range of interaction between two neighboring particles is very small compared with the mean distance between particles of the gas. Therefore, in evaluating the statistical averages of the collision effects, e.g., the calculation of mean free path, we need to account for binary collisions only. It is not so with charged particles for which the interaction force, known as coulomb force, is effective at considerable distances; thus, the motion of a given particle influences the motion of many particles in its neighborhood. In other words, each charged particle moves under the influences of many charged particles in the plasma. This long-ranged nature of particle interaction causes much difficulty in the evaluation of collision integrals that are involved in the analysis of plasma kinetics. Many alternates have been suggested to circumvent this difficulty in order to develop a consistent kinetic theory of plasmas. It is not possible to say at the present time that full satisfactory answers have been derived or that schemes are available for their derivation which are non-controversial.

It may be briefly mentioned here that among these alternatives, Bogliubov's approach (Ref. 11) which is based primarily on the fact that a definite sequence of relaxation processes take place in a gas which transforms it from any arbitrarily prescribed initial condition appears most promising. In his approach, the first relaxation is that in which the gas

molecules adjust to their correct pair distribution function. The next relaxation is that which allows for the adjustment of the function describing the distribution of the particles according to state velocity. This second relaxation is usually described as the Boltzmann stage. The third and last stage is that in which the continuum variables of the ensemble, density, pressure and temperature adjust to the environmental conditions. Attempts are then made to expand the dynamics of adjustment, or relaxation of the appropriate distribution functions, in a series in which the coupling constant or constant of expansion is directly proportional to the frequency by which the adjustments are taking place. Although this approach has led to some rather elegant formalisms at the present time, the state of advancement using this program does not compare to that already achieved with the modified Boltzmann equation that takes into account the long-range nature of interaction by separating the plasma into two domains with respect to a particular test particle. First, there is a region in the immediate neighborhood of the test particle in which the effect of coulomb interaction is treated much like a short-range interaction, in the sense, they are [illegible] cut off at a specified finite range from the test particle. Second, there is the region, exterior to this cut-off range, in which the interaction effect of the surrounding particle charges is considered collectively as if it were an external force field acting upon the test particle. The size of the first region may be

characterized by the Debye radius

$$R_D = \left(\frac{k\,T}{4\pi n_e e^2}\right)^{1/2} \tag{4.1}$$

where T is the plasma temperature; e, the electron charge; n_e, the electron density; k, Boltzmann constant. The significance of the Debye radius will be further discussed in this report. It should be noted here that more sophisticated treatment concerning the interaction in the first region has been used. However for a weak rarefied plasma which is considered here, the afore mentioned model appears sufficient.

4.4 General Considerations of Flow Problems in the Ionosphere

The aerodynamics of an ascending rocket in the atmosphere may be used as an illustration of the extensive change in basic flow characteristics from the condition of continuum at low altitude, then the transition state at intermediate altitude, say about 100 Km, and finally the free molecule state at high altitude. The division of these flow regimes with respect to a given moving body, becomes considerably modified when the neutral medium is replaced by a plasma. For one thing, the mean free paths of the particle species of the medium are different from that of the neutral particles due to long-range interaction between the charged particles. A more important factor is that such a moving body will normally become negatively charged on account of the

higher rate of electron influx than ion from the surrounding plasma. This is made possible by the higher thermal speeds of electrons. The negative potential on the body will have an electrostatic field in its neighborhood. The free stream plasma will be so disturbed by the presence of the negatively charged body that large electrostatic forces are set up such that cluster of positive ions will migrate to the neighborhood and form a ion sheath thus restoring electric neutrality of ambient plasma in the large.

To illustrate the physical structure as well as the thickness of this sheath, which is a significant parameter in plasma dynamics, we consider a small mass point moving at an extremely low subsonic speed in a plasma, the electrostatic potential distribution in the sheath is governed by the Poisson equation, assuming singly charged ions,

$$\nabla^2 \phi = 4 \pi e (n_e - n_i) \tag{4.2}$$

in which the term on the right hand side represents the net charges due to the presence of isolated electrons and ions. The solution to equation (4.2) for a stationary mass point is,

$$\phi = \frac{\text{const.}}{r} e^{-r/R_D} \tag{4.3}$$

where $R_D = (K T_e / 4 \pi n_e e^2)^{1/2}$, called Debye radius, is the distance at which the electrostatic potential ϕ has become 1/e times the value it would have with no other charged particles present, and is a measure of the distance over which the potential can vary significantly from ambient pressure.

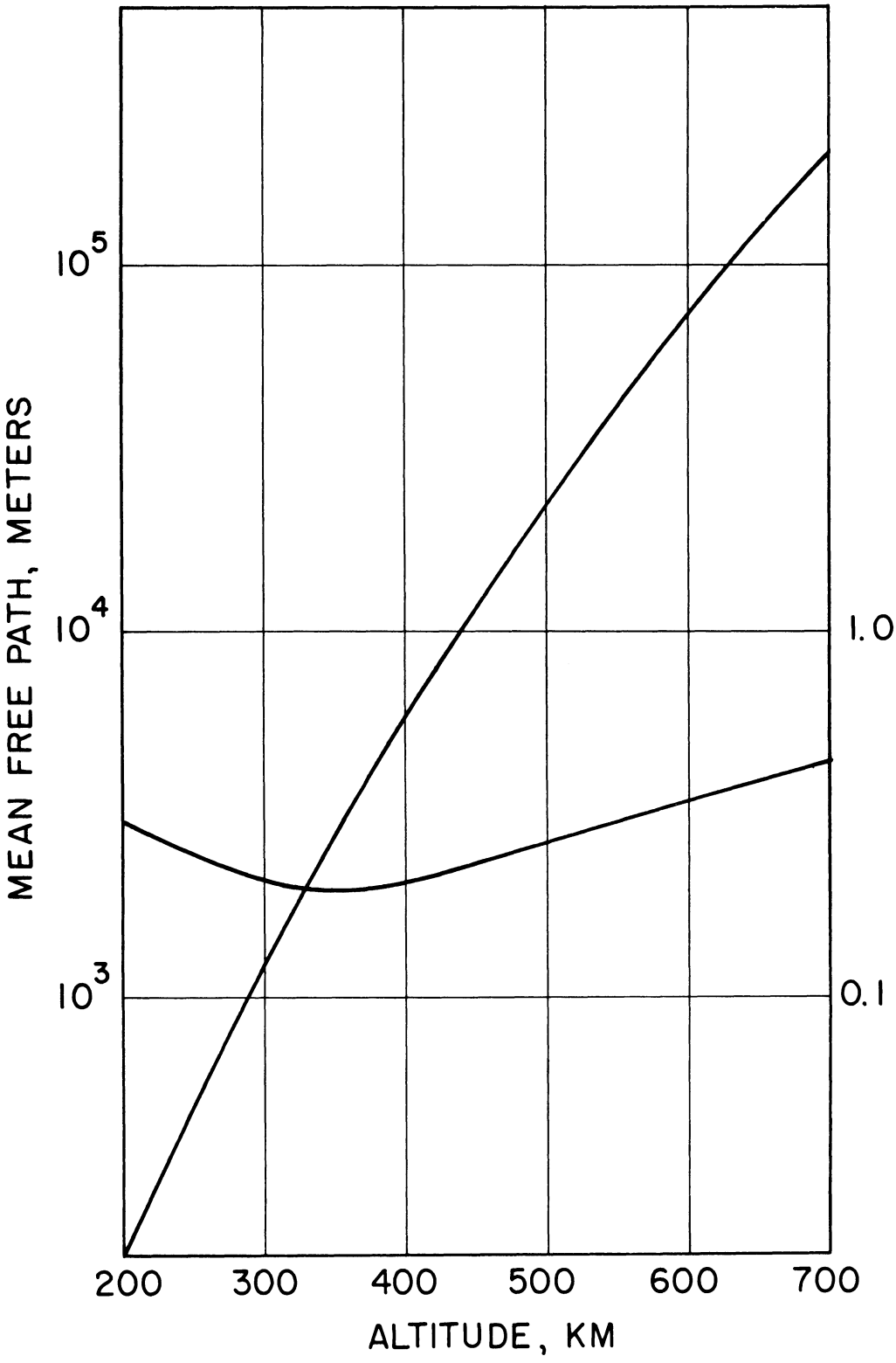

MEAN FREE PATH AND DEBYE DISTANCE AS FUNCTIONS OF ALTITUDES

Fig. 4-1

A physical interpretation to the above solution can be made: note that the factor $\frac{1}{r}$ is appropriate to a single ion in a vacuum, the factor exp $(- r/R_D)$ represents the influence of the plasma.

In the general case with a body of finite size moving at high speeds, the electron and ion densities (n_e and n_i) must be considered as functions of the translational speed of the body. Among other factors, the sheath will be distorted from the symmetric ring shape and its thickness will no longer be uniform. This will be discussed later.

The Debye radius R_D and the mean free path λ of the atmospheric neutral particles are plotted as functions of altitude in Figure (4-1).

It is well known that the contemporary methods of treating flow problems can be classified into two alternatives: the continuum approach and the particle approach. The difference between these two has been over-emphasized in the literature. In the first approach, the gas (including plasma) is viewed as smeared over the whole of space. A basic criterion to justify this viewpoint is that a length characterizing the granular structure of the particle motion such as the mean free path λ in the case of neutral particles or Debye radius $\Lambda^{(R_D)}$ in the case of plasma, should be small compared to a significant size parameter of the flow field, such as the characteristic length (L) of the body in question. In the second approach, the view is held that the space is mostly vacant and the occurrences of particles are such special events that they must be

treated with the individual respect that is theirs due. Obviously this is only true when $\lambda >> L$ in the case of neutral gases; $R_D >> L$, ionized gases.

The distinction between the points of view is not so clear as was once supposed, in view of the particular manner these approaches are handled. The theory of flow of gases consists of an appropriate blending of the mechanics of particles and mathematics of statistics. In the particle approach, the large amount of information concerning the mechanics of the particles involved must be condensed by means of statistical averaging processes. This is necessary in order to cut off the uninteresting physical informations which the basic formulation contains and thus to make the problem mathematically tractable. It is clear that the distinction ultimately resides in whether the average occurs before or after the analysis, i.e., whether statistics precede or follow mechanics. Of course, the specific manner of taking the statistical averages in the particle approach must be delicately handled in treating a rarefied flow problem.

For a qualitative description of the flow regimes in the ionosphere we may use the following criteria:

(1) Continuum flow, if λ and $R_D << L$

(2) Free molecule neutral gas flow
Quasi-continuum 'plasma' flow } if $R_D << L << \lambda$

(3) Free molecule gas and 'plasma' flow, if $L << R_D$.

Note that $R_D << \lambda$ is assumed in (2) and (3); also, we assume here that plasma is considered as a separate gas which does not interact with the neutral particles in the region of interest.

One can, of course, refine the division of flow regimes to include the transition regime as intermediate between free molecule and continuum states.

In treating the flow problems in the ionosphere the interaction of the charged particles with the solid surface must be considered. The physical process thus involved is still a matter of some controversy. One hypothesis is to consider the surface as a third body for re-combination, e.g., an ion, after hitting the solid surface, becomes neutralized by an electron and emitted as a neutral particle. One should, however, be cautious in using such an hypothesis when the kinetic energy of the impinging particle is near the energy range for sputtering effect to be significant.

4.5 Mathematical Formulation of Flow Kinetics in the Ionosphere

In the following discussion we deliberately leave out the geomagnetic field effect, the approximation thus obtained should not be used for the ionosphere at an extreme altitude where the magnetic field becomes the dominating influence. The gravitational forces on the particles are also excluded. This can be justified for problems where the characteristic length of the flow field in question is small compared with the local scale height (see§4.3 of this report).

In most problems of ionospheric measurements from a sounding rocket or satellite, the electrostatic potential (Φ) in the immediate neighborhood of measuring probe, which is immerged in the electrohydrodynamic disturbances created by the moving body, is of utmost interest. The potential distribution is governed by the Poisson equation:

$$\nabla^2 \Phi = 4\pi e (n_e - n_i) \tag{4.2}$$

which is prescribed in terms of the local concentrations of ions (n_i) and electrons (n_e). Therefore, to build a consistent theory of potential distribution, we need to know the rigorous expression of ion and electron distribution functions which can be obtained, for a rarefied plasma as the ionosphere, as the solutions to the Boltzmann-Vlasov equations for the two charge species:

$$\frac{\partial f}{\partial t} + \vec{v} \cdot \frac{\partial f}{\partial \vec{r}} + \frac{e}{m} \frac{\partial \Phi}{\partial \vec{r}} \cdot \frac{\partial f}{\partial \vec{v}} = 0 \tag{4.4}$$

where $f(\vec{r}, \vec{v}, t)$ is the distribution function for either ions or electrons with correspondingly prescribed $(e/m)\partial\Phi/\partial\vec{r}$. $\vec{v}$ is the particle velocity and $\vec{r}$ is the particle displacement.

Note that in equation (4.4) the change of $f(\vec{r}, \vec{v}, t)$ due to "binary collisons," as discussed in §4.3, has been neglected because of the tenuous nature of the ionosphere, while the collective motion effects due to charge separation appear in the last term on the left hand side in the form of an external force field acting upon the particles.

To complete the formulation of the problem, we must specify the boundary conditions which express the process of impinging of the charged particles at the body.

4.6 Solutions to Problems of Ionospheric Interest

We chose to treat two problems of geophysical interest. The first contribution (see Appendix I) deals with the electrostatic potential distribution in the sheath near the frontal part of a moving body. The aim of this analysis is to supply some useful information pertaining to the measurements of ionosphere with Langmuir probes, etc. The second contribution (see Appendix II) attempts to clarify much of the existing confusion concerning the electrohydrodynamic wake behind a moving body in an ionosphere. As an initial study of this complex problem, we chose a body of finite size moving at a subsonic speed in order to make the analysis tractable. It is our opinion that some significant revelation concerning the structure of wake has been made through this analysis.

5. Miscellaneous Problems of Geophysical Interest

5.1 Skin Temperature of a Sounding Rocket

In sounding rocket design, a problem of great interest is the strength of the structure which may possibly be weakened by the sudden and intense heat input from aerodynamic energy conversion. The heat conduction theory, usually based on the simple assumption of constant heat transfer coefficient, apparently does not apply to the problem in question because of the highly transient nature of the heat input function.

We have solved a problem pertaining to the skin temperature of a sounding rocket (see Appendix III) which may have a time-dependent heat transfer coefficient.

5.2 Free Convection Problems

A flow phenomenon, basic to the dynamics of the atmosphere is the free convection generated by the coupling of temperature gradient with external force field (gravity). To treat this hydrodynamic problem properly one has to start with the Navier-Stokes equation of motion which is highly non-linear. The mathematical difficulty involved with this non-linear boundary value problem is well known.

In an attempt to understand the basic nature of this interaction between gravity and thermal gradient effects for a flow medium, we set up a relatively simple problem that incorporates with this interesting interaction phenomenon. We use a flow in a cavity with temperature gradient and external (centrifugal) force (see Appendix VIII), and found some intricating results with the aid of IBM 704 computer.

We then proceed to treat a specific feature, the stagnation phenomenon, of this type of flow in a cavity and obtain some interesting results (see Appendix IX) which may be of interest to the cooling of gas turbine blades rotating at very high speeds.

5.3 Molecular Distribution Function and H-Theorem

Thirteen years ago, H. Grad published his memoir of thirteen-moment distribution which was claimed to be of uniform validity in the non-equilibrium processes of gas kinetics. It is supposed to be a theory of wider applicability than Chapman-Enskog's. It turns out that his claim is not exactly valid although it does represent a new approach which has been very influential upon later works.

The key to Grad's theory is the new formulation of the molecular distribution function in terms of thirteen moments, in an order of approximation higher than that of Navier-Stokes. Grad's thirteen-moment distribution is essentially a hypothesis. P. B. Hays has shown that the thirteen-moment distribution of Grad can be derived by invoking the H-theorem of Boltzmann (Appendix XII).

6. Conclusions and Suggestions

The present study has made an ambitious attempt to analyze a very wide spectrum of geophysical problems extending from free convection phenomena, sphere drag, transition flow aerodynamics to electrohydrodynamics of ionosphere. In a short period of three years, one does not expect to resolve all the problems, perhaps not even one, mentioned here. The nature of these problems is such that it is unlikely to see some one solving any of these over night; rather, one is expected to clear the obstacles little by little with continuous effort.

In the mean time, the understanding of the physical problem thus gained would always be helpful in improving the contemporary geophysical experiments, e.g., the need for measurement of the skin temperature of a falling sphere in order to make sphere drag in the rarefied atmosphere determinable, is a typical example. The current measurements of electron temperature and concentration of the ionosphere are even more susceptible to improvement because of the complex nature and primitive status of the rarefied plasma dynamics.

Repeated emphases have been made in this report about the desirability of coordinating the geophysical experiments with gas dynamical studies in the rocket sounding programs. One simple guiding principle of this approach is to make the geophysical measurements redundant such that the over-determinateness of the unknown quantity of gas dynamics can be used to reveal some physical insight of it. For instance, it would be very useful geophysically

and gas-dynamically to set up a rocket probing, in the ascending trajectory of which pitot tube is used to measure the ambient density with the release of a falling sphere near the peak of the trajectory; the ambient density, below the peak altitude can be thus re-determined. In so doing, we can cross-calibrate the sphere drag and the pitot pressure both of which are knowledge basic to the science of rarefied gas dynamics.

The exosphere phenomenon which pertains to the escape of atmospheric particles from the earth's gravitational field at the fringe of the atmosphere (see Appendix XI) presents a gas kinetic problem of unusual interest. Although lately there have been several papers in the literature (see, for instance, Öpik and Singer, 1961) dealing with the molecular aspect of the exosphere, it appears, however, that a fundamental aspect of the problem has been ignored, namely, whether there is a dynamic equilibrium between the outer atmosphere of the earth and the interplanetary gas, the existence of which is still a matter of controversy.

REFERENCES

1. Liu, V. C., "On a Pitot-Tube Method of Upper-Atmosphere Measurements," J. G. Res., June 1956.

2. Liu, V. C., "On the Drag of a Sphere at Extremely High Speeds," J. App. Phys., February 1958.

3. Liu, V. C., "On Pitot Pressure in an Almost-Free-Molecule Flow - A Physical Theory for Rarefied Gas Flows," JAS, 1958.

4. Liu, V. C., "On the Drag of a Flat Plate at Zero Incidence in an Almost-Free-Molecule Flow," J. Fluid Mech., 1959.

5. Liu, V. C., and Inger, G. R., "On Almost-Free-Molecule Flow Through an Orifice," JAS, 1960.

6. Chapman, S., and Cowling, T. G., "Mathematical Theory of Non-Uniform Gases," Cambridge, 1957.

7. Patterson, G. N., "Molecular Flow of Gases," Wiley, 1956.

8. Baker, R. M. L., Jr., and Charwat, A. F., "Transitional Connection to the Drag of a Sphere in Free Molecular Flow," Phys. Fluids, 1958.

9. Wang-Chang, C. S. W., "On the Dispersion of Sound in Helium," APL/JHU CM-467 (1948), The University of Michigan.

10. Öpik, E. J., and Singer, S. F., "Distribution of Density in a Planetary Atmosphere," Phys. Fluids, 1961.

11. Bogoliubov, N. N., "Problems of a dynamic theory in statistical physics" Geophys. Res. Paper #70 (trans. by Gora, E. K.)

7. Acknowledgement

This work was sponsored by Geophysics Research Directorate, Office of Aerospace Research, U. S. Air Force whose cooperation and support is gratefully acknowledged.

Finally, we would like to thank Dr. C. Stergis for his constant interest in this work and Dr. H. L. Pond for his help in monitoring the project.

Appendix I

On the Sheath Surrounding a Metallic Body in a Very Rarefied Plasma

(Contributed by Paul B. Hays)

Abstract

A nonlinear kinetic analysis of the sheath isolating the forward face of a metallic body is developed. The theory is valid for arbitrary bodies of small curvature moving supersonically through a highly rarefied n-component plasma. An interesting similarity results when there are no negative ions present. In this case the sheath is dependent only upon n-normal mach numbers and ion density ratios. The universal sheath resulting merely shifts relative to the body in order to satisfy the condition that the potential is the surface potential at the body.

Introduction

Direct observations of the properties of the ionosphere have become common with the present sounding rockets and satellite vehicles as measuring platforms. However, most of these studies suffer to some degree because of the complex plasma sheath which separates the measuring device from the ambient rarefied plasma. A great deal is known about this phenomena for bodies at rest (i.e. the Langmuir Probe studies), however, little work has been done for moving bodies. The work that has been done in this area is concerned mainly with the properties of the wake behind the body.[1, 2, 3, 4]# While these discussions have been useful in a qualitative sense, they are of little value to the experimental scientist who is concerned with the precise conditions which exist in the neighborhood of his device. The present paper will deal with these problems which must be faced when actual measurements are made with an instrument contained in or in the proximity of a large odd shaped body.

Of course, it would be entirely unreasonable to expect that this can be done without some restricting conditions. However, these restrictions are not as severe as one would expect. In fact, there are only three major restrictions. First, the section of the body being considered must have a normal mach number greater than 1.0. Secondly, the radius of curvature of the body in the neighborhood of interest must be very much greater than the debye length characterizing the plasma. Thirdly, the surface potential of the body must be negative. Under these conditions one finds that the sheath separating the body from the rarefied plasma is well defined and characterized only by the normal mach number and the surface potential. (i.e., The surface potential is nondimensionalized by ambient plasma kinetic potential.) This last remark applies to a plasma containing only one species of ions. However, the extension to a realistic multicomponent plasma is trivial. The sheath of the n-component plasma is characterized by the surface potential, n mach numbers based upon various species, and n-number density ratios. This result is given in the discussion to follow, however, the numerical results are for a two component plasma containing singly ionized particles and electrons.

#Refer to the numbers of References listed at the end of this appendix.

General Discussion

The motion of a highly rarefied plasma consisting of ions, electrons, and neutral particles is governed by a set of Boltzmann species equations coupled by the overall electric field and the "collision" interactions. These can be written schematically as follows:

$$\frac{\partial f_i}{\partial t} + \vec{v} \cdot \frac{\partial f_i}{\partial \vec{x}} + \frac{Z_i e \vec{E}}{M_i} \cdot \frac{\partial f_i}{\partial \vec{v}} = C_i \qquad i = 1 \ldots N \qquad 1\text{-}1$$

$$\frac{\partial f_e}{\partial t} + \vec{v} \cdot \frac{\partial f_e}{\partial \vec{x}} - \frac{e\vec{E}}{M} \cdot \frac{\partial f_e}{\partial \vec{v}} = C_e$$

The overall electric field E is derived from the smoothed charge density and the "collision" terms C contain all the fluctuation contributions. In this paper the plasma will be assumed to be so rarefied that the fluctuation terms are unimportant. This condition is only realistic in the immediate neighborhood of the body and the effects over large distances must be introduced by the boundary conditions. Thus the problem degenerates to the solution of a set of Landau-Vlasov equations[#] coupled by the electric field. Notice that for the neutral particles, where $Z_i = 0$, the equations for these particles are uncoupled from those of the other species when collisions are neglected. Thus the usual free molecular solutions hold for these particles.

The formal solution to the Landau-Vlasov equations is well-known and may be stated verbally as follows: The distribution function for any species in a collision free plasma is a constant along the trace of the particle path in the phase space. However, this is of little value in the general case because the electric field depends upon the distribution function and thus the particle traces are unknown. This is not a problem in all cases as is pointed out by Bernstein, et al.[5] For special cases where planar, cylindrical, and spherical symmetry exists these conditions may be written in terms of the momentum, and energies of the particles. A more detailed discussion of this phenomena will be given later. The problem now is to demonstrate that the general case may be approximated accurately with a simple one dimensional model which can be evaluated in general without recourse to exact particle tracing.

[#]Also called Boltzmann-Vlasov equations

Aside from the details of the basic equations the boundary conditions must be specified. In this paper we will be considering metallic bodies which act to recombine all charged particles which reach the surface. This imposes a restriction on the energy of the particles being used. If the impact energy is very high one must then consider the reflection of particles and foreign particles which are sputtered from the surface. However, this doesn't appear to be a problem for the particle energies encountered within the ionosphere. Thus it will be assumed that all particles impinging on the surface are reflected as neutral particles. Secondly, a condition must be imposed on the distribution function at the edge of the sheath. Here one must in essence take the "collision" phenomena into account. This is most simply taken care of by assuming that the distribution function is maxwellian at infinity. One will notice that this condition is not satisfied by the Landau-Vlasov equation, but, as pointed out by Yoshihara[6], it is a physically realistic condition.

Consider a large body which may be characterized by a length R. For this discussion let the body be spherical and the length R be the radius. It has been shown by Jastrow and Pearse[7] that near the stagnation point the sheath has a thickness of the order $\sqrt{-2\frac{e\phi_o}{KT_e}}\,\lambda_D$ for a large body where $R \gg \lambda_D$. This value proves to be valid over much of the forward surface of the sphere. Now extending this order of magnitude analysis one may give the electric field the value $\phi_o / \sqrt{-2\frac{e\phi_o}{KT_e}}\,\lambda_D$ within the sheath.

Now one may use the information given above to compute the region of influence that a boundary point[1] exerts within the sheath. This is illustrated in figure 1-1. Notice that the region of influence is actually a convenient fiction as there is really no sharp boundary. However, it is possible to define two limiting velocities which will give a definite region for practical consideration. These velocities represent the extreme deviations for particles with a random velocity equal to the mean thermal speed. These velocities are:

$$\vec{V}_1 = u_{\infty_x}\vec{i} + (u_{\infty_y} + C_M)\vec{j}$$

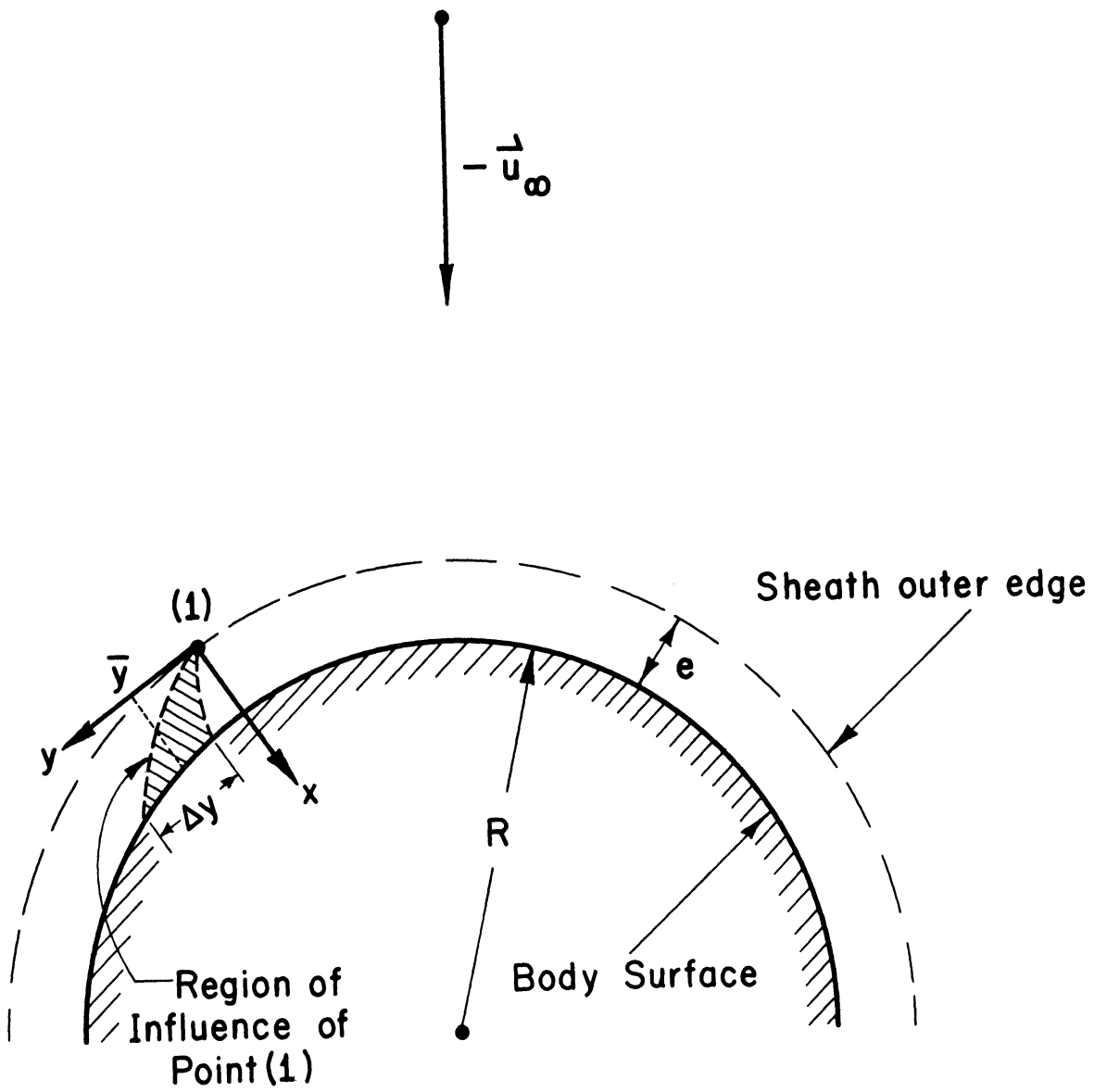

Fig. I-1 SHEATH GEOMETRY

and

$$\vec{V}_2 = u_{\infty_x}\vec{i} + (u_{\infty_y} - C_M)\vec{j}$$

A particle entering the sheath with either of these velocities will strike the body in a time

$$\Delta t = \frac{2\ell}{u_{\infty_x}} \quad \frac{1}{\gamma}\left[\sqrt{\gamma+1} - 1\right] \qquad 1\text{-}2$$

where

$$\gamma = \frac{-Z_i \frac{e\phi_o}{KT_o}}{M_{\infty_x}} .$$

The region of influence is defined by two lengths $\bar{y}$ and Δy given below.

$$\frac{\bar{y}}{\lambda_D} = 2\sqrt{\frac{2}{Z_i}} \quad M_{\infty_y} \left[\sqrt{\gamma+1} - 1\right] \qquad 1\text{-}3$$

$$\frac{\Delta y}{\lambda_D} = 2\sqrt{\frac{2}{Z_i \gamma}} \left[\sqrt{\gamma+1} - 1\right]$$

Thus the criterion that the sheath be a local phenomena which is essentially one dimensional in that $\bar{y}/R$ and $\Delta y/R$ are very small. This becomes the criteria that

$$\frac{M_{\infty_y}}{\sqrt{\gamma}} \quad \left[\sqrt{\gamma+1} - 1\right] \frac{1}{(R/\lambda_D)} << 1$$

and $\qquad 1\text{-}4$

$$\frac{1}{\sqrt{\gamma}} \left[\sqrt{\gamma+1} - 1\right] \frac{1}{(R/\lambda_D)} << 1$$

These conditions are subject to the sheath being approximately thickness given above. This requirement is essentially that the ion and electron

number densities be very close to the ambient at the distance ℓ from the surface. These conditions are satisfied if

$$\operatorname{erfc}(M_{\infty_x}) \ll 1$$

and 1-5

$$\sqrt{-\frac{e\phi_o}{KT_e}} \gg 1$$

These criteria are conditions on the ion and electron densities at the edge of the sheath. These will be discussed in more detail in a later section. Hence in review one may state that the sheath is essentially a local one-dimensional phenomena when the following criteria are satisfied.

$$\frac{M_{\infty_y}}{(R/\lambda_D)} \ll 1, \quad \frac{1}{(R/\lambda_D)} \ll 1$$

1-6

$$\operatorname{erfc}(M_{\infty_x}) \ll 1, \quad \frac{-e\phi_o}{KT_e} \gg 1$$

One-dimensional Sheath Computation

The previous discussion has shown that near the stagnation point of a large metallic body moving through a highly rarefied plasma the sheath is nearly one dimensional. Thus one may proceed to solve the problem of a one-dimensional sheath and then apply it locally to the general body subject to the condition (1-6) outlined above.

One proceeds by first determining the distribution function for a particle in a one-dimensional electrostatic potential field where no metallic boundaries exist. The potential field is assumed to drop to zero when $x \to \infty$. The distribution function for the jth species at infinity is given as,

$$f_j(\infty, \vec{V}) = n_{\infty_j} \left(\frac{\beta_{\infty_j}}{\pi}\right)^{3/2} e^{-\beta_{\infty_j}\left[(u-u_\infty)^2 + (v-v_\infty)^2 + w^2\right]} \qquad 1\text{-}7$$

However due to the planar nature of the electrostatic field one may characterize the particle motions by three parameters:

$$\left.\begin{aligned} v &= v_{\infty} \\ w &= w_{\infty} \\ \frac{m_j}{2} u^2 + Z_j e\phi &= E \end{aligned}\right\} \qquad 1\text{-}8$$

However one knows that at any point x the distribution function is the same as it is at infinity for a given particle, but that the particle has changed its position in the velocity space. This change is known as a function of the potential field and thus the distribution function is

$$f_j(\phi, \vec{V}) = n_{\infty_j} \left(\frac{\beta_{\infty_j}}{\pi}\right)^{3/2} e^{-\beta_{\infty_j}\left[\left(\pm\sqrt{u^2 + 2Z_j \frac{e\phi(x)}{m}} - u_{\infty}\right)^2\right.} \qquad 1\text{-}9$$

$$\left. + (v - v_{\infty})^2 + (w - w_{\infty})^2\right]$$

Where the + is for particles from $-\infty$, and - is for particles from $+\infty$.

One now introduces the planar metallic surface at x = 0 and imposes the recombination criterion at this surface. For negatively charged bodies the distribution becomes truncated and takes the form given below for positive and negatively charged particles.

A) Positively charged particles ($Z_j > 0$)

$$f_j(\phi, \vec{V}) = n_{\infty_j} \left(\frac{\beta_{\infty_j}}{\pi}\right) e^{-\beta_{\infty_j}\left[\left(-\sqrt{u^2 + 2Z_j \frac{e\phi(x)}{m}} - u_{\infty}\right)^2\right.} \qquad 1\text{-}10$$

$$\left. + (v - v_{\infty})^2 + (w - w_{\infty})^2\right]$$

$$\text{for } -\infty < u < -\sqrt{\frac{-2eZ_j\phi(x)}{m}}$$

$$= 0 \quad \text{otherwise.}$$

B) Negatively charged particles ($Z_j < 0$)

$$f_j(\phi, \vec{V}) = n_{\infty_j} \left(\frac{\beta_{\infty_j}}{\pi} \right)^{3/2} e^{-\beta_{\infty_j} \left[\left(-\sqrt{u^2 + 2Z_j \frac{e\phi(x)}{m}} - u_\infty \right)^2 + (v - v_\infty)^2 + (w - w_\infty)^2 \right]} \qquad 1\text{-}11$$

$$\text{for } -\infty < u < +\sqrt{\frac{2eZ_j}{m} (\phi_o - \phi_{(x)})}$$

$$= 0 \quad \text{otherwise.}$$

At this point it is obvious that the formulation is not complete as the potential field is yet unspecified. This problem is solved by taking the density moments of these distribution functions and satisfying the compatibility condition that they satisfy the Poisson equation for the potential field.

$$\frac{d^2\phi}{dx^2} = \frac{-e}{\varepsilon_o} \sum_{j=1}^{N} Z_j \int_{\infty}^{\infty} f(\phi, \vec{V})\, d\vec{V} \qquad 1\text{-}12$$

Nondimensionalizing by the mean speeds of the particle, the debye length, and the thermal energy yields the following set of equations that must be solved for ϕ as a function as x.

$$\frac{d^2\phi'}{dx'^2} = - \sum_{j=1}^{N} Z_j n_j' \left(\frac{n_{\infty_j}}{n_{\infty_e}} \right) \qquad 1\text{-}13$$

where

$$n_j' = \frac{1}{\sqrt{\pi}} \int_{\sqrt{-Z_j \phi_j'(x)}}^{\infty} e^{-\left(\sqrt{u^2 + Z_j \phi_j'} - M_{\infty_{x_j}} \right)^2} \quad (Z_j\ 0) \qquad 1\text{-}14$$

$$n_j' = \frac{1}{\sqrt{\pi}} \int_{\sqrt{+Z_j(\phi'_{o_j} - \phi'_j)}}^{\infty} e^{-\left(\sqrt{u^2 + Z_j\phi'_j} - M_{\infty_{x_j}}\right)^2} du \qquad (Z_j < 0) \qquad 1\text{-}15$$

where

$$\left.\begin{aligned} \phi' &= \frac{e\phi}{KT_e} & \phi_j' &= \phi' \, (Te/Tj) \\ x' &= x/\lambda_D & n_j' &= n_j/n_{\infty_j} \\ M_{\infty_{x_j}} &= -u_\infty \sqrt{\beta_{\infty_j}} & & \end{aligned}\right\} \qquad 1\text{-}16$$

For electrons the solution becomes rather simple as $M_{x_e} << 1$, hence one may neglect it in the integral for the density. Thus,

$$n_e' = \frac{e^{\phi'}}{2} \left(1 + \operatorname{erf} \sqrt{\phi' - \phi'_o}\right) \qquad 1\text{-}17$$

However one observes that as $x \rightarrow \infty$ n_e' should tend to one, but this condition is not satisfied if $\phi \rightarrow 0$. Thus it is necessary that a condition be placed on ϕ'_o such that this is realized. This condition is that

$$\operatorname{erfc} \left(\sqrt{-\phi_o}\right) << 1 \qquad 1\text{-}18$$

which was one of the conditions introduced initially in (6).

The equations 1-13, 1-14 and 1-15 are highly nonlinear and thus not readily amenable to closed form solution. This is not a great handicap in many cases for there exists an approximate similarity which is valid as long as there are no negative ions. That is the equations are independent of the surface potential in that case and the only effect of changing this potential is to displace the sheath outward or inward. This will become clear as the solution is presented below. We shall however simplify the computations in this brief paper by considering only a two component plasma consisting of singly ionized positive ions and electrons with a common temperature. Under this condition the problem becomes easily amenable to numerical solution. This is stated formally below.

A. Mathematical formulation

$$\frac{d^2\phi}{dx'^2} = e^{\phi'} - \frac{1}{\sqrt{\pi}} \int_{\sqrt{-\phi'}}^{\infty} e^{-\left(\sqrt{u^2 + \phi'} - M_{\infty_x}\right)^2} du \qquad 1\text{-}19$$

B. Boundary Condition

Here one has some latitude in choosing the boundary conditions. A very general solution may be obtained by first taking an asymptotic solution for small ϕ then extending this to large values of $|\phi|$ numerically.

For large distances from the body where ϕ becomes small (1-19) may be linearized to yield

$$\frac{d^2\phi'}{dx'^2} = \frac{\operatorname{erfc} M_{\infty_x}}{2} + \phi \qquad 1\text{-}20$$

The solution to this equation for convergence at $x \longrightarrow + \infty$ is

$$\phi = \phi'(o)e^{-x'} - \frac{\operatorname{erfc} M_{\infty_x}}{2} \qquad 1\text{-}21$$

$$\frac{d\phi'}{dx'} = -\phi'(o)e^{-x}$$

One notices here that the final condition of the criteria (1-6) is demonstrated in (1-21). That is if the sheath is to have an effective finite size then erfc (M_{∞_x}) must be very much less than one.

Thus it is obvious from equation (1-21) that the boundary condition need not be given at the body surface. Rather they may be chosen at a point within the sheath where the asymptotic solution is valid, then the computation may be continued backward into the sheath to any desired ϕ'_o. When this is carried out the result will be valid for any ϕ'_o and will only yield a shifting of the profile as ϕ'_o is changed.

A numerical solution of equation (1-19) has been completed for various normal mach numbers, M_{∞_x} and is presented in figure (1-2). The reference distance, x = 0, was determined by the surface potential. Figure 1-2

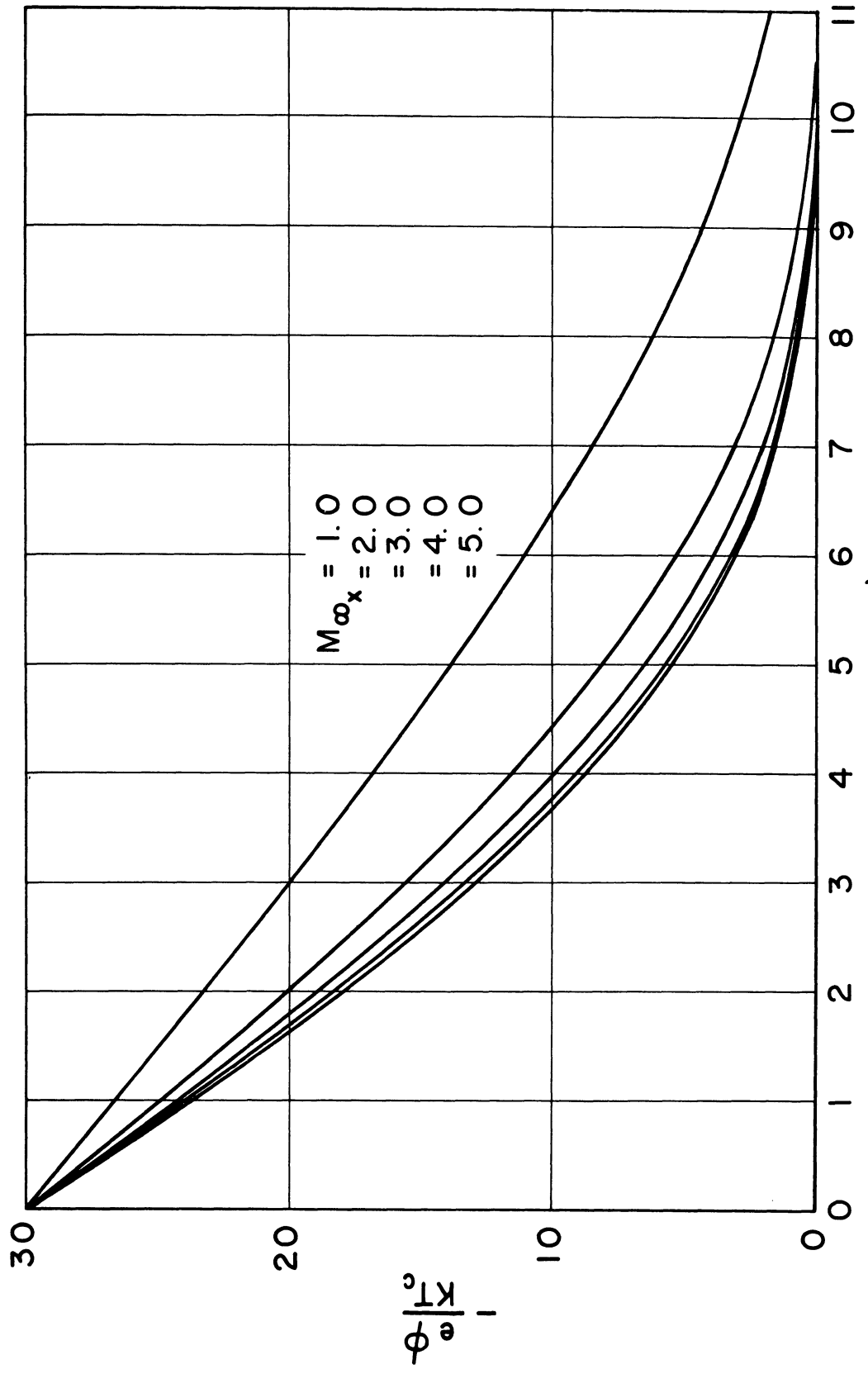

Fig. I-2 ELECTROSTATIC POTENTIAL vs. DISTANCE FOR VARIOUS NORMAL MACH NUMBERS.

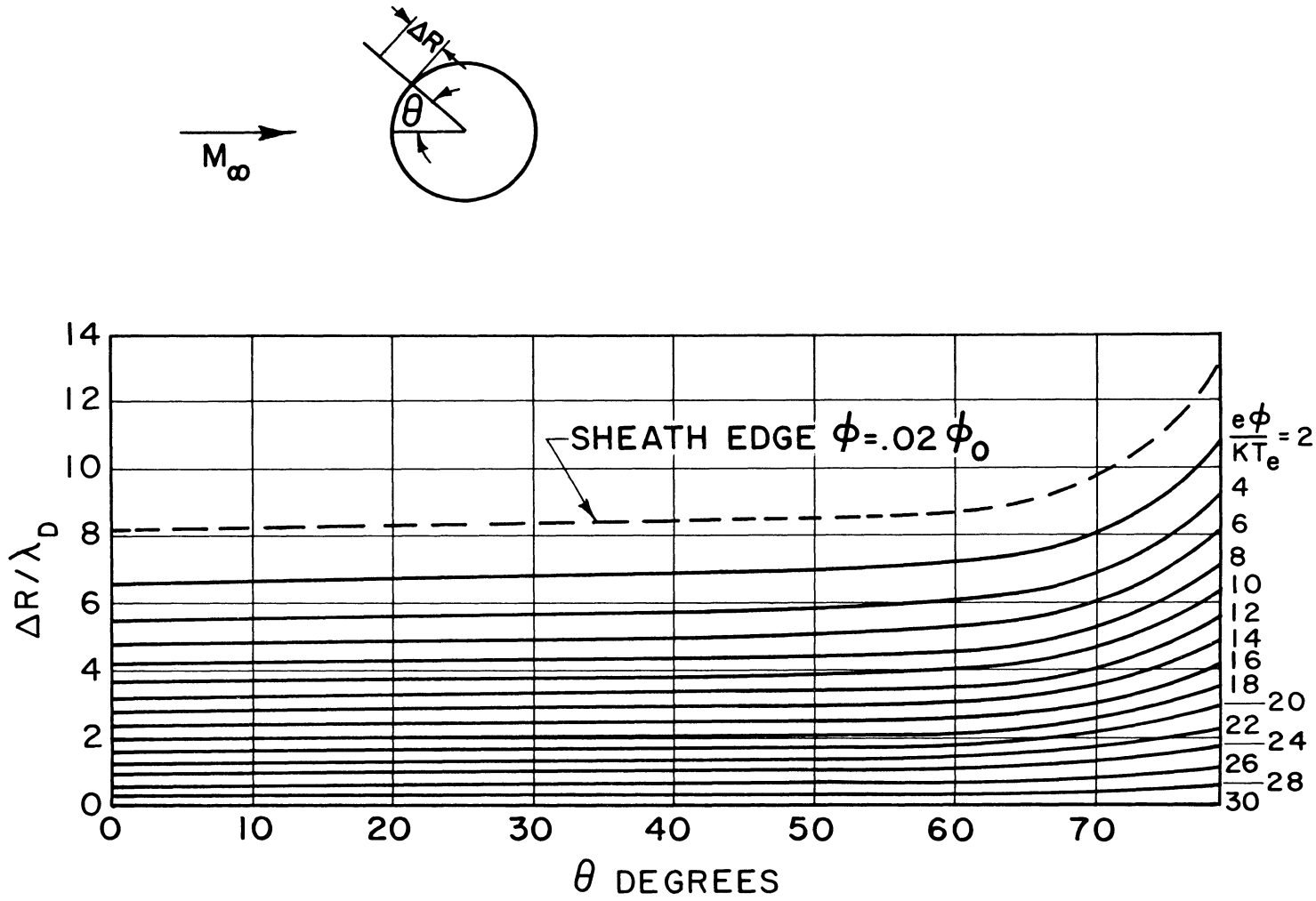

Fig. I-3 CONTOUR PLOT OF EQUI POTENTIAL LINES FOR SPHERICAL AND CYLINDRICAL BODIES

$\frac{e\phi_0}{KT_e} = 30.0$, $M_\infty = 5.0$

shows a potential profile which has been shifted corresponding to a surface potential $\phi'_o = 30$ and normal mach numbers M_{∞_x} from 1 to 5.

The results of this study were then applied to the sheath surrounding the stagnation point of a large spherical body. (Note: These are identical to the results for the corresponding cylinder.) These data are presented in figure 1-3 as contour plots of the electrostatic potential surface. It is interesting to notice that these results indicate the validity of the criteria obtained in the order of magnitude analysis. The region near the stagnation point does appear to change very slowly with distance along the sphere. Also the divergence near 80^o indicates two things. First, the one-dimensional solution is breaking down, however, this is predicted by the criteria (1-6) as the $M_{\infty_x} \cong 1.0$. Secondly, the sheath is thickening as is required in order to merge into the wake. This of course is expected and one would not expect the results in this region to be of quantitative value. However, one observes that the entire sheath forward of about 70^o is predicted by the theory.

Conclusion

The theory discussed above is able to predict the sheath surrounding a body of large curvature over most of its forward face. The limits of validity on the theory have been shown to be

$$\frac{M_{\infty_y}}{(R/\lambda_D)} << 1 \quad , \qquad \frac{1}{(R/\lambda_D)} << 1$$

$$\text{erfc}\,(M_{\infty_y}) << 1 \quad , \qquad \frac{-e\phi_o}{KT_e} >> 1 \, .$$

Thus the present theory is a valuable tool when applied to satellite vehicles carrying instrumentation which is affected by the local plasma. The results of the theory yield the distribution function, the electrostatic potential, the charge density and other moments of the distribution function at any point in the sheath. The numerical computations given herein have only been carried out for the potential field. This was done only to prove the validity of the method, however, the extension to other quantities can be carried out very easily using numerical methods.

Symbols

C_M	Mean particle speed
e	Electron charge
$\vec{E}$	Electric field
f	Distribution function
K	Boltzmann constant
ℓ	Approximate sheath thickness $\sqrt{\frac{-2e\phi_o}{KT_e}}\ \lambda_D$
m	Electron mass
M	Ion mass
M_{∞_x}	Normal Mach number u_{∞_x}/C_M
M_{∞_y}	Tangential Mach number u_{∞_y}/C_M
n	Number density
R	Radius of curvature of body
t	Time
Δt	Time for a particle to traverse the sheath
T	Temperature
$\vec{u}_\infty$	Mean velocity of fluid at infinity
$\vec{V}$	Particle speed
x	Distance normal to the body
y	Distance along the body
y	See equation (1-3)
Δy	See equation (1-3)
Z	Number of electrons stripped from an ion
β	$1/C_M^2$
λ_D	Debye length, $(\varepsilon_o KT_e/n_{o_e} e^2)^{\frac{1}{2}}$
ϕ	Electrostatic potential

Super- and Subscripts

$(\ )'$	Nondimensional quantity
$(\ )_o$	Condition at body surface
$(\ )_\infty$	Condition at infinity
$(\ )_j$	Property of j^{th} species
$(\ )_e$	Property of electron

References

1. L. Kraus and K. M. Watson, Phys. Fluids, 1, 480, (1958).

2. S. Rand, Phys. Fluids, 2, 649 (1959).

3. S. Rand, Phys. Fluids, 3, 265 (1960).

4. A. Ron and G. Kalman, Annals of Physics, 11, 240 (1960).

5. I. B. Bernstein and I. N. Rabinowitz, Phys. Fluids, 2, 112 (1959).

6. H. Yoshihara, Phys. Fluids, 4, 1361 (1961).

7 R. Jastrow and C. A. Pearse, J. Geophysical Research, 62, 3, 413 (1957).

Appendix II

On the Potential Field Surrounding a Large Metallic Body Moving Subsonically through a Rarefied Plasma

(Contributed by Paul B. Hays and V. C. Liu)

Abstract

The interactions between a highly rarefied plasma and a moving metallic body are investigated from the kinetic point of view. The present investigation considers cases where the free stream mach number is less than 1.0 and the body radius of curvature is very much greater than the debye length. Under these conditions the sheath may be separated into two regions, an inner nonlinear region, and an outer "linear" region. The inner region is treated by a one-dimensional nonlinear theory. The outer region is treated by using a perturbation on the "free molecular" solution for neutral particles. These two solutions are joined to form the complete sheath surrounding the body. The results of the theory are then illustrated with an example of a metallic sphere moving with mach number 0.2.

Introduction

The interest in electrostatic interactions within a plasma has increased substantially in the past decade. This increase has no doubt been spurred on by our ability to place measuring instruments in regions of the atmosphere where these interactions are important. In general, interactions of this type are caused by two factors. First, the instrument or instrument platform may have an electrostatic potential different from the ambient plasma. This causes particles with charges of one sign to be attracted to the body, and of the other sign to be repelled. In the steady state this results in the charge separation and currents associated with the sheath. Secondly, the existence of a solid surface induces a distortion in the distribution functions of the various types of particles. This distortion is dependent upon the character of the particles under consideration and thus will cause charge separation and currents. These properties of the plasma are of great interest in that they may be used to determine the character of the ambient plasma from the currents and other properties measured in an artificially disturbed region. Thus in order to take advantage of these properties and to cancel spurious effects it is essential that a sound theoretical foundation be established for these phenomena. Unfortunately the mathematical representations of these phenomena are highly nonlinear and not readily amenable to solution.

Recently a number of papers have been published which investigate these problems using various perturbation techniques.[1, 2, 3, 4#] These investigations have mostly increased our understanding of the basic physics underlying these interactions. However, most of these studies have been directed toward the details of the wakes behind infinitesimal point charges. This yields the perturbations in the field due to the scattering by the body as a potential well, however the effects of the body surface are absent. The metallic surface acts as a third body to recombine the charged particles which strike it. Hence the distribution functions for the ions are vastly modified near the surface and this can be the dominant disturbance in many cases. Thus it is necessary to consider the extreme where the conversion of ions and electrons to neutrals at the body surface is the dominant effect. S. Rand[3] has considered such a case in his solution for the large disc, however his solution must be considered carefully due to the breakdown of the assumption of linearity in the wake region near the body. His method

#Refer to the numbers of References listed at end of this appendix.

also suffers in that the charge distribution on the body must be known a priori, however this should in general result from the analysis. This represents one of the difficulties inherent in the consideration of large metallic bodies. Here the surface of the body is an equipotential surface and one cannot predict the surface charge distribution a priori.

The present analysis will attempt to circumvent these problems by using a perturbation technique based upon the distribution function of a neutral particle as a zeroth iterate. Secondly, a rather general solution for the Poisson equation will be derived under the condition that the electrons are in thermodynamic equilibrium and that the body surface is an equipotential surface. This solution for the electrostatic potential will be subject to the condition that $e\phi/KT_e << 1$ (i.e. that the electron density may be approximated by a linear term) and the body having small curvature. These conditions appear to be rather restrictive, but they will allow qualitative solutions for arbitrarily shaped bodies under various conditions. Finally this solution for regions where $\frac{e\phi}{KT_e} << 1$ will be supplemented with an inner ~~inner~~ solution which will hold in those regions near the body where $\frac{e\phi}{KT_e} >> 1$. The ability of these two solutions to be united to form the entire flow field about the body will be shown to depend upon the free stream mach number being subsonic.

General Considerations

When a large conducting body moves through a highly rarefied plasma it acts primarily as a sink for ionized particles. That is, it causes all charged particles which impinge upon its surface to yield their charge and be rejected as neutral particles. The result of this recombination is that the ion and electron distribution functions must be discontinuous in the velocity space. This is, of course, obvious if one considers the analogous case for neutral particles which are unaffected by an electrostatic field. In this extreme, neglecting the reflection of particles from the body, the distribution function is equal to the ambient distribution except in those regions of the velocity space where a particle would have to pass through the body in order to reach the point being considered. Those velocities where a particle would pass just tangent to the body define the discontinuity. On one side of this surface in velocity space the distribution is the ambient,

on the other it is zero. The mechanism is identical in the case of charged particles except that the ambient distribution is distorted due to the curved particle trajectories and the boundaries of the discontinuity are twisted due to this same effect. Thus one must initially face the fact that simple perturbations on the ambient distribution function cannot yield useful results.

It appears after this brief introduction that a rigorous solution for the distribution functions in the presence of a metallic body presents quite a formidable task. However, it is reasonable to consider one effect to be dominant and carry the others as perturbations. This has been done by Kraus and Watson[1] in their discussion of the wake behind a charged body. In their solution they entirely neglected the effect of the recombination of ions at the body surface and considered only the distortions due to the potential field. We shall approach the problem from the other extreme where the body is very large and consequently the recombination is dominant. However, it will be necessary to consider the distortions of the distribution function by the potential field at least as a perturbation in this case.

In order to clarify the succeeding discussion we shall define the restriction that we are going to use in the following study. First, in order that the recombination effect be the main effect, the body must have a characteristic dimension very much larger than the debye length. Secondly, the potential field will be treated as a perturbation quantity. That is, at every point in the field the potential energy must be very much less than the average kinetic energy of the ions. These conditions become the following relations:

$$R/\lambda_D \gg 1 \qquad 2\text{-}1$$

$$\left| \frac{e\phi}{KT_e} \right| \ll 1 \qquad 2\text{-}2$$

Here R is the characteristic length of the body and ϕ is the electrostatic potential at any point in the field. Condition 2 will require more careful discussion later in this analysis. The reason for this is that the potential is not an independent parameter, but results from the analysis. Thus placing a restriction upon this parameter will restrict the number of physical problems which can be considered.

The final assumption that we shall make is that the velocity of the body is very much lower than the mean electron speed. This is actually more of a statement of fact than an assumption due to the extremely high electron thermal speeds. This assumption allows one to use the Boltzmann distribution for the electrons if the surface of the body has a highly negative potential (i.e. $-\frac{e\phi_b}{KT_e} >> 1$). This is true only to the extent that the effects of the body are only significant for electrons with very large velocity. These electrons, however, do not effect the density moment significantly. The major difficulty associated with this simplification is that it violates the criterion that $\left|\frac{e\phi}{KT_e}\right| << 1$. In order to incorporate this simplification we will consider the possibility of separating this nonlinear region from the major region of the field where $\left|\frac{e\phi}{KT_e}\right| << 1$. It is always possible to do this formally, however, for this separation to be of practical value two conditions must be satisfied. First, the "inner" region must be thin. Secondly, no particles are reflected from the inner region into the exterior region. If these conditions are true then the inner region has the nature of a boundary layer in that the exterior solution may be obtained without knowledge of the details of the inner solution.

The criterion that the inner region be thin is needed so that one may specify the general shape of the interface without detailed knowledge of the inner solution. The thinness criterion is also required in order to make the inner solution be a one-dimensional effect. If the inner solution were not nearly one dimensional than the problem would still be beyond our present methods of analysis. Secondly, the criterion that very few particles be reflected from the inner region is required in order to specify the boundary condition on the distribution function at the interface. If a large number of particles were reflected, then this boundary condition would require a detailed knowledge of the trajectories within the inner region. Here again the benefit of the separation would be lost. If both of these conditions are satisfied then one may proceed to study the inner and exterior region separately. In general, one will specify the interface and solve both the inner and exterior fields from the information given on this surface. This information is that the distribution function is zero for all velocities such that $\vec{V}\cdot\vec{n} > 0$, (i.e., $\vec{n}$, a unit normal vector at the interface) and that the interface potential

is a constant. The constant value for the interface potential is unspecified initially and will be determined by the exterior solution.

At this point in our development much of what has been said is in the nature of speculation; however, conceptually the argument seems plausible. The final reasonability lies in the results of the theoretical discussion to follow. If the results compare favorably then we have outlined a realistic approach to the physical problem. This will prove to be true with the qualification that the free stream mach number must be small.

In review we may outline our assumptions as follows:

1. The metallic body being considered is very much larger than the debye length.
2. The sheath surrounding this body is divided into a outer sheath where $\left|\frac{e\phi}{KT_e}\right| << 1$ and a thin inner transition sheath where this criterion is violated.
3. The interface surface is specified a priori and the actual body will be determined from the transitional solution.

The major restriction on this theory is that the inner sheath must be thin. This will result in restrictions being placed upon the mach number of the moving body.

Outer Sheath Solution

In the outer sheath the fundamental assumption is that $\left|\frac{e\phi}{KT_e}\right| << 1$. Secondly, the plasma is extremely rarefied, thus the collision-like effects may be neglected. Finally, the electron distribution may be approximated by linearized Boltzmann distribution as discussed above. Thus the basic relations used for this region for a singly ionized plasma may be given as

$$\frac{\partial f_i}{\partial t} + \vec{V} \cdot \frac{\partial f_i}{\partial \vec{x}} + \frac{e\vec{E}}{M_i} \cdot \frac{\partial f_i}{\partial \vec{V}} = 0 \qquad 2\text{-}3$$

where

$$\nabla^2\phi = + \frac{e}{\mathcal{E}_o} \left\{ n_{\infty_e} \left(1 + \frac{e\phi}{KT_e}\right) - \int_{\vec{V}} f_i d\vec{V} \right\}$$

$$\vec{E} = - \vec{\nabla}\phi . \qquad 2\text{-}4$$

Here the plasma consists of electrons and a single species of ionized particles of mass M_1 and charge e. In order that these equations have a solution boundary conditions must be applied at infinity and at the interface.

A. At infinity the potential tends to zero and the distribution tends to a maxwellian. This form of the distribution function is determined by the ambient plasma state and the body velocity.

B. On the interface we assume that $\phi \to \phi_o$. This condition will also determine the outer boundary condition on the transitional solution. Secondly, the distribution function will be zero for all particles entering the outer region. That is no ions are allowed to be reflected within the transitional region.

These conditions along with equations 2-3 and 2-4 completely determine the external sheath if the interface position is specified initially. The solution of this set is still formidable in its present form. However, this is not final since we have not used the fact that the potential field is small. In order to use this information we shall consider expanding the distribution function in terms of some characteristic potential value. It is reasonable to do this if the distribution function is a weak function of the potential field. This is eventually an ad hoc approach which is used to show that equations 2-3 and 2-4 may be replaced by a hierarchy of simplified perturbation equations. Thus we shall assume that the distribution function may be written as

$$f = f^{(o)} + Nf^{(1)} + N^2 f^{(2)} + \ldots \qquad 2\text{-}5$$

where $N = \frac{e\phi_o}{KT_e}$. In this case we have chosen the characteristic potential as the interface potential, however, this procedure is valid for any potential which characterizes a given problem. Now in order to simplify the analysis we nondimensionalize the equation using the following parameters.

$$t' = \frac{t\,\bar{e}}{\lambda_D} \qquad x' = \frac{x}{\lambda_D} \qquad \vec{V}' = \frac{\vec{V}}{\bar{C}}$$

$$\bar{\phi} = \frac{\phi}{\phi_o} \qquad f' = f\,\frac{\bar{C}^3}{n_\infty}$$

where $\bar{C}$ is the mean particle speed, λ_D is the debye length, ϕ_o is the interface potential, and n_∞ is the ambient particle density.

Introducing 2-5 and 2-6 into equations 2-3 and 2-4 yields the equations:

$$D(f^{(o)'} + Nf^{(1)'} + N^2 f^{(2)'} + \ldots) = N \frac{\partial \phi'}{\partial \vec{x}'} \cdot \frac{\partial}{\partial \vec{V}'}(f^{(o)'} + Nf^{(1)'} + N^2 f^{(2)'} + \ldots) \qquad 2\text{-}7$$

where

$$\nabla^2 \phi' - \phi' = -\frac{1}{N}\left\{\int_{\vec{V}'} \sum_{j=0}^{\infty} N^j f^{(j)'} \, dV' - 1.0\right\}. \qquad 2\text{-}8$$

One notices here that ϕ' is of order $[1]$ and further if the dependence of f on ϕ is small then all of the $f^{(j)}$'s are of the same or of lower order than $f^{(o)}$. Thus one may approximate 2-7 by the system of perturbation equations listed below.

$$\left.\begin{aligned} \frac{Df^{(o)'}}{Dt'} &= 0 \\ \frac{Df^{(1)'}}{Dt'} &= \frac{\partial \phi'}{\partial \vec{x}} \cdot \frac{\partial f^{(o)'}}{\partial \vec{V}'} \\ \frac{Df^{(n)'}}{Dt'} &= \frac{\partial \phi'}{\partial \vec{x}} \cdot \frac{\partial f^{(n-1)'}}{\partial \vec{V}'} \end{aligned}\right\} \qquad 2\text{-}9$$

We notice that the function ϕ' is still depends upon all of the distribution functions. However one observes from 2-8 that the highest order terms in ϕ are retained if we keep only the first two terms, i.e.

$$\nabla^2 \phi' - \phi' \cong \frac{+1}{N}\left\{1 - \int_{\vec{V}'} (f^{(o)} + Nf^{(1)}) \, d\vec{V}'\right\}$$

We may write this as

$$\phi' \cong \phi'^{(o)} + \phi'^{(1)} = \bar{\phi}'$$

where

$$\nabla^2\phi'^{(o)} - \phi'^{(o)} = \frac{-1}{N}\left\{\int_{\vec{V}'} f^{(o)} d\vec{V} - 1\right\}$$

$$\nabla^2\phi'^{(1)} - \phi'^{(1)} = -\int_{\vec{V}'} f^{(1)}\, d\vec{V} \qquad 2\text{-}10$$

Using these approximate relations the basic set of equations is modified to the form:

$$\frac{Df^{(o)'}}{Dt} = 0 \qquad 2\text{-}11a$$

$$\frac{Df^{(1)'}}{Dt'} \cdot \frac{\partial\phi'^{(1)}}{\partial\vec{X}} \cdot \frac{\partial f^{(o)'}}{\partial\vec{V}} = \frac{\partial\phi'^{(o)}}{\partial\vec{X}} \cdot \frac{\partial f^{(o)'}}{\partial\vec{V}} \qquad 2\text{-}11b$$

$$\frac{Df^{(n)'}}{Dt} = + \frac{\partial\bar{\phi}'}{\partial\vec{X}'} \cdot \frac{\partial f^{(n-1)'}}{\partial\vec{V}} \qquad 2\text{-}11c$$

These equations still contain all of the essential features of the original equations. The coupling between the distribution function and ϕ is contained in equation 2-11b. The basic equations are strikingly similar to the linearized Landau-Vlasov equations[#] for a uniform plasma. The exception is that the background distribution function is time and space dependent. i.e., From equation 2-11a,

$$f^{(o)} = f(\vec{X}' - \vec{V}'t', \vec{V}', 0)\, L(\vec{X}', \vec{V}', t') = f_{F.M.} \qquad 2\text{-}12$$

where $L(\vec{X}',\vec{V}', t')$ is zero for particles which pass through the body and is one otherwise. This solution is commonly called the free molecular solution. In many cases if one is interested only in gross effects the cross coupling in equation 2-11b may be neglected. This is equivalent to neglecting the potential ϕ' compared to ϕ'_o. To this order one may formally write the solution to the distribution function as:

[#]Or Boltzmann-Vlasov equations.

$$f' \tilde{=} \left(f'(\vec{X}-\vec{V}t,\ \vec{V},\ 0) + N \int_0^t H'(X - \vec{V}(t-\xi),\ \vec{V},\ \xi)\,d\xi\right) L'(\vec{X}', \vec{V}', t') \quad 2\text{-}13$$

where

$$H' = \frac{\partial \phi'^{(o)}}{\partial \vec{X}} \cdot \frac{\partial f^{(o)'}}{\partial \vec{V}}$$

In terms of dimensional quantities this becomes,

$$f(\vec{X}, \vec{V}, t) \tilde{=} \left\{ f(\vec{X}-\vec{V}t,\ \vec{V},\ 0) + \frac{e}{M_i} \int_0^t H(\vec{X}-\vec{V}(t-\xi), \vec{V}, \xi)\,d\xi \right\} L(\vec{X}, \vec{V}, t) \quad 2\text{-}13a$$

where

$$H = \frac{\partial \phi^{(o)}}{\partial \vec{X}} \cdot \frac{\partial f^{(o)}}{\partial \vec{V}}$$

and

$$\nabla^2 \phi^{(o)} - \frac{e\phi^{(o)}}{KT_e} = \frac{e}{\varepsilon_o} \left\{ 1 - \int_{\vec{V}} f(\vec{X}-\vec{V}t, \vec{V}, 0)\, L(\vec{X}, \vec{V}, t)\, d\vec{V} \right\} \quad 2\text{-}14$$

One observes here that the greatest single problem remaining is to evaluate the potential field in terms of the density moment of $f^{(o)}$. This is in general the practical problem which will decide the general usefulness of the approximate solution obtained at this point. In the next section we shall develop a series type solution to equation 2-14 for the potential in terms of an arbitrary density variation.

Approximate solution for the potential field

The following section will be devoted to solving the Poissons equation for the electrostatic field.

$$\nabla^2 \phi^{(n)} - \frac{e\phi^{(n)}}{KT_e} = - \frac{e}{\varepsilon_o} n_o \left(\frac{\Delta n}{n_o}\right)_n$$

In general this equation cannot be solved analytically for an arbitrary ion density function, however it will be shown that under certain condition a valid approximation may be obtained without previous knowledge of the ion density. In order to solve this equation the boundary conditions must be specified.

Boundary Conditions

For this problem the interface is at a constant potential $\phi(s) = \phi_o$. Secondly, the potential must tend to zero as the distance from the body tends to infinity.

Greens Function Solution

The solution obtained here will be given for a large spherical interface, (i.e. $R_o >> \lambda_D$). This is done only for convenience and will be extended later in the analysis. Now in order to proceed in the most general sense the equation for the potential is nondimensionalized as follows:

$$\nabla^2\phi' - \phi' = -\frac{\Delta n}{n_o}(r') \qquad 2\text{-}15$$

where

$$\phi' = \frac{e\phi^{(n)}}{KT_e}, \quad x' = \frac{x}{\lambda_D}.$$

This equation may be solved formally in terms of the Greens function ψ in the following form,

$$\phi'(r') = \frac{1}{4\pi}\iiint_{\tau_o}\frac{\Delta n}{n_o}\psi\, d\tau_o + \frac{1}{4\pi}\iint_{s_i}\phi\frac{\partial\psi}{\partial n}\, ds_i$$

$$-\frac{1}{4\pi}\iint_{s_i}\frac{\partial\phi}{\partial n}\psi\, ds_i \qquad 2\text{-}16$$

where ψ satisfies the adjoint homogeneous equation, *

*See Reference 5.

$$\nabla^2 \psi - \psi = 0$$

with boundary conditions that $\psi \longrightarrow 0$ as $\vec{r} \longrightarrow \infty$. However one observes that one additional condition on ψ is required because $\partial\phi/\partial n$ is not known on the interface. This condition is that $\psi = 0$ on the interface.

The Greens function will now be developed satisfying the condition stated above, i.e.:

Adjoint Homogeneous Equation

$$\nabla^2 \psi - \psi = 0 \qquad 2\text{-}17$$

Boundary Condition

a) $\psi = 0$ when $|r'| = a'$

b) $\psi \longrightarrow 0$ as $r' \longrightarrow \infty$

c) and further that ψ has the required singularity at the point P in the field where a charge of magnitude 4π is located.

A transformation is made to spherical coordinates yielding the equation:

$$\frac{1}{r'} \frac{\partial^2 r'\psi}{\partial r'^2} + \frac{1}{r'^2 \sin\theta} \frac{\partial}{\partial\theta} \left(\sin\theta \frac{\partial\psi}{\partial\theta}\right) - \psi = 0 \qquad 2\text{-}18$$

Note: Dependence upon azimuth angle is not included as the field is axially symmetrical.

This equation is separable yielding the two equations:

$$(1 - \mu^2) \frac{d^2 \Theta}{d\mu^2} - 2\mu \frac{d\Theta}{d\mu} + n(n+1)\Theta = 0 \qquad 2\text{-}19$$

where $\mu = \cos\theta$

and

$$\frac{1}{r'R} d^2 \frac{r'R}{dr'^2} + \frac{1}{r'^2} \left[-n(n+1)\right] - 1 = 0 \qquad 2\text{-}20$$

where

$$\psi = R\,\Theta.$$

Equation 2-19 is recognized immediately as Legendre's equation, hence,

$$\Theta = P_n(\mu). \qquad 2\text{-}21$$

It can easily be shown that the solution to 2-20 is

$$R = \frac{e^{-r'}}{r'^{n+1}} \quad \text{or} \quad r^n e^{-r'} \qquad 2\text{-}22$$

Both of these solutions satisfy the boundary condition at infinity, however th first is easier to work with. Thus choosing the first solution one has the following general form for the function ψ .

$$\psi = \sum_{n=0}^{\infty} a_n \frac{e^{-r}}{r^{n+1}} P_n(\mu) + \frac{e^{-r''}(r,\mu)}{r''(r,\mu)} \qquad 2\text{-}23$$

Here the series is used to satisfy the condition that $\psi = 0$ when $r = a$ and the last term is the solution for a point charge shielded by electrons.

See the diagram below for an explanation of the variables.

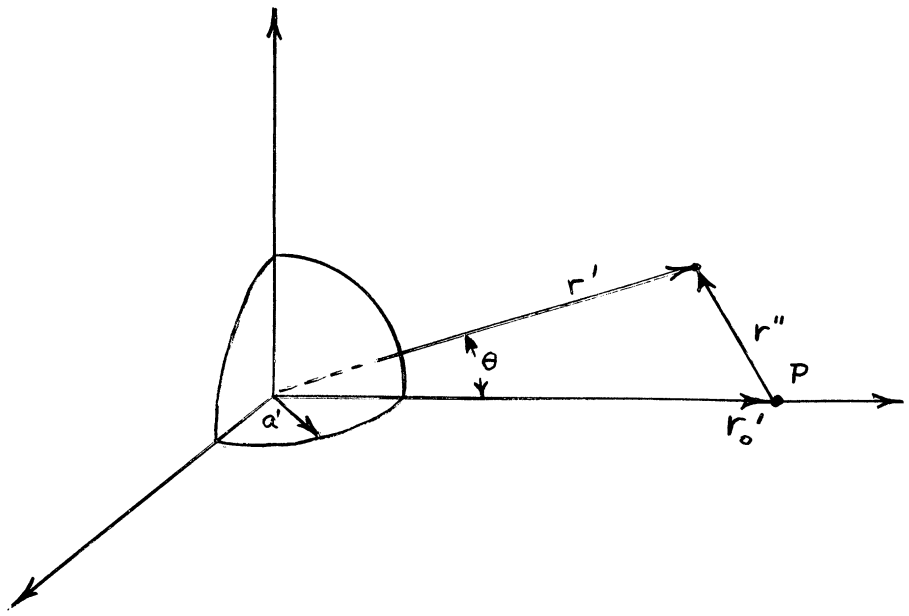

All that is required now is to evaluate the coefficients under the condition that $\psi = 0$ when $r = a$.

This condition is simply that

$$\sum_{n=0}^{\infty} Q_n \frac{e^{-a'}}{a'^{n+1}} P_n(\mu) + \frac{e^{-r''(a',\mu)}}{r''(a',\mu)} = 0 \qquad 2\text{-}24$$

Multiplying through by $P_m(\mu)$ and integrating with respect to μ yield the final relation for the coefficients.

$$Q_m = \frac{-(2m+1)}{2} \frac{a'^{m+1}}{e^{-a'}} \int_{-1}^{+1} P_m(\mu) \frac{e^{-r''(a',\mu)}}{r''(a',\mu)} \, d\mu \qquad 2\text{-}25$$

One must now evaluate the above integral. Let

$$I_m = \int_{-1}^{+1} \frac{e^{-r''(a',\mu)}}{r(a',\mu)} P_m(\mu) d\mu \qquad 2\text{-}26$$

Now transform to coordinates $\rho' = r''(a,\mu)$. Then,

$$I_m = \frac{1}{ar_o} \int_{r'_o - a'}^{r'_o + a'} P_m\left(\frac{r'^2_o + a'^2 - \rho'^2}{2a'r'_o}\right) e^{-\rho'} \, d\rho' \, . \qquad 2\text{-}27$$

Again one must make some realistic assumption in order to evaluate this integral. In the regions of the atmosphere being considered it is well known that the debye length is small, hence for relatively large bodies of the order of tens of centimeters a is a very large number. Thus $r_o + a$ is a very large number and is called infinity here. Apply the transformation $u = \rho - r_o + a = \rho - z_o$ to 2-27 which yields:

$$I_m \cong \frac{e^{-z'_o}}{a'r'_o} \int_{o}^{\infty} P_m \left(1 - \frac{u^2 + 2z'_o u}{2a'r'_o}\right) e^{-u} \, du. \qquad 2\text{-}28$$

Now the expansion for $P_m(x)$ will be introduced.

$$P_m(x) = \frac{1}{2^m} \sum_{\nu=0}^{\left[\frac{m}{2}\right]} \frac{(-1)(2m-2\nu)!}{\nu!(m-\nu)!(m-2\nu)!} x'^{m-2} \qquad 2\text{-}29$$

where $\left[\frac{m}{2}\right]$ denotes the integer n, such that $n \leq \frac{m}{2} \leq n+1$. At this point we make the following observation. Due to the extremely large value of $2ar_o$ we may assume that

$$\frac{u^2 + 2z'_o u}{2a'r'_o} << 1 \qquad 2\text{-}30$$

for the important interval in the integration. Then:

$$I_m \simeq \frac{e^{-z'_o}}{a'r'_o} \int_o^\infty \frac{1}{2^m} \sum_{\nu=0}^{\left[\frac{m}{2}\right]} \frac{(-1)^\nu (2m-2\nu)!}{\nu!(m-\nu)!(m-2\nu)!} \left\{1 - \frac{m-2\nu}{2a'r'_o}(u^2 + 2z'_o u)\right\} e^{-u}\, du \qquad 2\text{-}31$$

$$= \frac{e^{-z'_o}}{a'r'_o} \left\{ \frac{1}{2^m} \sum_{\nu=0}^{\left[\frac{m}{2}\right]} \frac{(-1)^\nu (2m-2\nu)!}{\nu!(m-\nu)!(m-2\nu)!} \left[1 - \frac{m-2}{2a'r'_o}(2 + 2z'_o)\right] \right.$$

But for points near the body, which is all that one will find to be of interest, the last term is negligible, thus one finds that

$$I_m = \frac{e^{-z'_o}}{a'r'_o} P_m(1) = \frac{e^{-z'_o}}{a'r'_o} \qquad 2\text{-}32$$

Thus the coefficients Q_m have been determined, i.e.

$$Q_m = -\frac{(2m+1)}{2a'r'_o} \frac{a'^{m+1}}{e^{-a'}} e^{-z'_o} \qquad 2\text{-}33$$

This yields the final form for the Greens function.

$$\psi = \frac{e^{-r''(r,\mu)}}{r''(r,\mu)} - \frac{e^{-(z'_o + r'-a')}}{a'r'_o} \sum_{m=0}^{\infty} \frac{2m+1}{2} \left(\frac{a'}{r'}\right)^{m+1} P_m(\mu) \qquad 2\text{-}34$$

Up to this stage the only assumption of major consequence is that $(z_o/a^2) \lll 1$. This is a physically realistic assumption due to the extremely sharp damping exerted by the electrons in the region of the test charge. This is in effect the ability of the electrons to shield any local discontinuity from the rest of the field. One may further assume that a/a+z = 1, allowing the above series to be summed. This greatly simplifies the work of integration which must succeed this development.

$$\psi \cong \frac{e^{-r''(r,\mu)}}{r''(r,\mu)} - e^{-(r'-a')} \frac{e^{-\sqrt{x'^2 + y'^2 + z'^2_o}}}{\sqrt{x'^2 + y'^2 + z'^2_o}}$$

$$\cong \frac{e^{-\sqrt{x'^2 + y'^2 + (z'-z'_o)^2}}}{\sqrt{x'^2 + y'^2 + (z'-z'_o)^2}} - \frac{e^{-z'} e^{-\sqrt{x'^2 + y'^2 + z'^2_o}}}{\sqrt{x'^2 + y'^2 + z'^2_o}} \qquad 2\text{-}35$$

Here rectangular coordinates based at the surface of the sphere have been introduced.

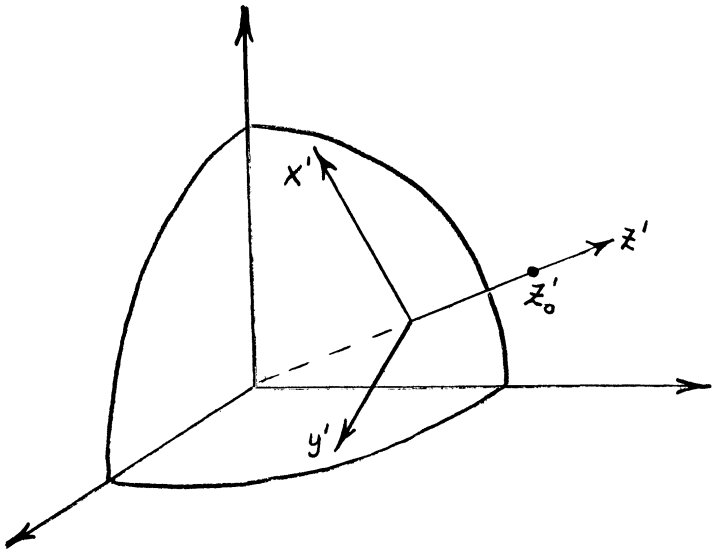

Evaluation of the Potential

The next step is to evaluate the potential using the Green's function developed above. The surface integral of $\frac{\partial \psi}{\partial n}$ is easily evaluated yielding the following form for $\phi(z_o)$

$$\phi'(z_o) = \phi_o' e^{-z_o'} + \frac{1}{4\pi} \iiint_{z>0} \frac{\Delta n_i}{n_{i\infty}} \psi dx'dy'dz' \qquad 2\text{-}36$$

We note here that the only major assumption introduced thus far is that the radius of curvature of the body is much larger than z'. This is equivalent to assuming that the body appears as a plane isolating the half space $z > 0$. This yields a valid solution for the potential about all bodies which have small curvature. Thus the results developed from this point on will be valid for a body of any shape which has a small curvature.

The final evaluation of the potential involves the weighted integral of the density. However due to the sharp damping of the ψ function one may expand the density in a Taylor series about the point under consideration.

$$\frac{\Delta n}{n_\infty} = \frac{\Delta n}{n_\infty}\bigg|_{z_o'} + \frac{\partial}{\partial x'}\left(\frac{\Delta n}{n_\infty}\right)\bigg|_{z_o'} x' + \frac{\partial}{\partial y'}\left(\frac{\Delta n}{n_\infty}\right)\bigg|_{z_o'} y' + \frac{\partial}{\partial z'}\left(\frac{\Delta n}{n_\infty}\right)\bigg|_{z_o} (z' - z_o')$$

$$+ \tfrac{1}{2}\frac{\partial^2 \left(\frac{\Delta n}{n_\infty}\right)}{\partial x'^2}\bigg|_{z_o'} x'^2 + \tfrac{1}{2}\frac{\partial^2}{\partial y'^2}\left(\frac{\Delta n}{n_\infty}\right)\bigg|_{z_o'} y'^2 + \tfrac{1}{2}\frac{\partial^2}{\partial z'^2}\left(\frac{\Delta n}{n_\infty}\right)\bigg|_{z_o'} (z'-z_o')^2 \qquad 2\text{-}37$$

$$+ \ldots$$

This series has been truncated with the quadratic terms for simplicity, however, it can be carried to any degree of accuracy required. These integrals are tedious, but elementary, thus only the results will be given. To terms quadratic in x, y, and z the results are given below.

$$\phi'(z_o) = \phi'_o e^{-z'_o} + \left.\frac{\Delta n}{n_\infty}\right|_{z'_o} (1 - e^{-z'_o})$$

$$+ \left.\frac{\partial}{\partial z'}\left(\frac{\Delta n_i}{n_\infty}\right)\right|_{z'_o} z'_o e^{-z'_o} + \left(\frac{\partial^2}{\partial x'^2}\left(\frac{\Delta n}{n_\infty}\right) + \frac{\partial^2}{\partial y'^2}\frac{\Delta n}{n_\infty}\right)_{z_o}\left[1 - 3/4 z'_o e^{-z'_o}\right] \qquad 2\text{-}38$$

$$+ \left.\frac{\partial^2 \frac{\Delta n}{n_\infty}}{\partial z'^2}\right|_{z'_o}\left[1 - \left(\frac{z'^2_o}{2} + 1\right) e^{-z'_o}\right] + \ldots$$

This result yields a value for $\phi' = \phi'_o$ at the interface and appears to have the correct limit far from the body. This outer limits may be considered as follows. If the potential were taken such that electrical neutrality existed then,

$$\phi'^{(o)} = \Delta n_i / n_{i_\infty} \,. \qquad 2\text{-}39$$

However the next iterate would be that

$$\phi^{(1)'} = \Delta n_i / n_{i_\infty} + \nabla^2 \phi^o = \frac{\Delta n_i}{n_{i_\infty}} + \nabla^2 \frac{\Delta n_i}{n_{i_\infty}} \,. \qquad 2\text{-}40$$

But this exactly what the above solution yields far from the body. Note that the next higher iterate would involve forth derivatives and hence it is possible to neglect these in slowly varying density fields.

Note:

This lends some credibility to the possibility of using an iterative solution to the nonlinear Poisson's equation, i.e., in regions far from a metallic body the nonlinear solution should approach

$$\phi' = \log (n_i/n_{i_\infty}) + \nabla^2 \log (n_i/n_{i_\infty}) + \ldots$$

Review of Exterior Solution

We have constructed a theory for the exterior sheath surrounding a large metallic body. This solution depends upon three main assumptions.

1. The curvature of the body is very small.
2. The sheath may be resolved into two sections, an inner sheath, and an outer sheath.
3. The potential outside of the interface between the two sheaths is small such that $\left|e\phi/KT_e\right| << 1$.

Under these conditions one obtains the approximate solution for the distribution function in the outer sheath.

$$f(X, V, t) = \left\{ f(\vec{X}-\vec{V}t, \vec{V}, 0) + \frac{e}{M_i} \int_0^t H(\vec{X}-\vec{V}(t-\xi), \vec{V}, \xi)d\xi \right\} L(\vec{X}, \vec{V}, t) \qquad 2\text{-}41$$

where

$$H(\vec{X}, \vec{V}, t) = \frac{\partial \phi^{(o)}}{\partial \vec{X}} \quad \frac{\partial f(\vec{X}-\vec{V}t, \vec{V}, 0)L(\vec{X}, \vec{V}, t)}{\partial \vec{V}} \qquad 2\text{-}42$$

$$\frac{e\phi^{(o)}}{KT_e} = \frac{e\phi_o}{KT_e} e^{-z/\lambda_D} + \frac{\Delta n}{n_\infty} \Big|_z (1-e^{-z/\lambda_D}) \qquad 2\text{-}43$$

$$+ \frac{\partial}{\partial z} \frac{\Delta n}{n_\infty} (e^{-z/\lambda_D} + \lambda_D^2 \left(\frac{\partial^2}{\partial x^2} \frac{\Delta n}{n_\infty} + \frac{\partial^2}{\partial y^2} \frac{\Delta n}{n_\infty} \right) \left[1 - 3/4\, z/\lambda_D\, e^{-z/\lambda_D} \right]$$

$$+ \lambda_D^2 \partial^2 \frac{\frac{\Delta n}{n_\infty}}{\partial z^2} \left[1 - \left(\frac{z^2}{2\lambda_D^2} + 1 \right) e^{-z/\lambda_D} \right] + \ldots$$

$$\frac{\Delta n}{n_\infty} = \frac{1}{n_\infty} \left\{ \int_{\vec{V}} f(\vec{X}-\vec{V}t, \vec{V}, 0)L(\vec{X}, \vec{V}, t)d\vec{V} - n_\infty \right\} \qquad 2\text{-}44$$

This solution is complete in the exterior region if the interface is known (i.e., if the interface is known then L(X, V, t) is known). The next problem is to determine the interface shape in terms of the body shape, or the converse problem. The next section will be devoted to obtaining an approximate solution for inner sheath.

Inner Sheath Solution

The inner sheath depends upon the condition at the interface and the body surface potential. If this region is thin as is required by our original discussion then the inner solution is eventually one dimensional. There is an "exact" solution for this problem if the condition at the interface are known. Exact here refers to a solution under the assumption that there is no scattering due to collision-like effects. This solution was discussed by the present author in a previous paper[6], thus only the results will be given here. The distribution function for the electron still may be approximated by the Boltzmann distribution. The ions, however, have a distribution function given by,

$$f(z, \vec{V}, t) = f(0, u-u_o, v-v_o, -\sqrt{w^2 + \frac{2e}{M_i}\phi(z) - w_o}). \qquad 2\text{-}45$$

where the subscript (o) refers to the interface. w is perpendicular to the interface directed into the outer sheath. See diagram below.

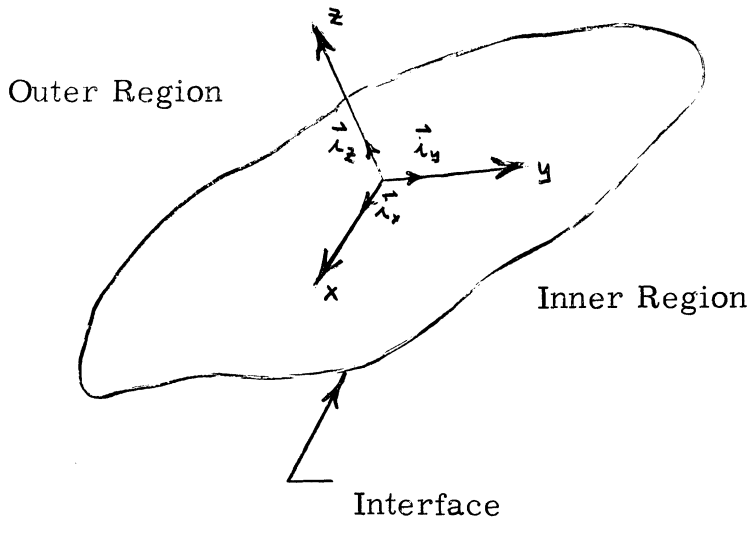

The solution given here is a quasi-steady solution depending upon the rate of change of this field being slow in a time period $\tau = \sqrt{\beta}\lambda_D = 1/\omega_{p_i}$ (i.e., ion plasma frequency).

In order to obtain the condition at the interface one may neglect the perturbation in the outer solution due to the potential in the first approximation. For a large body this distribution depends only upon the angle of the local normal to the free stream velocity. For a maxwellian velocity distribution the approximate distribution at the interface is:

$$f(o, \vec{V}, t) = n_\infty \left(\frac{\beta_\infty}{\pi}\right)^{3/2} e^{-\beta_\infty\left[(u-u_o)^2 + (v-v_o)^2 + (w-w_o)^2\right]} \quad w < 0 \qquad 2\text{-}46$$

$$= 0 \quad w > 0$$

where

$$\left.\begin{aligned} u_o &= -\vec{i}_x \cdot \vec{u}_\infty \\ v_o &= -\vec{i}_y \cdot \vec{u}_\infty \\ w_o &= -\vec{i}_z \cdot \vec{u}_\infty \end{aligned}\right\}$$

where $\vec{u}_\infty$ = velocity of the body.

Thus the ion distribution function within the inner sheath is given by

$$f(\vec{z}, \vec{V}, t) = n_\infty \left(\frac{\beta_\infty}{\pi}\right)^{3/2} e^{-\beta_\infty\left[\left(\sqrt{w^2 + \frac{2e}{M_i}(\phi-\phi_o)} - w_o\right)^2 + (v-v_o)^2 + (u-u_o)^2\right]} \qquad 2\text{-}47$$

$$\text{for } w < -\sqrt{\frac{2e}{m}(\phi_o - \phi)}$$

$$= 0 \qquad \text{for } w > -\sqrt{\frac{2e}{m}(\phi_o - \phi)}$$

The ion density at any point is then given by

$$n(\vec{z}, t) = n_\infty \sqrt{\frac{\beta_\infty}{\pi}} \int_{-\sqrt{\frac{2e}{m}(\phi_o-\phi)}}^{\infty} e^{-\left(\sqrt{\beta_\infty w^2 + \frac{e}{KT_e}(\phi-\phi_o)} - \sqrt{\beta_\infty} w_o\right)^2} dw \qquad 2\text{-}48$$

and thus the potential in the inner sheath satisfies the equation:

$$\nabla^2\phi = +\frac{e}{\epsilon_o} n_o \left(e^{\frac{e\phi}{KT_e}} - \frac{1}{\sqrt{\pi}} \int_{\sqrt{\frac{e}{KT_e}(\phi_o - \phi)}}^{\infty} e^{-\left(\sqrt{w'^2 + \frac{e}{KT_e}(\phi - \phi_o)} - \beta u_{\infty o} \right)^2} dw' \right) \quad 2\text{-}49$$

where

$$\phi = \phi_o, \quad \frac{\partial\phi}{\partial x} = \frac{\partial\phi}{\partial x}\Big|_o \text{ at } z = 0$$

and the sheath thickness is given by

$$\Delta z = z \text{ where } \phi = \phi_b$$

The interface solution can be carried out very easily by numerical means, however we shall consider a simple order of magnitude method such as that used by Jastrow and Pearse[7] for simplicity. Jastrow and Pearse assume that within the nonlinear sheath the electron density is zero and the ion density is equal to the density at the edge of the sheath. This yields a parabolic approximation to the sheath given by:

$$\frac{e\phi}{KT_e} = -\tfrac{1}{2}\left(\frac{n_o}{n_\infty}\right)\left(\frac{z}{\lambda_D}\right)^2 + \frac{\partial\frac{e\phi_o}{KT_e}}{\partial\frac{x}{\lambda_D}} \lambda_D + e^{\frac{\phi_o}{KT_e}} \quad 2\text{-}50$$

For small ϕ_o and $\partial\frac{\phi_o}{\partial x}$ one may neglect these compared to ϕ_{body}. Thus the inner sheath thickness is of the order,

$$\frac{\Delta z}{\lambda_D} = -\sqrt{\frac{2\, e\phi_b}{KT_e}\left(\frac{n_\infty}{n_o}\right)} \quad . \quad 2\text{-}51$$

The criterion that the inner sheath be thin is satisfied if

$$\frac{\Delta z}{R} << 1 \quad 2\text{-}52$$

or

$$\frac{1}{(R/\lambda_D)}\sqrt{\frac{-2\ e\phi_b}{\frac{KT_e}{(n_o/n_\infty)}}} << 1 \qquad 2\text{-}52a$$

If we neglect the potential field effects in the outer sheath one may compute n_b as follows:

$$n_b = \frac{n_\infty}{2}(1 + \text{erf}\sqrt{\beta_\infty}\, u_o) \qquad 2\text{-}53$$

Therefore the criterion for thinness of the inner sheath is,

$$\frac{1}{(R/\lambda_D)}\sqrt{\frac{-4\ e\phi_b}{\frac{KT_e}{1 + \text{erf}\,(\sqrt{\beta_\infty}\, u_o)}}} << 1 \qquad 2\text{-}54$$

where

$$u_o = \vec{i} \cdot \vec{u}_\infty$$

The worst case occurs where $u_o = -u_\infty$ and here the criterion becomes:

$$\text{erfc}\,(\sqrt{\beta_\infty}\, u_\infty) >> \frac{-4\ e\phi_b}{\frac{KT_e}{(R/\lambda_D)^2}} \qquad 2\text{-}55$$

For example if $e\phi_b/KT_e = 10$ and $R/\lambda_D = 100$ then

$$\sqrt{\beta_\infty}\, u_\infty << 1.50$$

Thus one observes that in this case the two sheath separation can only be valid for subsonic flows. The exact criterion in each case depends strongly upon the body size and the surface potential.

Computation of the Complete Sheath

At this point the details of the analysis are essentially finished, however the means by which these results are combined to yield the complete sheath must yet be examined. Before we consider this task it might be well to discuss this process from a more basic viewpoint. First let us consider the basic relations for the potential field.

$$\nabla^2\phi' = e^{\phi'} - n_i/n_\infty \qquad 2\text{-}56$$

For large bodies the major contribution to this equation will be the term:

$$\frac{d^2\phi'}{dr^2} \simeq e^{\phi'} - n_i/n_\infty \qquad 2\text{-}57$$

if n_i/n_∞ is a weak function of θ. From this approximation we note that if n_i/n_∞ increases nonatomically from the body there can be only one inflection point in ϕ'. That is there are no isolated bumps in the potential field. In our case this means that there can be no maximum in the exterior potential field. For if these were to occur it would require that the interface potential would be at a higher potential then that in the exterior field. However, we know that the interface potential satisfies the condition that $e\phi_0/KT_e \ll 1$ and the body satisfies the condition $e\phi_b/KT_e \gg 1$. Thus there would be at least two inflection points in the potential field. Hence the interface potential must be less than or equal to the lowest possible potential in the exterior solution.

This requirement is that $\partial\phi/\partial z$ at the interface is always positive. Differentiating equation 2-38 by z and dropping the quadratic terms yields the criterion that,

$$\frac{e\phi_0}{KT_e} < \frac{n_i - n_\infty}{n_\infty} + \frac{\partial}{\partial z}\left(\frac{n_i - n_\infty}{n_\infty}\right) - \ldots \qquad 2\text{-}58$$

at any point on the interface. Neglecting the derivative terms we find that the worst case occurs when $n_\infty - n_i$ is a maximum which corresponds to the wake. For a spherical interface they may be replaced by the requirement that,

$$\frac{e\phi_o}{KT_e} < -\tfrac{1}{2}\,(1 + \operatorname{erf}\sqrt{\beta_\infty}\,u_\infty)\,. \qquad 2\text{-}59$$

Hence for our criterion $e\phi_o/KT_e \ll 1$ to be even approximately accurate the mach number must be small. One should not be unduly alarmed by the apparent difficulty even if the criterion is not completely satisfied in the wake. The reason for this is that the region where the exterior solution is in error will be small and does not have a large effect on the rest of the field. Thus one may choose any value for the interface potential consistent with the above criterion. Any criterion will lead to some small errors in the immediate vicinity of the interface, however, the main results will be valid throughout the field.

Using this information we shall outline the method of solution. For the simplest cases one chooses the shape for the interface initially. This can be done by taking the body shape and correcting it for the inner sheath by using the approximate formula 2-51 for the displacement distance.

$$\frac{\Delta z}{\lambda_D} \cong \sqrt{\frac{-4\,\dfrac{e\phi_b}{KT_e}}{\operatorname{erfc}\,(\sqrt{\beta_\infty}\,\vec{\lambda}_i \cdot \vec{u}_\infty)}} \qquad 2\text{-}60$$

Thus for a spherical body the interface would take the shape,

$$r_I = \lambda_D \sqrt{\frac{-4\,\dfrac{e\phi_b}{KT_e}}{1 + \operatorname{erf}\,(\sqrt{\beta_\infty}\,u_\infty \cos\theta)}} + a\,. \qquad 2\text{-}61$$

However in many cases it is easier to start with a simple interface shape and compute the body shape after exterior solution is complete.

In order to illustrate the method and to indicate the region in which the linear approximation breaks down the zeroth iteration has been completed for an interface which has a diameter of 40 debye lengths. The surface of the interface was kept at a potential $e\phi_o/KT_e = 0.3$. The mach number of the sphere was chosen to be 0.2. The free molecular distribution function for the sphere is given below.

$$f_{F.M.} = n_\infty \left(\frac{\beta_{\infty_i}}{\pi}\right)^{3/2} e^{-\beta_{o_i}\left[(u+u_\infty)^2 + v^2 + w^2\right]}$$

2-62

$$\text{for } \left|\frac{\bar{v} \times \bar{r}}{|v|}\right| > a \text{ and } \vec{v} \cdot \vec{r} > 0$$

$$= 0 \text{ for } \left|\frac{\vec{v} \times \vec{r}}{|v|}\right| \leq a \text{ or } \vec{v} \cdot \vec{r} < 0$$

where

v = particle velocity

r = radius vector from center of sphere to the point at which the distribution function is required

a = radius of sphere

This distribution function integrates to yield the free molecular density given below

$$\frac{\Delta n_{F.M.}}{n_o} = \frac{n_{F.M.} - n_\infty}{n_\infty} = -\tfrac{1}{2} + e^{-\beta_{\infty_i} u_\infty^2 \sin^2\theta} \cdot$$

2-63

$$\int_o^\infty \varsigma e^{-\varsigma^2} J_o(2i\sqrt{\beta_{\infty_i}} u_\infty \sin\theta\, \varsigma) \cdot \operatorname{erf}\left(\frac{\varsigma}{\tan\sigma_o} + \sqrt{\beta_{\infty_i}} u_\infty \cos\theta\right) d\varsigma$$

where $\theta = \cos^{-1}\left(\dfrac{\vec{r} \cdot \vec{u}_\infty}{|ru_\infty|}\right)$

$\sigma_o = \sin^{-1}(a/r)$

$J_o(ix)$ = Bessel function of imagining argument.

The final integral was computed numerically and used to compute the zeroth order potential field surrounding the sphere.

The exterior field around the spherical interface moving with M_∞ = 0.2 is plotted in figureII-1 as contour lines of the potential. The approximate inner sheath distance derived from equation 2-60 has been used to indicate the actual body shape which would produce this interface and exterior field. Here we have chosen the body surface potential $e\phi_b/KT_e = -5.0$. Notice that the case we have chosen violates the condition that the inner sheath is thin, however this was done purposely in order to show these regions clearly. In this case the inner sheath has a thickness of about $4\lambda_D$ and the external field has characteristic dimensions of the order of the body size. Thus the external field should approximate the actual external field of the given body quite well. The area very close to the interface which is indicated by the cross hatching will not accurately depict the real potential field, but this is only a small portion of the total field. The details of the inner solution have not been completed in this case.

From the graphical presentation of the solution given in figureII-1 the major features of the problem become clear. The exterior sheath is distorted as is expected due to the motion of the body. One also observes that the exterior sheath is very large due to the effects of the recombination of ions at the body surface. Secondly, the inner sheath represents a small portion of the entire sheath. Here we have used a case where this is marginal, however, in general the region covered by the external solution is proportional to the body size and the inner sheath is of constant thickness. Thus for a large body of the order of a meter in diameter the inner sheath would represent a very small portion of the field in most regions of the earth's atmosphere.

Conclusion

An approximate theory has been developed to compute the electrostatic sheath surrounding a large metallic body moving subsonically through a rarefied plasma. This theory is based upon the assumption that:

1. The body radius of curvature is very much larger than the debye length,
2. The surface potential satisfies the condition $e\phi_b/KT_e \gg 1$,
3. The mach number of the body, $\sqrt{\beta_\infty}u_\infty$, is very much less than 1.0.

Under these conditions it has been demonstrated that the sheath may be subdivided into inner and outer regions, where the outer region is treated by a linear perturbation theory, and the inner region by a one-dimensional nonlinear theory. This method is similar to the boundary layer theory in continuum dynamics. Our theory is approximate, but it does yield the qualitative features of the entire field surrounding a large body.

The main advantage of such a theory is not in its practical application, but in the general insight which can be obtained from it. The preliminary results which have been obtained so far indicate that many of the limitations present at this stage may be circumvented with further work. For example, the errors found in the transition region between the inner and outer solutions can be eliminated by introducing a more complex condition on the interface potential field. Secondly the interior solution may be improved by considering the effects of curvature in this region. Thus the methods and analysis presented in this review represent an intermediate stage in the development of a unified theory, not the final result.

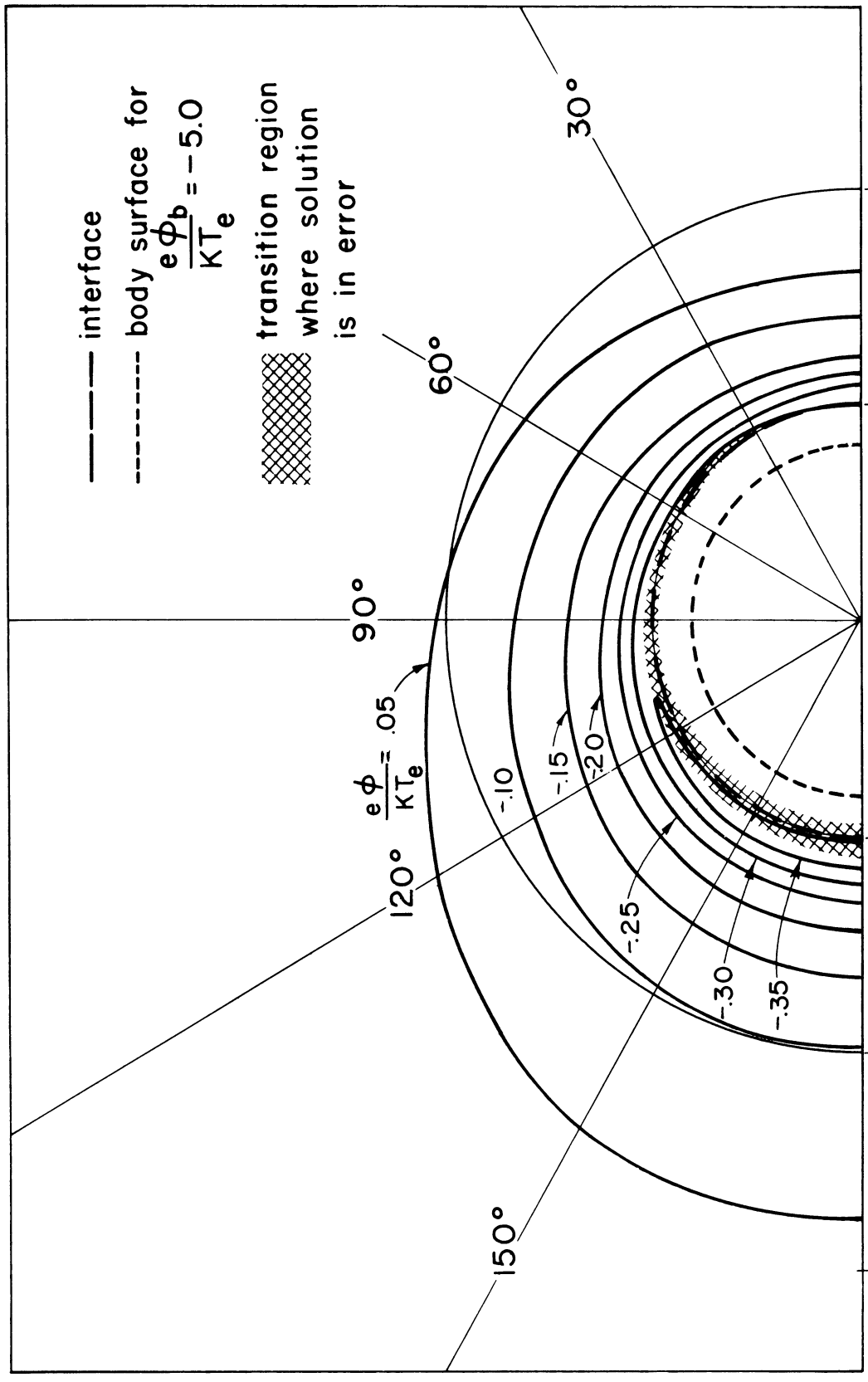

Fig. II-1 EXTERIOR POTENTIAL FIELD FOR A SPHERICAL INTERFACE OF RADIUS $r = 20\lambda_o$, $\frac{e\phi_I}{KT_e} = -.3, \sqrt{\beta}u_\infty = .2$

Symbols

a	Radius of sphere
$\bar{c}$	Most probable particle speed
$\frac{D}{Dt} = \frac{\partial}{\partial t} + \vec{v} \cdot \frac{\partial}{\partial \vec{x}}$	Substantial derivative
$\vec{E}$	Electric field
ε_o	Dielectric constant of vacuum
e	Electron charge
f	Distribution function
H	See equation 2-13
I_m	Integral in equation 2-25
K	Boltzmann constant
$L(\vec{X}, \vec{V}, t)$	Discontinuous function used in free molecular distribution function.
M_∞	$\sqrt{\beta}\, u_\infty$ mach number
M	Mass of particle
n	number density
N	$\frac{e\phi_o}{KT_e}$ nondimensional interface potential
P_n	Legendre polynomial
Q_n	Coefficient in Greens function expression
R	Radial eigen function and radius of curvature of body
T	Temperature
$\vec{u}_\infty$	Body velocity
$\vec{v}$	Particle velocity
$\vec{x}$	Position vector
z	Distance from interface
β	$1/c^2$
λ_D	Debye length
ϕ	Electrostatic potential
ψ	Greens function
Θ	Angular eigen function
μ	$\cos \theta$

Symbols (continued)

Super- and Subscripts

$( )'$	Nondimensional quantity
$( )^{(j)}$	j^{th} iterate
$( )_b$	Refers to body surface
$( )_e$	Refers to electrons
$( )_i$	Refers to ions
$( )_o$	Refers to interface
$( )_\infty$	Refers to condition far from body.

References

1. L. Kraus and K. M. Watson, Phys. Fluids 1, 480 (1959).

2. S. Rand, Phys. Fluids 2, 649 (1959).

3. S. Rand, Phys. Fluids 3, 265 (1960).

4. A. Ron and G. Kalman, Annals of Phys. 11, 240 (1960).

5. C. Lanczos, "Linear Differential Operators", Van Nostrand, London, 1961.

6. Appendix I of this report.

7. R. Jastrow and E. Pearse, J. Geophys. Research 62, 413 (1957).

APPENDIX III

ON THERMAL SKIN EFFECT

Contributed by

V. C. Liu and Y. S. Lim

I. Introduction

A heat transfer problem of unusual interest involves a physical process such that a highly transient temperature and extremely large thermal gradient are encountered within a thin layer at the surface of a heat-conducting body. This is often called skin heating problem. It occurs in the aerodynamic heating of the skin of a highly accelerated sounding rocket, the explosive heating of a gun barrel and the combustion chamber of a rocket engine.

This thermal skin problem, important as it is, has not always been treated in comply with sufficient physical reality. For instance, the heat flux input to the skin is often considered as proportional to the temperature difference between the hot gas and the skin; the proportionality constant used is the convective heat transfer coefficient. This can be justified only for the heat convection process at a reasonably steady rate. It is well known that the convective heat transfer coefficient, of aerodynamic origin, depends on the Reynolds number (Re) and the free stream velocity, both of which vary rapidly with time under the special heating conditions mentioned in the last paragraph.

The problem can be divided into two parts: (1) the study of the rate of convective heat transfer across the "boundary layer" formed

at the skin of the body, (2) calculation of the temperature distribution within the body in the immediate neighborhood of the exposed skin. The present note treats the second part only; however, the boundary condition related to the heat flux is made to accommodate a time-dependent function. This is a new feature which distinguishes the present analysis from the previous works.

To illustrate the physical phenomenon of the thermal skin effect we use a one-dimensional case with a simple time-dependent function for the aerodynamic heat transfer coefficient. It should be noted that the characteristic feature of the thermal skin effect is that the depth of penetration of the heat flux into the wall in a characteristic time of interest is often small in comparison with total thickness of the wall. This justifies the rise of the following simplifications in the idealized model to be used: Firstly, the wall may be considered as a semi-infinite solid bounded by a plane surface; Secondly, all thermal gradients other than the one normal to the wall can be considered as negligibly small.

II. Mathematical Formulation

The problem of determining the skin temperature of a one-dimension boundary solid with surface conducting linearly varying with time is described by the following equations:

$$\frac{\partial V}{\partial t} = k \frac{\partial^2 V}{\partial x^2} \tag{1}$$

$$V(x, o) = 0 \qquad V(\infty, t) = 0 \tag{2}$$

$$V(o, t) = \phi(t) \tag{3}$$

$$-K \frac{\partial V}{\partial x} = h(t) \left[V_g - \phi(t) \right] \quad \text{at } x = 0 \tag{4}$$

$$h(t) = Bt \qquad V_g(t) = At \tag{5}$$

where V = temperature of the solid body

k = diffusivity

K = thermal conductivity

$h(t)$ = convective heat transfer coefficient, a function of t

V_g = gas temperature of the free stream

For convenience, dimensionless quantities of the dependent and independent variables are used. In this particular problem, the conversion of dimensionless quantities is as follows:

$$V \longrightarrow u \qquad u = \frac{V}{A\, a^{2/3}}$$

$$\phi \longrightarrow \varphi \qquad \varphi = \frac{\phi}{A\, a^{2/3}}$$

$$t \longrightarrow \tau \qquad \tau = \frac{t}{a^{2/3}}$$

$$x \longrightarrow \ell \qquad \ell = \frac{x}{K/B\,a^{2/3}}$$

$$h(t) \longrightarrow g(t) \qquad g(t) = \frac{h(t)}{B\,a^{2/3}}$$

$$V_g \longrightarrow u_g \qquad u_g = \frac{V_g}{A\,a^{2/3}}$$

where $a = \dfrac{K}{B\sqrt{k}}$, it is checked that

$$a^{2/3} = \left(\frac{K}{B}\right)^{2/3} k^{-1/3} = \left[T^{-1}\right]$$

$$A\,a^{2/3} = \left[V\right]$$

$$\frac{K}{B\,a^{2/3}} = \left[\frac{K\,k}{B}\right]^{1/3} = \left[L\right]$$

since $k = \left[L^2\,T^{-1}\right]$

$$K = Q\,L^{-1}\,T^{-1}\,v^{-1}$$

$$h = Q\,L^{-2}\,T^{-1}\,v^{-1} \quad \text{or} \quad B = \left[Q\,L^{-2}\,T^{-2}\,v^{-1}\right]$$

Substituting the dimensionless quantities into the original equations we have the normalized equations:

$$\frac{\partial u}{\partial t} = \frac{\partial^2 u}{\partial \ell^2} \qquad (1a)$$

$$u(\ell, o) = 0, \quad u(\infty, \tau) = 0 \qquad (2a)$$

$$u(o, \tau) = \varphi(\tau) \qquad (3a)$$

$$-\frac{\partial u}{\partial \ell} = g(\tau)\left[u_g(\tau) - \varphi(\tau)\right] \qquad (4a)$$

$$g(\tau) = \tau, \quad u_g = \tau \qquad (5a)$$

III. Methods of Solving the Problems

The important point in this problem is that h is assumed to be a linear function of t, i.e., $h(t) = At$, which is usually assumed to be a constant in ordinary heat transfer problems.

The first step in solving this problem is to take the Laplace transform with respect to τ. A nonhomogeneous linear differential equation with variable coefficients is found for the dependent variable $\bar{\varphi}(s)$ (which is the Laplace transform of $\varphi(t)$). The solution of the differential equation is then expressed in a series form of asymptotic expansion.

Then by taking the inverse transform it gives the expression for the temperature at the boundary (skin temperature). From the temperature at the boundary, one can calculate the temperature inside the solid using the well known expression:

$$V(x,t) = \frac{x}{2\sqrt{\pi k}} \int_0^t \phi(\lambda) \frac{e^{-\frac{x^2}{4k(t-\lambda)}}}{(t-\lambda)^{3/2}} d\lambda \qquad (6)$$

or

$$V(x,t) = \frac{x}{2\sqrt{\pi k}} \int_0^t \phi(t-\lambda) \frac{e^{-\frac{x^2}{4k\lambda}}}{\lambda^{3/2}} d\lambda \qquad (7)$$

IV. Analysis

$$g(\tau) = \tau \,, \quad u_g = \tau \qquad \text{or} \qquad \left[h(t) = Bt \,, \; V_g(t) = At \right]$$

From (1a) the Laplace transform is

$$s\,\bar{u}(\ell, s) = \bar{u}_{\ell\ell} \qquad \text{(A bar - denotes the transform)} \tag{8}$$

the solution of which is

$$\bar{u}(\ell, s) = c_1 e^{-\ell\sqrt{s}} + c_2 e^{+\ell\sqrt{s}}$$

With the boundary condition (2a), it is found that

$$\bar{u}(\ell, s) = \bar{\varphi}(s)\, e^{-\ell\sqrt{s}} \tag{9}$$

Taking the Laplace transform for (4a):

$$L\left[-\frac{\partial u}{\partial \ell}\right] = L\left[\tau^2 - \tau\,\varphi(\tau)\right] = \frac{2}{s^3} + \frac{d\bar{\varphi}(s)}{ds}, \quad \ell = 0$$

but

$$L\left[-\frac{\partial u}{\partial \ell}\right]_{\ell=0} = -\frac{\partial}{\partial \ell}\left(L\left[u(\ell,\tau)\right]\right) = -\frac{\partial}{\partial \ell}\left[\bar{\varphi}(s)\, e^{-\ell\sqrt{s}}\right]_{\ell=0} =$$

$$= \sqrt{s}\;\bar{\varphi}(s) \tag{10}$$

since interchange of operations is permissible. Then a differential equation is obtained:

$$\sqrt{s}\;\bar{\varphi}(s) = \frac{2}{s^3} + \frac{d\bar{\varphi}}{ds}$$

or

$$\frac{d\bar{\varphi}}{ds} - \sqrt{s}\,\bar{\varphi} = \frac{-2}{s^3} \tag{11}$$

With the integrating factor $e^{-\frac{2}{3}s^{3/2}}$ we have

$$e^{-\frac{2}{3}s^{3/2}}\,\bar{\varphi}(s)\Big|_{s}^{\infty} = \int_s^{\infty} \frac{-2}{s^3}\, e^{-\frac{2}{3}s^{3/2}}\, ds$$

so that

$$\bar{\varphi}(s) = 2\, e^{\frac{2}{3}s^{3/2}} \int_s^{\infty} \frac{e^{-\frac{2}{3}s^{3/2}}}{s^3}\, ds \tag{12}$$

Now consider s as real variable and let $y = \frac{2}{3} s^{3/2}$

$$s = (\tfrac{3}{2})^{\frac{2}{3}} y^{2/3} , \qquad ds = (\tfrac{3}{2})^{-\frac{1}{3}} y^{-\frac{1}{3}} dy$$

$$\bar{\varphi} = 2 e^{y} \int_{y}^{\infty} \frac{e^{-y}}{(\frac{3}{2})^{2} y^{2}} (\tfrac{3}{2})^{-\frac{1}{3}} y^{-\frac{1}{3}} dy = \frac{8}{9} (\tfrac{2}{3})^{\frac{1}{3}} e^{y} \int_{y}^{\infty} \frac{e^{-y}}{y^{7/3}} dy$$

$$\bar{\varphi} = \frac{8}{9} (\tfrac{2}{3})^{1/3} e^{y} \int_{y}^{\infty} e^{-y} y^{-\frac{4}{3}-1} dy \qquad (13)$$

The integral is the incomplete Gamma function which can be expressed in terms of a confluent hypergeometric series $\Psi(a, c, y)$ (see pp. 226, Bateman, Vol. 1).

$$\bar{\varphi} = \frac{8}{9} (\tfrac{2}{3})^{\frac{1}{3}} e^{y} e^{-y} \Psi(\tfrac{7}{3}, \tfrac{7}{3}; y) = \frac{8}{9} (\tfrac{2}{3})^{\frac{1}{3}} \Psi(\tfrac{7}{3}, \tfrac{7}{3}; y) \qquad (14)$$

For large value of y and s, Ψ can be expanded into series form

$$\bar{\varphi} = \frac{8}{9} (\tfrac{2}{3})^{\frac{1}{3}} \left[\sum_{n=0}^{n} \frac{(-1)^{n} (\frac{7}{3})_{n} (\frac{7}{3} - \frac{7}{3} + 1)_{n}}{n!} y^{-\frac{7}{3}-n} + 0(|y|^{-\frac{7}{3}-n-1}) \right] \qquad (15)$$

$n = 0, 1, 2 \cdots$, $y \longrightarrow \infty$ [see pp. 278 Bateman, Vol. 1.]

Although this is a divergent series as $n \longrightarrow \infty$, it is actually an approximate solution for finite n and large value of y. This is the property of asymptotic expansion, so:

$$\bar{\varphi} = \frac{8}{9}\left(\frac{2}{3}\right)^{\frac{1}{3}}\left[\sum_{n=0}^{n}(-1)^n \frac{\Gamma(\frac{7}{3}+n)}{\Gamma(\frac{7}{3})}\frac{\Gamma(n+1)}{\Gamma(1)}\frac{1}{n!}\, y^{-\frac{7}{3}-n} + \cdots\right]$$

$$= \frac{8}{9}\left(\frac{2}{3}\right)^{\frac{1}{2}}\left[\sum_{n=0}^{n}(-1)^n \frac{\Gamma(\frac{7}{3}+n)}{\Gamma(\frac{7}{3})}\, y^{-\frac{7}{3}-n} + \cdots\right]$$

where $(1)_n = \dfrac{\Gamma(n+1)}{\Gamma(1)} = n!$.

$$\bar{\varphi}(s) = \frac{8}{9}\left(\frac{2}{3}\right)^{\frac{1}{3}}\left[\sum_{n=0}^{n}(-1)^n \frac{\Gamma(\frac{7}{3}+n)}{\Gamma(\frac{7}{3})}\left(\frac{2}{3}\right)^{-\frac{7}{3}-n} s^{-\frac{7}{2}-\frac{3n}{2}} + \cdots\right]$$

$$= 2\left[\sum_{n=0}^{n}(-1)^n \frac{\Gamma(\frac{7}{3}+n)}{\Gamma(\frac{7}{3})}\left(\frac{2}{3}\right)^{-n} s^{-\frac{7}{2}-\frac{3n}{2}} + \cdots\right]$$

$$= \left[\frac{2}{S^{7/2}} - \sum_{m=0}^{M_1}\frac{7.10.13.\ldots(6m+7)}{2^{2m}}\frac{1}{s^{3m+5}} + \sum_{m=1}^{M_2}\frac{7.10.13.\ldots(6m+4)}{2^{2m-1}}\frac{1}{s^{3m+7/2}} + \cdots\right] \quad (16)$$

This solution is exactly the same as obtained from integration by parts if we carry out the integration of equation (12).

Taking the inverse transform, we have,

$$\varphi(\tau) = \frac{2^4}{1.3.5\sqrt{\pi}}\tau^{5/2} - \sum_{m=0}^{M_1}\frac{7.10.13\ldots(6m+7)}{2^{2m}}\frac{\tau^{3m+4}}{(3m+4)!} + \sum_{m=1}^{M_2}\frac{7.10.13\ldots(6m+4)}{2^{2m-1}}\frac{2^{3m+3}\,\tau^{3m+\frac{5}{2}}}{1.3.5\ldots(6m+5)\sqrt{\pi}} + \cdots \quad (17)$$

In examining these two series in the above equation, we found that even for $M_1 \longrightarrow \infty$ and $M_2 \longrightarrow \infty$, these two series are convergent for finite value of τ. This can be shown as follows:

For the first series, we have:

$$\lim_{m\to\infty} \frac{u_{m+1}}{u_m} = \lim_{m\to\infty} \frac{(6m+10)(6m+13)}{2^2} \frac{\tau^3}{(3m+5)(3m+6)(3m+7)} = 0$$

for finite τ.

For the second series, we have:

$$\lim_{m\to\infty} \frac{u_{m+1}}{u_m} = \lim_{m\to\infty} \frac{(6m+7)(6m+10)\,2\cdot\tau^3}{(6m+7)(6m+9)(6m+11)} = 0 \text{ for finite } \tau.$$

Therefore, as long as τ is finite, the representation of an infinite convergent series for the solution is valid. Then equation (17) becomes:

$$\varphi(\tau) = \frac{2^4}{1.3.5\sqrt{\pi}}\tau^{5/2} - \sum_{m=0}^{\infty} \frac{7.10.13\ldots(6m+7)}{2^{2m}} \frac{\tau^{3m+4}}{(3m+4)!}$$

$$+ \sum_{m=1}^{\infty} \frac{7.10.13\ldots(6m+4)}{1.3.5\ldots(6m+5)} \frac{2^{m+4}}{\sqrt{\pi}} \tau^{3m+\frac{5}{2}} \qquad (18)$$

We have for the first few terms:

$$\varphi(\tau) = \frac{2^4}{1.3.5\sqrt{\pi}}\tau^{5/2} - \frac{7}{4!}\tau^4 + \frac{7.10.2^5}{1.3.5.7.9.11}\tau^{11/2}$$

$$- \frac{7.10.13}{2^2\,7!}\tau^7 + \frac{7.10.13.16\cdot 2^6}{1.3.5.7.9.11.13.15.17\sqrt{\pi}}\tau^{17/2}$$

$$- \frac{7.10.13.16.19}{2^4\,10!}\tau^{10} + \left(\frac{7.10.13.16.19.22\cdot 2^7}{1.3.5.7.9.11.13.15.17.19.21.23\sqrt{\pi}}\right)\cdot$$

$$\left(\tau^{\frac{23}{2}}\right) + \ldots.$$

$$\varphi(\tau) = 0.604\tau^{5/2} - 0.2915\tau^{4} + 0.1212\tau^{11/2} - 0.04513\tau^{7} + 0.0152\tau^{17/2} - 0.004765\tau^{10} + 0.001385\tau^{23/2} + \ldots.$$

For τ in the range 0 - 1.3, the function $\varphi(\tau)$ is tabulated below:

τ	$\varphi(\tau)$
0	0
0.1	0.00189
0.3	0.02720
0.5	0.00902
0.7	0.19020
1.0	0.39640
1.3	0.64970

This is plotted in Figure (III-1).

Iv. Conclusion and Discussion

An accurate knowledge of the temperature and the thermal gradient at the surface of a body under a sudden and extreme heating is very important in engineering design. These are pertinent informations in deciding whether a certain structural member so involved will crack or not under a thermal shock.

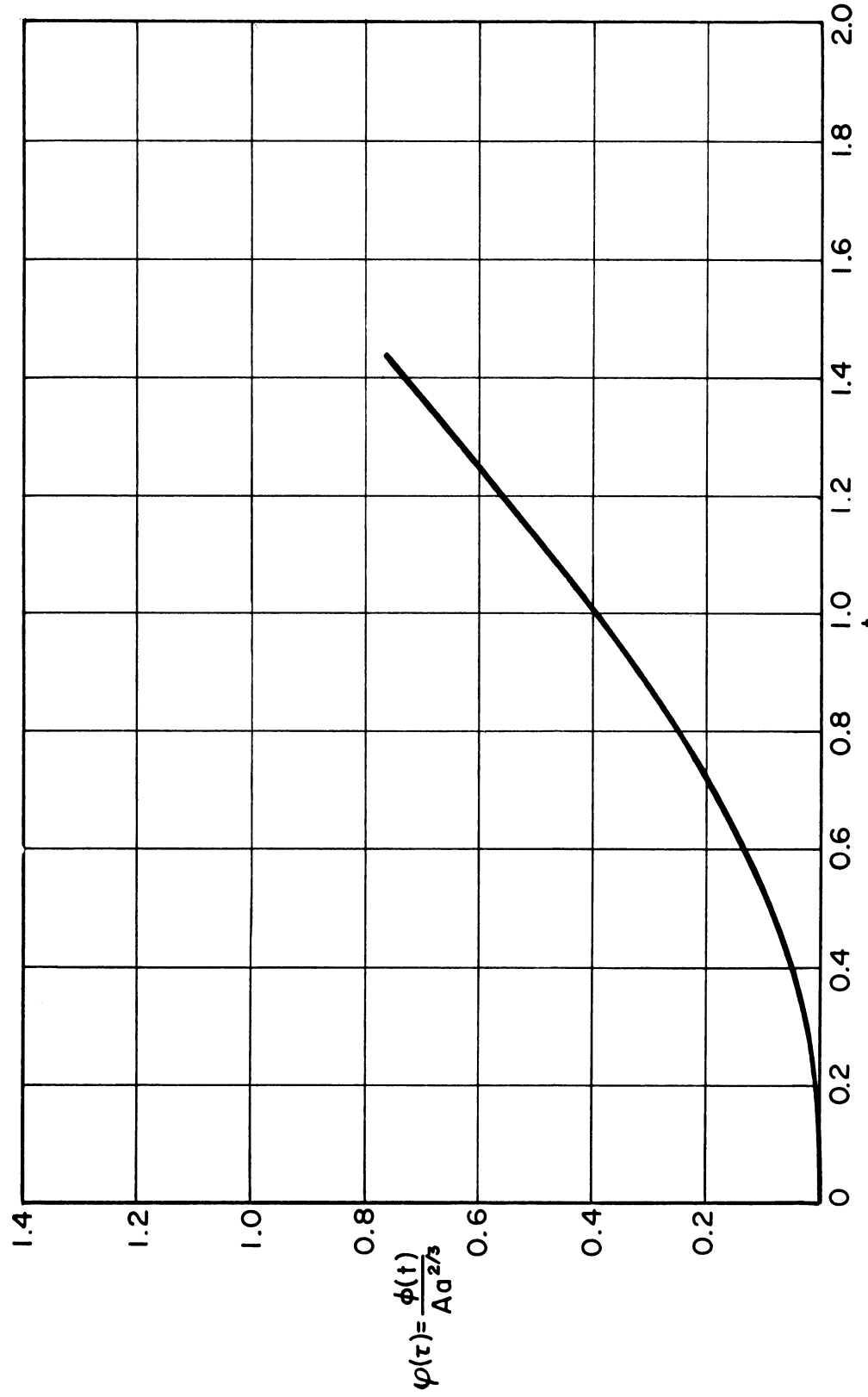
1.4
1.2
1.0
0.8
0.6
0.4
0.2
$\varphi(\tau)=\frac{\phi(t)}{Aa^{2/3}}$
0
0.2
0.4
0.6
0.8
1.0
1.2
1.4
1.6
1.8
2.0
$\tau=\frac{t}{a^{2/3}}$

Fig. III - 1

The thermal demands on the material of the inner surfaces of gun bores and combustion chambers, as well as the skin of a sounding rocket, are very severe. It is known that the lifetime of gun barrels depends on the surface temperature reached after a series of shots. The ablation of rocket skin during flight is also a known fact.

All of these points the need for a precise determination of the thermal skin phenomenon. In this note, we have improved the accuracy of conventional heat conduction analysis by a successful use of a time-dependent function for the convective heat transfer coefficient.

V. Reference

H. Bateman (Erdélyi, etc. ed.), "Higher Transcendental Functions," Volume I and II.

Appendix IV

ON THE AERODYNAMIC DRAG OF SPHERE

Contributed by

V. C. Liu

(written as a scientific report for this project, Oct. 1961)

ON THE AERODYNAMIC DRAG OF SPHERE

BY

V. C. LIU

SUMMARY

The purpose of this report is to review and interpret the present state of knowledge concerning sphere drag especially for the case with rarefied gas media. Supersonic sphere drag at low and intermediate Reynolds number has been of particular interest to the upper air measurements and space vehicle re-entry studies.

In the report recent experimental measurements and results that have contributed to the understanding of rarefied gas dynamic effect on sphere drag are briefly described and interpreted. Several contemporary theories fruitfully bearing on the issue are also discussed.

On the basis of the present study, suggestions to improve the falling sphere experiment of upper air measurement are made.

(I) INTRODUCTION

The characteristic Symmetry and Simplicity in geometry make the spherical body a favorite aerodynamic model for flow studies as well as for sounding probe in upper air measurements and ballistic range calibrations. In such experiments, the sphere drag is invariably chosen as a characteristic aerodynamic parameter. Recent developments in space research such as the determination of atmospheric density from satellite observation and the decay of satellite orbits as well as the accurate prediction of the impact point of vehicles that re-enter the atmosphere from orbital and space missions have added new significance to the problem of sphere drag.

Measurements of the sphere drag have been made by various means over a wide range of Reynolds numbers and Mach numbers in many countries. These results are not without significant disagreements; some of these disagreements of early results, especially in the measurements of sphere drags at high Reynolds numbers and low subsonic speeds, are attributed to the effect of free stream turbulence, among other factors (Goldstein 1938).

It appears that the first Systematic compilation of sphere drag data was made by Goldstein (1938). The sphere drag data up to that time were mostly for the flows at low subsonic speeds for which the compressibility effect is insignificant. Goldstein's collection covers a wide range of Reynolds number. His primary interest was to establish the critical Reynolds number relative to the free stream turbulence present in the measurements.

During the forties and earlier fifties, interests in ballistic problems brought forth extensive measurements on sphere drag with high speed wind tunnels and ballistic ranges. A comprehensive compilation of sphere drag data covering a wider range of Mach numbers than the earlier one was presented by May and Witt (1953) of the Naval Ordinance Laboratory. The main objective in this collection was to establish the Mach number effect on sphere drag and also to explore the rarefied gas dynamic effect (i. e. the low Reynolds number effect) with the fragmental and controversial data available then from the earlier low density wind tunnel measurements (Kane 1951, Sherman 1951 and Jensen 1951). In the early days of low density experiments incomplete knowledge of the flow structure in the test section with resulting uncertainties about the sphere wake, hence the base drag, made the measured sphere drags in the low density wind tunnels doubtful in value.

The use of falling sphere method to measure the upper atmospheric density (Liu 1950, Liu 1951, Bartman, Chaney, Jones and Liu 1956) has introduced a new wrinkle to the importance of sphere drag. In such experiment, accurate sphere drag coefficients at wide ranges of Reynolds numbers and Mach numbers are one of the prerequisites. On the other hand, precision-instrumented falling sphere experiments can also serve as a free flight calibration of the sphere drag provided the ambient density is known. The availability of such free flight drag of falling sphere in the upper atmosphere becomes an invaluable asset as independent check of the sphere drag obtained in laboratory tests. The agreement of these results (Liu 1959) removes some of the doubts about the accuracy of the sphere drag obtained in the laboratory tests.

It is obvious from the composite contour plot of sphere drag coefficient against Mach number and Reynolds number (see Figure 2) that the sphere drag corresponding to the intermediate Reynolds numbers ($1 \leq Re < 1000$) and supersonic speeds still remains essentially unknown.

Experimental difficulties in obtaining the sphere drag in a rarefied medium accounts for the lack of information in this transition flow regime. From the viewpoint of the falling sphere experiment, the sphere drag coefficient in question corresponds to the measurement of ambient density at the approximate altitude region of 100 km which happens to be an atmospheric layer of great geophysical interest. From the aerodynamic standpoint experimental information on sphere drag in the transition flow regime would be of utmost importance in the analytical studies of the transition flows - an important missing link in the science of fluid mechanics.

In the last few years extensive works have been done concerning supersonic sphere drag at the intermediate Reynolds numbers, particularly the recent measurements at the University of Toronto which appears to have supplied the experimental knowledge that links, in a limited sense, the known results of the free molecule flow theory and of the continuum flow. The present report on the status of sphere drag aims at clarifying the rarefied gas dynamic effect on the sphere drag and also recommending some points of vital interest to the falling sphere experiment on the basis of the recent studies.

(II) MEASUREMENTS OF SUPERSONIC SPHERE DRAG AT INTERMEDIATE REYNOLDS NUMBERS

Recent experiments of interest are described as follows:

(a) Institute of Aerophysics, University of Toronto (Sreekanth 1961 and Deleeuw 1961). The measurements were made in the UTIA Low Density Wind Tunnel which is the continuous, open circuit type with a vacuum pump drive designed to operate at Mach numbers up to 5, over a static pressure range from 1 to 70 micron Hg. In the

present experiment, an axially symmetric open jet nozzle designed to give a Mach number of 2 at a static pressure of about 20 micron Hg. was used in the sphere drag measurements. The force measurements were made by a remote control beam-type balance. The mean free path of the air in the test flow was 0.049 inches and the model sizes were such that Knudsen numbers in the range 0.1 to 0.8 based on the diameter of the sphere were covered.

The drag coefficient of the spheres as a function of Knudsen number is plotted in Figure 1. The important finding in the experimental results is that the free molecule flow and experiment will most likely agree at Knudsen number only slightly larger than unity.

(b) Jet Propulsion Laboratory, California Institute of Technology (Wegener and Ashkenas 1961). The experiments were performed in a low density supersonic wind tunnel with a uniquely designed displacement technique for force measurements. The tunnel was designed to have a continuous flow in a Mach number range of 3.8 - 4.3 for free stream static pressures of 30-100 micron Hg.

The drag coefficient of the spheres as a function of Knudsen number is shown in Figure 1.

(c) Rand (Masson, Morris and Bloxsom 1960). The tests were conducted in a hotshot-type wind tunnel in which high-enthalpy stagnation conditions were produced by the electrical discharge of a bank of capacitors through electrodes into a stagnation chamber containing gas. The stagnation chamber was separated from a conical nozzle by a frangible diaphragm which was burst by the high pressures generated in the stagnation chamber when the electrical charge was released. The flow process in the test section consisted of a starting shock with a series of trailing disturbances, followed by a period of steady flow.

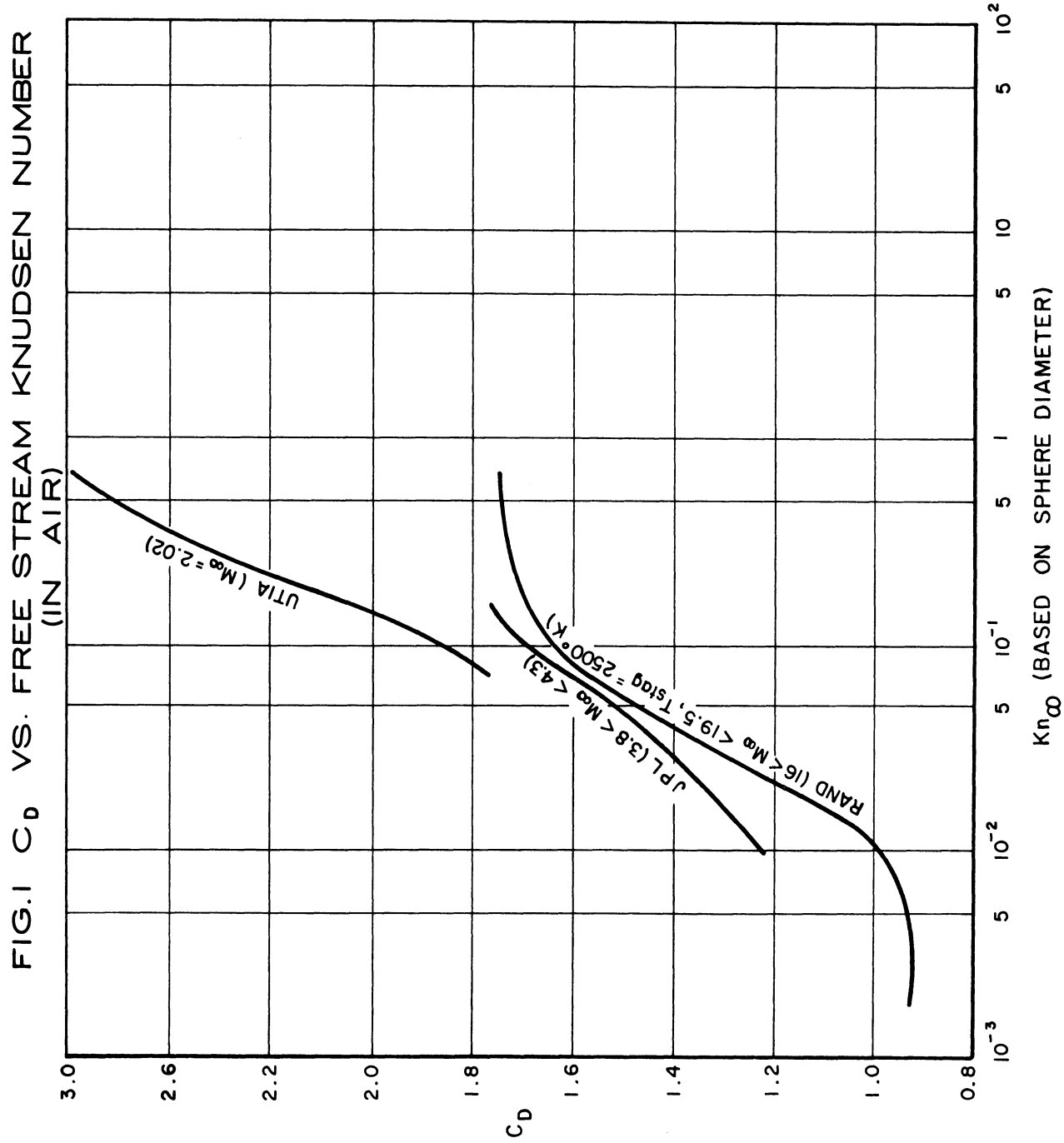
FIG. 1 C_D VS. FREE STREAM KNUDSEN NUMBER (IN AIR)
UTIA ($M_\infty = 2.02$)
JPL ($3.8 < M_\infty < 4.3$)
RAND ($16 < M_\infty < 19.5$, $T_{stag} = 2500°K$)
C_D
Kn_∞ (BASED ON SPHERE DIAMETER)
3.0
2.6
2.2
2.0
1.8
1.6
1.4
1.2
1.0
0.8
10^{-3}
5
10^{-2}
5
10^{-1}
5
1
5
10
5
10^{2}

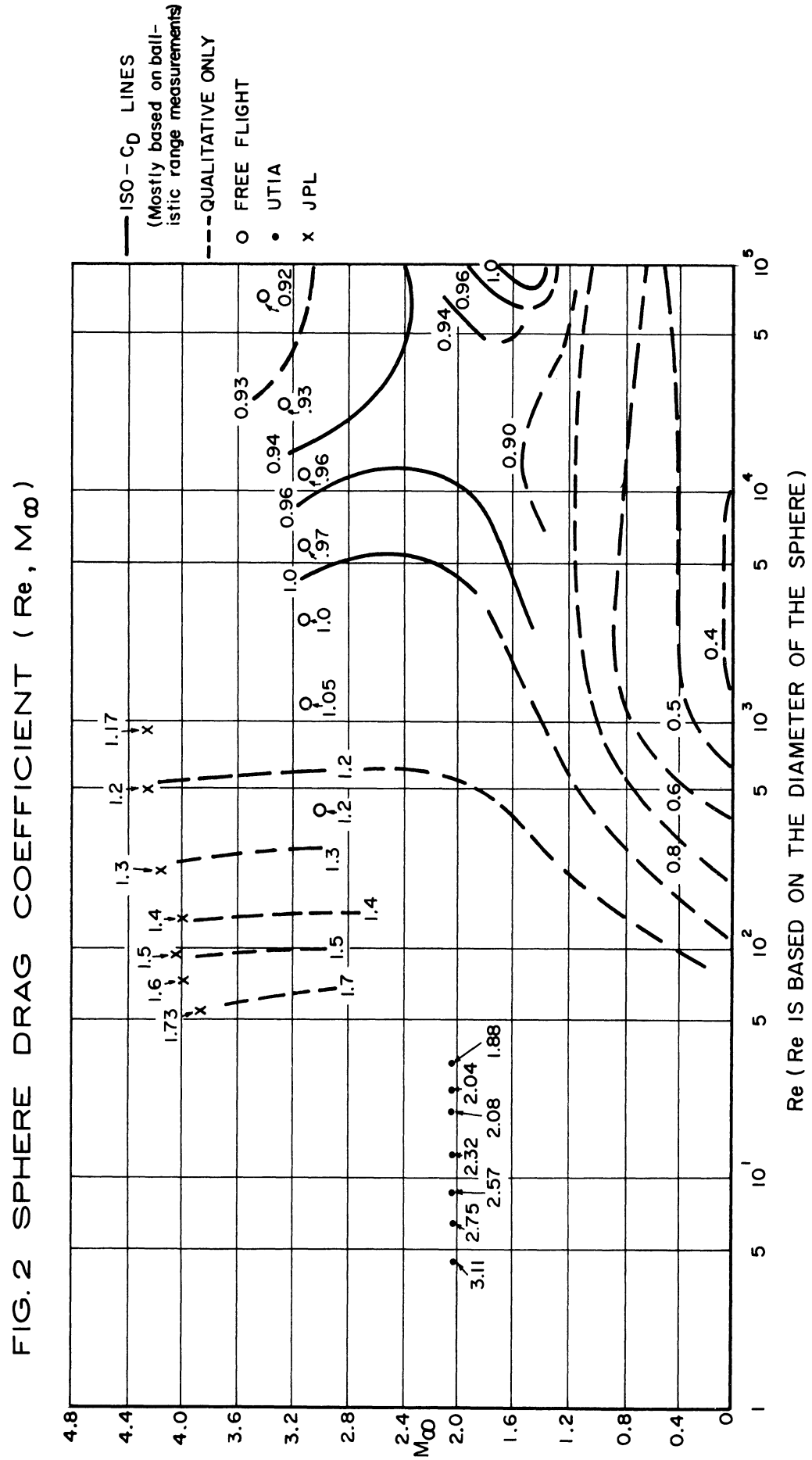

FIG. 2 SPHERE DRAG COEFFICIENT (Re , M_∞)

The starting shock was reflected from the end of the tank and returned upstream, and the steady-flow period was terminated when the effects of this reflected shock reached the test section. The time available for testing in the steady flow amounts about 2-5 microseconds.

The Mach numbers and Reynolds numbers in the test section cover the ranges 11-60 and 30-15,000 respectively. The interesting point of these measured results is that they cover practically the entire range of the transition flow regime; at the continuum end, the data check with the value ($C_D \approx 0.92$) predicted earlier by theory of sphere drag at extreme speeds (Liu 1957), and at the opposite end the theoretical free molecule value of $C_D \approx 2$ for spheres at hypersonic speeds also agrees with the measured results. The measured results in this experiment are preliminary in nature; much of the experimental uncertainties involved need to be re-examined and evaluated. The drag coefficient vs. free stream Knudsen number is also shown in Figure 1.

The above results of sphere drag have been plotted in Figure 2 as a function of Reynolds number and Mach number in constant drag coefficient curves. It is noted that on the basis of the recent measured sphere drag data the earlier contour C_D (Liu 1959) has been revised accordingly.

(III) THEORIES OF SPHERE DRAG

In spite of the geometric simplicity of a sphere the aerodynamic theory of sphere drag has met with only very limited successs. There is not a general theory of sphere drag that is uniformly valid over extensive ranges of Mach number and Reynolds number. Among the special theories there are the well-known Stokes theory and its extensions by Oseen (Schlichting 1955), Millikan (1923) and Epstein (1924) which is applicable to the case of extremely low speeds and low Reynolds number. With

a sphere in an ultra-low density flows for which the free molecule hypothesis is valid, the drag formula is known provided the momentum accommodation coefficient for the surface interaction between the gas particles and the solid wall is given. Qualified success in sphere drag theory has been developed for the case of extremely high speed flows at high Reynolds numbers.

The purpose of the following reviews of the contemporary theories on supersonic sphere drag is to establish the pertinent parameters that govern the mechanism of flow in question and to point out additional measurements needed to improve the accuracy of the falling sphere experiments.

(a) Free molecule theory of sphere drag. The characteristics of the free-molecule flows is that the gas medium is sufficiently rarefied so that the gaseous mean free path is everywhere much greater than the sphere diameter, so that collisions between the molecules and the solid boundary dominate over intermolecular collisions. The neglect of the intermolecular collision effects greatly simplifies the gas kinetic treatment of the sphere drag. The result of calculation for sphere drag assuming diffuse reflection is (Emmons 1958):

$$C_{D_{F.M.}} = \frac{\exp(-S_\infty^2/2)}{\pi^{\frac{1}{2}} S_\infty^3}(1+2S_\infty^2) + \frac{4S_\infty^4 + 4S_\infty^2 - 1}{2S_\infty^4}\,\mathrm{erf}\,S_\infty + \frac{2(\pi)^{\frac{1}{2}}}{3S_w}$$

if the oncoming molecules are re-emitted diffusely at a speed ratio S_w corresponding to some degree of accommodation to the wall conditions. Note that the speed ratio S_∞ denotes the ratio between the mass velocity and the most probable random velocity of the free stream.

(b) Drag of a sphere in an almost free-molecule flow. As the ratio of the gaseous mean free path to the sphere diameter decreases, the intermolecular collision effects that are neglected in the free-molecule flow analysis assume more and more importance in determining the

aerodynamic drag. In the case where such intermolecular collision effects are still small but not negligible compared with the gas-boundary collision effect, one may set up an almost-free-molecule hypothesis that the probability of a reflected molecule colliding twice with the incident molecules, before it is deflected away, is negligible compared with the probability of its colliding only once. The single collision effects are calculated on the basis of Maxwellian distribution for the molecular velocities. It is further assumed that molecules are reflected diffusely from the solid wall without preferred direction (Liu 1958, Liu 1959; Baker and Charwat 1958).

The application of the single collision theory to the calculation of sphere drag leads to:

$$C_D = C_{D_{F.M.}} - 0.15\,Re\left(\frac{T_\infty}{T_w}\right)^{\frac{1}{2}}$$

Where T_w is the wall temperature; T_∞ the free stream temperature, while $C_{D_{F.M.}}$ is the sphere drag coefficient based on free-molecule flow theory.

It is significant to note that the wall temperature of the sphere should be measured (Liu 1951b) in experimental investigation and falling sphere experiments in order to remove an uncertainity in sphere drag determination.

(c) Theory of sphere drag at extreme speeds considering real gas effects. The gas kinetic theory of sphere drag thus far discussed does not take into account the effect of complex molecular structure which, e.g., can lead to dissociation at high temperatures. In the case of a very fast moving sphere in a continuous medium, one may introduce a simplified shock model consisting of a nose shock following the exact contour of the frontal half of the sphere and with the rear half of the sphere exposed to a narrow vacuum half shell. The sphere pressure drag can be calculated

with the use of the oblique shock relations with an equivalent isentropic exponent γ_e to account for the chemical dissociation of the molecules behind the shock wave (Liu 1957):

$$C_D = \frac{2}{\gamma_e + 1} + \frac{4}{(\gamma_e + 1)M_\infty^2} + \frac{2}{\gamma_\infty M_\infty^2}$$

In the original derivation, Liu uses $\gamma_e = 1.15$ for air whereas Lampert (1961) recently suggests the use of $\gamma_e = 1.2$ based on more recent experimental results of dissociated gas mixtures at high temperatures.

(IV) DISCUSSIONS AND CONCLUSIONS

The task of presenting the sphere drag coefficient for the entire range of Mach number and Reynolds number is indeed challenging and would be rewarding considering the technical significance of the sphere drag problem. Aerodynamically it means a complete solution of a flow problem which so far has denied the best effort of the fluid dynamicists even for the simplest object. No claim is made in this report as to the fulfillment of this ambition; however, one sees clearly studies have been made recently to clear some of the obstacles to the eventual success such as the mild break through into the transition flow regime.

On the basis of the present study on sphere drag in a rarefied gas, we found that measurement of the wall temperature of the sphere drag is necessary in determining the sphere drag. This idea is worth noting both in the experimental investigation of sphere drag and in the falling sphere method of determining the upper atmospheric density.

SYMBOLS

C_D = Sphere drag force/ $\frac{1}{2} \rho_\infty V_\infty^2 (\pi d^2/4)$

$C_{D_{F.M.}}$ = C_D based on free-molecule flow theory

S_∞ = Free stream velocity V_∞/most probable molecular random speeds $\sqrt{2RT_\infty}$

S_w = $V_\infty / \sqrt{2RT_w}$

Re = Reynolds number $\frac{\rho V_\infty d}{\mu}$

M_∞ = Mach number $V_\infty / \sqrt{\gamma_\infty RT_\infty}$

T_∞ = Free stream temperature

T_w = Wall temperature

γ_e = Equivalent isentropic exponent

γ_∞ = Ratio of specific heat for the free stream

R = Gas constant

Kn = Knudsen number, gaseous mean free path/d

d = Sphere diameter

REFERENCES

Baker, R. M. L. Jr. & Charwat, A. F. (1958), "Transitional Correction To The Drag Of A Sphere In Free Molecule Flow." Phys. Fluids.

Bartman, F. L., Chaney, L. W., Jones, L. M., Liu, V. C. 1956, "Upper-Air Density And Temperature By The Falling-Sphere Method. J. App. Phys.

de Leeuw, J. H. (1961), "Communication On Sphere Drag Measurements." (Private correspondence.)

Emmons, H. W. (1958), "Fundamentals Of Gas Dynamics." Section H., vol. III., Princeton Series, High Speed Aerodynamics and Jet Propulsion.

Epstein, P. S. (1924), "On The Resistance Experienced By Spheres In Their Motion Through Gases." Phys. Rev.

Goldstein, S. (ed.) 1938, "Modern Development In Fluid Dynamics." vol. II., Oxford University Press.

Jensen, N. A. 1951, "Supplementary Data On Sphere Drag Tests," PTZ, University of California Inst. Eng. Res. HE-150-92.

Kane, E. D. 1951, "Sphere Drag Data At Supersonic Speeds And Low Reynolds Numbers." J. Aero. Sci.

Lampert, S. 1961, "Pressure Drag For A Sphere At Extreme Speeds." J. Aerospace Sci.

Liu, V. C. 1950, "Preliminary Investigation Of 'Sphere' Method Of Ambient Temperature Measurement." University of Michigan ERI, Atmospheric Phenomena at High Altitudes, Memo. No. 1 (unpublished).

Liu, V. C. 1951a, "On 'Sphere' Method Of Ambient Temperature Measurement In The Upper Atmosphere With Wind." University of Michigan, ERI, Atmospheric Phenomena at High Altitudes, Memo No. 3 (unpublished).

Liu, V. C. 1951b, "Estimation Of The Transient Skin Temperature Of A Falling Sphere." University of Michigan, ERI, Atmospheric Phenomena At High Altitudes, Memo No. 5 (unpublished).

Liu, V. C. 1957, "On The Drag Of A Sphere At Extremely High Speeds." J. App. Phys.

Liu, V. C. 1958, "On Pitot Pressure In An Almost-Free-Molecule Flow - A Physical Theory Of Flow Of The Rarefied Gases." J. Aero. Sci.

Liu, V. C. 1959, "On The Drag Of A Flat Plate At Zero Incidence In Almost-Free-Molecule Flow," J. Fluid Mech.

Liu, V. C. 1959, "Rarefied Gas Dynamical Considerations In The Rocket-Sounding Measurements." Aerodynamics Of The Upper Atmosphere, Rand Report R-339.

Masson, D. J., Morris, D. N., & Bloxsom, D. E. 1960, "Measurements Of Sphere Drag From Hypersonic Continuum To Free-Molecule Flow." Rand RM-2678.

Milikan, R. A. (1923), "Coefficients Of Slip In Gases And The Law Of Reflection Of Molecules From The Surface Of Solids And Liquids." Phys. Rev.

Schlichting, H. 1955, "Boundary Layer Theory." McGraw-Hill.

Sherman, F. S. 1951, "Notes On Sphere Drag Data." J. Aero. Sci.

Sreekanth, A. K. 1961, "Drag Measurements On Circular Cylinders And Spheres In The Transition Regime At A Mach Number Of 2." University of Toronto, UTIA Report No. 74.

Wegener, P. P. & Ashkenas, H. 1961, "Wind Tunnel Measurements Of Sphere Drag At Supersonic Speeds And Low Reynolds Numbers." J. Fluid Mech.

May, A. & Witt, W. R. 1953, "Free Flight Determinations Of The Drag Coefficients Of Spheres." J. Aero. Sci.

Appendix V

AN EMPIRICAL THEORY OF SPHERE DRAG IN TRANSITION FLOWS

Contributed by

V. C. Liu

Calibrations of sphere drag made in wind tunnels, ballistic ranges, etc., have been very helpful to the geophysical measurements using the device of a falling sphere. The aerodynamic drag coefficient (C_D) as a function of the free stream Mach number (M_∞) and Renolds number (Re_∞) has been the commonly accepted scheme of presentation except perhaps in cases of extremely high Mach numbers which are usually not of interest to the falling sphere experiments. This manner of presentation of C_D has the advantage of uniform validity over various Mach number and Reynolds number ranges, but is inconvenient for the users because of its three-dimensional plot and does not provide much physical insight into the nature of the sphere drag.

On the basis of the discussion in § 2 of this report, it is found that M_∞/Kn_∞ must be a significant parameter for the sphere drag in the transition flow regime. It is, of course, well known that $Re \sim M/Kn$. C_D as a function of Re_∞ or M_∞/Kn_∞ is shown in Figure (V-1). The data on C_D are from two independent sources of measurement (for references, see Appendix IV).

In the estimation of C_D at much lower Re_∞, one may use Figure (V-1) for extrapolation together with C_D for free molecule flows prescribed at given M_∞ and thermal condition at the surface of this sphere in question.

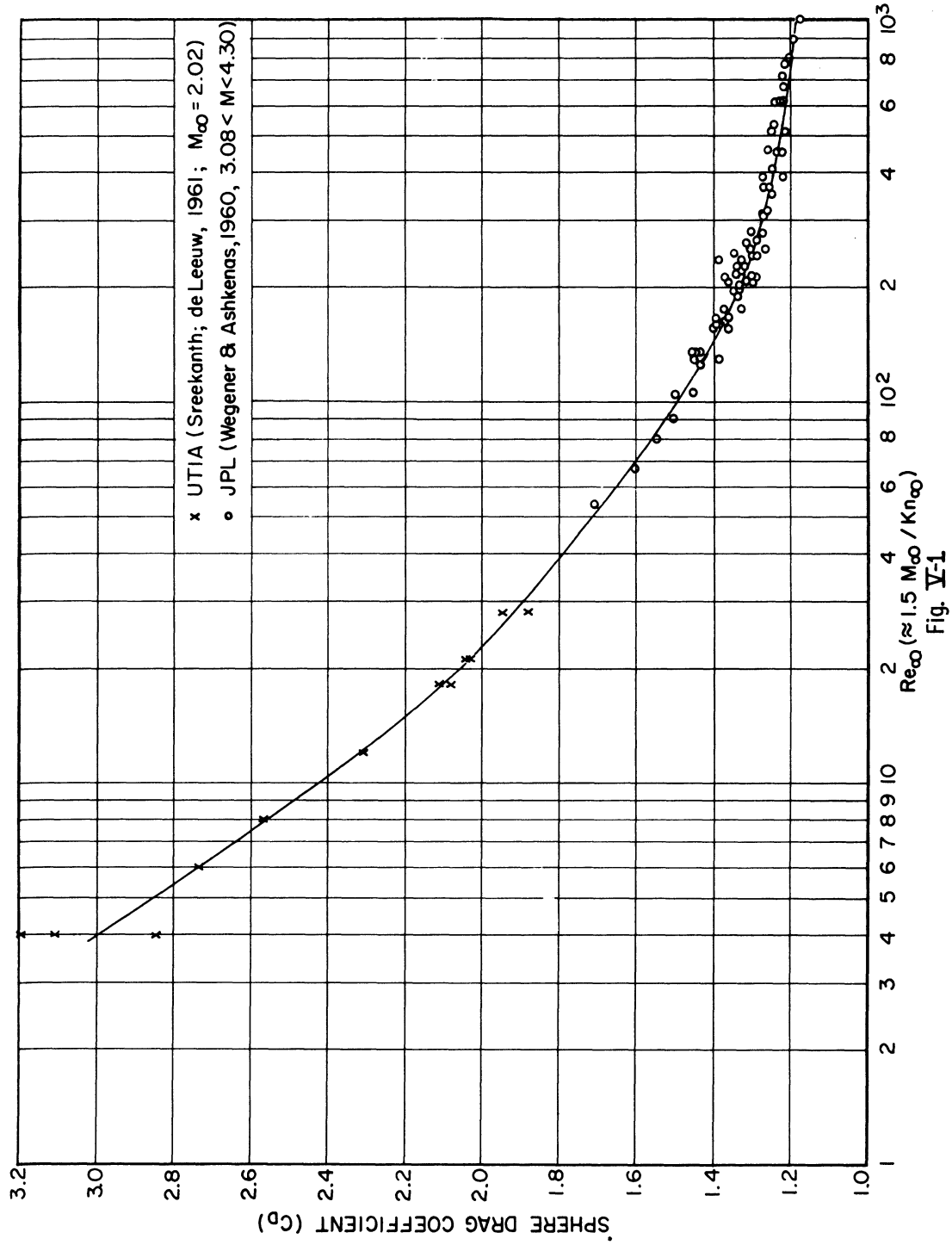
× UTIA (Sreekanth; de Leeuw, 1961; $M_\infty = 2.02$)
○ JPL (Wegener & Ashkenas, 1960, $3.08 < M < 4.30$)
SPHERE DRAG COEFFICIENT (C_D)
Re_∞ ($\approx 1.5\ M_\infty / Kn_\infty$)

Fig. V-1

APPENDIX VI

Propagation of Sound Waves in Rarfied Gases Under the Influence of an External Force Field

(Contributed by V. C. Liu and Paul B. Hays)

I. Introduction

The propagation of sound waves has always been a problem of unusual interest to gas dynamicists. In the simplest case, it represents a case of crowning success for the mathematical physics whereby the physical phenomenon is represented by an idealized model for which a simple elegant mathematical solution is obtained that checks remarkably well with measured results under the assumed conditions of the theory. This theoretical triumph, first achieved by Laplace in 1816, is much responsible for our physical insight into this intricate gas dynamical phenomenon.

Among the numerous applications of the theory of sound propagation in gases, one may mention the probing of the upper atmosphere by sound waves to measure the ambient temperature[1]*. Several questions naturally arise in connection with the propagation of sound waves in the rarefied atmosphere with or against gravity: (i) how will the amplitude, intensity and the phase velocities of the sound waves vary as it proceeds to the higher and higher altitude? (ii) what will happen to the sound waves when the mechanism of propagation of disturbance, namely the molecular collisions, is disrupted when an appreciable number of molecules in a rarefied gas cross a wave length without colliding?

The phenomena of absorption and dispersion are clear from the macroscopic viewpoint.[2] It is clear that at higher frequency or longer mean free path the thermal and velocity gradients between compression and rarefaction become so steep in the length scale of the mean free path that transport phenomena - heat conduction and viscosity - begin to cause absorption.

---

*Refer to references listed at the end of this note.

To answer the second inquiry, one must analyze the problem from the kinetic viewpoint. The kinetic theory of sound propagation in a rarefied monatomic gas without external force field has been given by Wang-Chang and Uhlenbeck.[3] The consideration of the influence of the external force field acting on the wave-carrier gas adds a new characteristic length parameter, namely the scale height H^*, to the problem. It is clear that when H is much larger than the mean free path (λ) of the gas and the wave length (Λ) of the wave, then the external force field, with or against which the waves propagate, does not give significant contribution to the "dispersion" of the waves. On the other hand, a new interesting physical phenomenon can be developed when all three parameters are of the same order.

In the following analysis of the dispersion of planar sound waves in a monatomic gas under the influence of an external force field, we choose a restricted case of isothermal gas in a potential force field (U).

2 Perturbation Analysis and the Linearized Boltzmann Equation

It is assumed that the wave-bearing medium is in thermodynamic equilibrium (f_e). The sound waves can be treated as small pressure disturbances from equilibrium, we are, therefore, justified in representing the molecular distribution function f ($\vec{x}$, $\vec{v}$, t) as a perturbed function of the following form:

$$f(\vec{x},\vec{v},t) = f_e(\vec{x},\vec{v})\left[1 + h(\vec{x},\vec{v},t)\right] \tag{1}$$

which satisfies the Boltzmann equation[4] for a monatomic gas of mass m in a force potential field U (x):

$$\frac{\partial f}{\partial t} + \vec{v}\cdot\frac{\partial f}{\partial \vec{x}} - \frac{1}{m}\frac{\partial U}{\partial \vec{x}}\cdot\frac{\partial f}{\partial \vec{v}} = \iiint d\vec{v}_1 \int\int d\varepsilon\, d\theta\, \sin\theta\, g\, I(g,\theta)(ff_1' - ff_1) \tag{2}$$

---

*$H\,(= kT/ma)$ may be defined as a distance in which the density of variable isothermal medium decreases to 1/e times its value at the initial station from which the distance is measured; "a" denotes the acceleration of the molecule of mass m.

In equation (1) the equilibrium distribution f_e is given by the Maxwell-Boltzmann law:

$$f_e = n_o \left(\frac{m}{2\pi RT}\right)^{3/2} e^{-\frac{m}{RT}[U + v^2/2]} \tag{3}$$

where n_o denotes the molecular density at $x = 0$; k, Boltzmann constant, T, temperature of the gas; v, molecular thermal speed.

In equation (2), the prime and the index 1 of the f's refer to the velocity variables alone, e.g., $f_1 = f(\vec{x}, \vec{v}, t)$, etc. I (g, θ) is the differential collision cross section corresponding to a turning of the relative velocity $g\ (= |v_1 - v|)$ over the angle θ into the solid angle $\sin\theta\, d\theta\, d\varepsilon$.

For molecules which interact like the Maxwellian model, i.e., when the force of interaction $= K r^{-5}$,

$$g I(g,\theta) = \frac{K}{RT} F(\theta) \tag{4}$$

Notice that by the assumption of perturbation, $h << 1$, we obtain the linearized Boltzmann equation (2), after the introduction of the dimensionless velocity: $\vec{c} = (m/2RT)^{1/2} \vec{v} \equiv \beta^{1/2} \vec{v}$

$$\sqrt{\beta}\frac{\partial h}{\partial t} + \vec{c}\cdot\frac{\partial h}{\partial \vec{x}} + \frac{\beta}{m}\frac{\partial U}{\partial \vec{x}}\cdot\frac{\partial h}{\partial \vec{c}} = n_o e^{-\frac{mU}{RT}} J(h) \tag{5}$$

where the collision integral:

$$J(h) = \pi^{-3/2} \iiint d\vec{c}_1 e^{-c_1^2} \iint d\varepsilon\, d\theta\, \sin\theta\, g\, I(g,\theta)(h' + h_1' - h - h_1) \tag{6}$$

The right hand side of equation (5) is conveniently expressed such that the collision integral J (h) preserves the mathematical form of that without the external force[3]; it was pointed out in reference (3)* that, for Maxwellian

*See also L. Waldmann[5]

model (4), the eigenfunctions ψ_{rl} of the collision operator J defined as:

$$J(\psi_{rl}) = \lambda_{rl}\,\psi_{rl} \tag{7}$$

where λ_{rl} is the eigenvalue, are the complete set of functions given by the product of Sonine polynomials with spherical harmonics[#] in the following normalized form:

$$\psi_{rl} = \sqrt{\frac{r!\,(l+1/2)}{\pi\,(l+\frac{1}{2}+r)!}}\; c^l\, P_l(\cos\phi)\, S^{(r)}_{l+1/2}(c^2) \tag{8}$$

Note that (8) forms a complete orthogonal set with weight function $\exp(-c^2)$ and the corresponding eigenvalues:

$$\lambda_{rl} = 2\pi\int_0^{\pi} d\theta\, \sin\theta\, F(\theta)\left[\cos^{2r+l}\frac{\theta}{2}\, P_l\left(\cos\frac{\theta}{2}\right) + \sin^{2r+l}\frac{\theta}{2}\, P_l\left(\cos\frac{\theta}{2}\right) - 1 - \delta_{r0}\,\delta_{l0}\right] \tag{9}$$

3 Propagation of plane sound waves along an external force field

Let the gravitational potential be: $U = gz + U_0$; the scale height: $H = (g\beta)^{-1}$. We have, from (5) and (6), the perturbed Boltzmann equation:

$$\sqrt{\beta}\,\frac{\partial h}{\partial t} + c_z\frac{\partial h}{\partial z} + \frac{1}{H}\frac{\partial h}{\partial c_z} = n_0 e^{-2z/H}\, J(h) \tag{10}$$

In the expansion for h we must introduce a more general expression than that in Ref. (3). Let

$$h = \sum\sum \alpha_{rl}(\vec{x}, t)\,\psi_{rl}(\vec{c}) \tag{11}$$

Equation (10), after the substitution of (11), multiplication by $\psi_{r'l'}\, e^{-c^2}$ and integration over $\vec{c}$, yields

$$\sqrt{\beta}\,\frac{\partial \alpha_{r'l'}}{\partial t} + \sum\sum\left(M_{rl,r'l'}\frac{\partial \alpha_{rl}}{\partial z} + \frac{N_{rl,r'l'}}{H}\,\alpha_{rl}\right) = n_0 e^{-2z/H}\,\alpha_{r'l'}\,\lambda_{r'l'} \tag{12}$$

where $M_{rl,r'l'} = \iiint d\vec{c}\, e^{-c^2} c_z\, \psi_{rl}\,\psi_{r'l'}$ and $N_{rl,r'l'} = \iiint d\vec{c}\, e^{-c^2}\frac{\partial \psi_{rl}}{\partial c_z}\,\psi_{r'l'}$

[#] Extensive use of these functions in the expansion for the normal solution to the Boltzmann equation was made much earlier by Burnett.(4)

The evaluation of equation (12), for the purpose of seeking the dispersion relation of the wave propagation, can be simplified by introducing the Fourier transform with respect to z and t, thus #

$$\omega_0\bar{\alpha}_{n'l'}(\sigma)-\sigma_0\left(1+\frac{2i}{H\sigma}\right)\left[(l'+1)\sqrt{\frac{l'+n'+3/2}{(2l'+1)(2l'+3)}}\,\bar{\alpha}_{n',l'+1}(\sigma)-l'\sqrt{\frac{n'+1}{(2l'+1)(2l'-1)}}\,\bar{\alpha}_{n'+1,l'-1}\right]$$

$$-\sigma_0\left(1+\frac{i}{H\sigma}\right)\left[l'\sqrt{\frac{l'+n'+1/2}{(2l'+1)(2l'-1)}}\,\bar{\alpha}_{n',l'-1}(\sigma)-(l'+1)\sqrt{\frac{n'}{(2l'+1)(2l'+3)}}\,\bar{\alpha}_{n'-1,l'+1}\right] \qquad (13)$$

$$=-i\lambda'_{n'l'}\,\bar{\alpha}_{n'l'}\left(\sigma+\frac{2i}{H}\right)$$

where $\bar{\alpha}_{n'l'}=\frac{1}{2\pi}\int dz\int dt\, e^{i(\sigma z-\omega t)}\alpha_{nl}(z,t)$,

$\omega_0=\omega/n_0\sqrt{2K/m}$, $\sigma_0=(\sigma/n_0)\sqrt{kT/K}$, $\sigma_0/\omega_0=(\sigma/\omega)/\sqrt{\beta}$, $\lambda'_{nl}=\lambda_{nl}\sqrt{kT/K}$.

4 Approximate solutions and the dispersion relation

First order approximation.

For the propagation of sound waves in the atmosphere, it is justifiable to assume $H\gg\sigma^{-1}$, hence we have the first order approximation to equation (13):

$$\left(\omega_0+i\lambda_{n'l'}\right)\bar{\alpha}_{nl}-\frac{2\lambda_{n'l'}}{H}\frac{\partial\bar{\alpha}_{n'l'}}{\partial\sigma}+\cdots\cdots \qquad (14)$$

Zeroth order approximation.

The neglect of the first order (derivative) terms of equation (14) results in a set of linear homogeneous algebraic equations which has a solution if determinant of its coefficients vanishes.

$$\left(\omega_0+i\lambda_{n'l'}\right)\alpha_{n'l'}-\sigma_0\left(1+\frac{2i}{H\sigma}\right)\left[(l'+1)\sqrt{\frac{l'+n'+3/2}{(2l'+1)(2l'+3)}}\,\alpha_{n',l'+1}-l'\sqrt{\frac{n'+1}{(2l'+1)(2l'+3)}}\,\alpha_{n'+1,l'-1}\right]$$

$$-\sigma_0\left(1+\frac{i}{H\sigma}\right)\left[l'\sqrt{\frac{l'+n'+1/2}{(2l'+1)(2l'-1)}}\,\alpha_{n',l'-1}-(l'+1)\sqrt{\frac{n'}{(2l'+1)(2l'+3)}}\,\alpha_{n'-1,l'+1}\right]=0 \qquad (15)$$

We may approach the solution of this infinite set in the same manner as in Ref. (3), i. e. in the order: $2r+l=0, 1, 2, \ldots\ldots$ Comparing with results in Ref. (3) our terms below the diagonal of determinant have a constant multiplier $(1+1/H\sigma)$; above, $(1+2i/H\sigma)$.

#Index o refers to the dimensionless quantity as defined below. σ is wave number.

We let these factors be Q_2 and Q_1 then the determinant has the form given below for the first eleven rows and columns.

We have expanded this using the same procedure of successive approximation as in Ref. (3). The result appears that for the first 8 rows and columns the determinant is exactly the same as in Ref. (3) except with σ_0 replaced by $\sqrt{Q_1 Q_2}\,\sigma_0$. We have not been able to prove that this is true in general, however it does appear that due to the special form of these equations that it appears so. Thus the "second approximation"[#] following that in Ref. (3) yields the dispersion relation:

$$\sigma_0 Q_1 Q_2 \cong \frac{6\omega_0^2}{5}\left[1-\frac{28}{15}\frac{i\omega_0}{A_2}-\frac{2^5\cdot 11}{3\cdot 5^2}\frac{\omega_0^2}{A_2}+\frac{2^5\cdot 37}{3\cdot 5^2}\frac{i\omega_0^3}{A_2^3}+\frac{2^7\cdot 56761}{3^3\cdot 5^4\cdot 7}\frac{\omega_0^4}{A_2^4}+\cdots\right] \quad (16)$$

Thus introducing the Q's and $H \gg \sigma^{-1}$, we have

$$\sigma\left(1+\frac{3i}{2H\sigma}\right) \cong \frac{\omega}{V_0}\left[1-\frac{7i\mu\omega}{3\rho V_0^2}-\frac{22}{3}\frac{\mu^2\omega^2}{\rho^2 V_0^4}+\frac{185}{6}\frac{i\mu^3\omega^3}{\rho^3 V_0^6}+\frac{56761}{126}\frac{\mu^4\omega^4}{\rho^4 V_0^8}\right] \quad (17)$$

Note that $V_0 = \sqrt{5kT/3m}$, we have[+]

$$\sigma_1 = \frac{\omega}{V} \cong \frac{\omega}{V_0}\left(1-2.99\frac{\mu^2\omega^2}{\rho^4 V_0^4}+56.7\frac{\mu^4\omega^4}{\rho^4 V_0^8}+\cdots\right) \quad (18)$$

and

$$\sigma_2 \cong \frac{\mu\omega^2}{\rho V_0^3}\left(1.17-11.93\frac{\mu^2\omega^2}{\rho^2 V_0^4}+\cdots\right)-\frac{3}{2H} \quad (19)$$

where for a sinusoidal input

$$\alpha_{rl}(z,t) = \alpha_{rl}(0,0)\, e^{i\left(\omega t-\frac{\omega}{V}z\right)} e^{\sigma_2 z}$$

For the case where gravitational force important

$$\alpha_{rl}(z,t) = \alpha_{rl}(z,t)\Big|_{\text{Ref (3)}}\, e^{-3z/2H}$$

α represents the amplitude of the received wave as a function of z and t.

[#] The second approximation here refers to the "Burnett" level of approximation in fluid mechanics; it should not be confused with the sucessive approximations discussed in (14) and (15).

[+] The complex wave number $\sigma = \sigma_1 - i\sigma_2$ where σ_1 is the dispersion coefficient, σ_2, the absorption coefficient.

5 Conclusions and discussions

Although the case of prime interest, namely when $H \sim \lambda \sim \Lambda$ has not been solved here, in fact the perturbation technique probably would not be effective for treating such problem, we have , however shown the qualitative trend for the general effect of an external force on the propagation of sound waves.

The damping action of the viscosity and heat conduction is more effective on the sound waves of shorter length. It increases with (λ/Λ) Under the condition $\lambda \sim \Lambda$, considerable number of molecules will move at thermal speed, which is of the same order as the sound speed, in one oscillation from the region of compression to that of rarfaction on account of the temperature and pressure differences. This equalization of temperature and pressure effectively checks the progress of the sound wave by dissipating its energy to thermal energy.

6 References

(1) Ratcliffe, J. A. (ed.) "Physics of the Upper Atmosphere", Acad., 1960.

(2) Lamb, H. "Hydrodynamics", Cambridge, 1932.

(3) Wang-Chang, C. S. and Uhlenbeck, G. E. "On the Propagation of Sound in Monatomic gases", Univ. of Mich. E. R. I. Project M999, Oct. 1952.

(4) Chapman, S. and Cowling, T. G. "Mathematical Theory of Nonuniform Gases", Cambridge, 1952.

(5) Waldmann, L. Transporterscheinungen von Mittleren Druck", Handbuch der Phys. vol. 12, Springer, 1958.

APPENDIX VII

ON THE ALMOST-FREE-MOLECULE FLOW THROUGH AN ORIFICE

(Contributed by V. C. Liu and G. R. Inger)

(Published in J. A. S., 1960)

On Almost-Free-Molecule Flow Through an Orifice†

V. C. Liu and G. R. Inger**
Professor and Graduate Student, Respectively,
Department of Aeronautical and Astronautical Engineering,
University of Michigan, Ann Arbor, Mich.
May 20, 1960

THE APPLICATION of the principle of almost-free-molecule flow, which is essentially a form of first-order Knudsen iteration of rarefied-gas dynamics, has shown some very encouraging results.[1, 2] The effusion of rarefied gases through an orifice into a vacuum is a very instructive problem for the purpose of studying the basic nature of rarefied-flow phenomena. The object of the present analysis is to provide a microscopic description of the flow parameters pertaining to the steady effusion from an orifice, the diameter (D) of which is of the same order or smaller than the mean free path (λ) of the reservoir gas. A thin diaphragm ($t/D << 1$) which has a small circular orifice separates a large high-pressure (p_1) reservoir from the low-pressure (p_2) region. The pressure ratio will be assumed large enough ($p_1/p_2 > 10^3$) to permit neglect of the back flow from the low-pressure side. This condition distinguishes the present problem from the pitot-pressure problem of reference 1.

Consider first the case of free-molecule effusion, where $\lambda >> D$ and molecules move through the orifice essentially independent of each other. The deviations of the resulting molecular distribution from its equilibrium state will be negligibly small and promptly wiped out by the intermolecular collisions, which always tend to set up and preserve the equilibrium state. The loss of molecules through the orifice, however, develops a trace of mass motion toward the orifice due to absence of those collisions that the lost molecules would have made with the ambient molecules on their return from the wall. This trace of orifice-bound mass motion grows in prominence as λ/D decreases. The principle of almost-free-molecule flow is applied here to calculate the molecular flux of the mass motion within the reservoir as a result of intermolecular collisions or their absence. The following physical model is devised for this purpose.

Imagine the orifice were closed with an imaginary disc of diameter D as the orifice; then equilibrium (Maxwellian) distribution of molecules in the reservoir would be restored through scattering of reflected molecules, from the imaginary disc, with the ambient molecules. It is postulated that the net molecular flux toward the orifice, inhibited by the scattering action of the imaginary reflected molecules, is equal to the difference between the true effusion flux through the orifice and its calculated value based on free-molecule hypothesis. It is assumed that this molecular flux, due to absence of scattering, amounts to only a small fraction of the corresponding free-molecule effusion flux. This implies that the present theory is valid only when D is not much larger than λ, so that the single-collision analysis used here is acceptable. The rate of collisions (N_{id}) between the molecular rays incident on, and reflected from the imaginary disc is calculated for rigid spheres on the basis of classical kinetic theory The cross section of the spheres is taken from the experimental

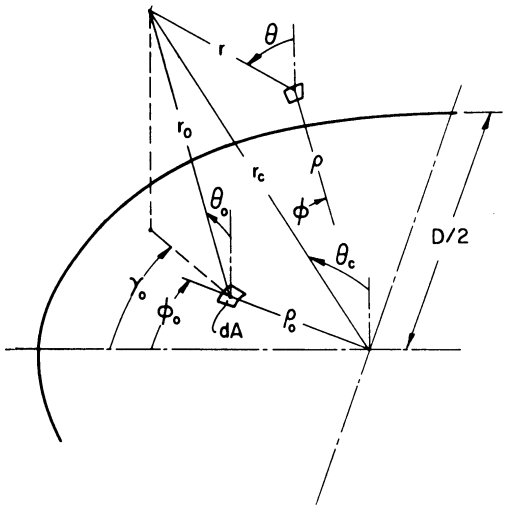

FIG. 1. Geometry of scattering analysis.

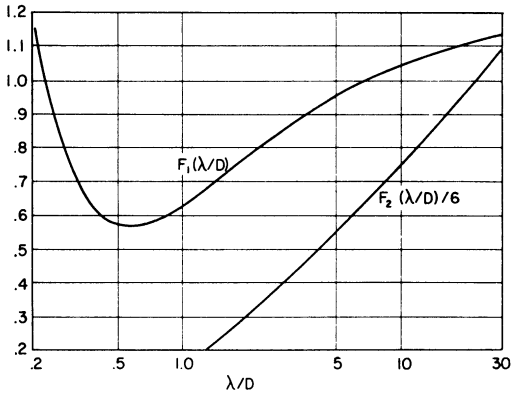

FIG. 2. Functions F_1 (λ/D) and $F_2(\lambda/D)$.

determination of the mean free path. It is assumed that every collision throws the incident molecule out of the impinging stream on the disc. This assumption can be justified only when λ is not very small compared to D. We assume that the molecules inside the "closed" reservoir are now in thermodynamic equilibrium with Maxwellian distribution. To determine the net contribution, through intermolecular collisions, of the hypothetical reflected molecules, we need to calculate the molecular flux (N_{dd}), originated from the diaphragm surrounding the orifice, that is thrown into the incident ray through their collisions with the reflected molecules from the disc. These molecules (N_{dd}) would otherwise not impinge on the orifice area. Thus, the net impingement inhibition for the imaginary reflection ray is equal to ($N_{id} - N_{dd}$).

Let N_d be reflected molecular flux from the disc, which is equal to $\pi D^2 nc/16$ where n = molecular density, c = mean thermal velocity; $E(E = 0.92/\lambda$ for air) the average collision expectancy per unit distance traveled by a single molecule moving through molecules under equilibrium (Maxwellian) distribution.[2]

† This investigation was part of a broad upper-air research program supported by the USAF Cambridge Research Center under contract No. AF19(604)-5477 with the University of Michigan.

** Now with Aerodynamic Research Group, Missile and Space Division, Douglas Aircraft Co., Santa Monica, Calif.

Reprinted from JOURNAL OF THE AEROSPACE SCIENCES

Referring to the coordinate system shown in Fig. 1, we obtain

$$\frac{N_{id}}{N_d} = \frac{E}{4\pi^2}\int_0^{2\pi} d\phi_0 \int_0^{2\pi} d\gamma_0 \int_0^{\pi/2} d\theta_0 \int_0^{D/2} d\rho_0 \int_0^{\infty} \frac{\rho_0 r_0 \sin\theta_0 \cos^2\theta_0 e^{-2r_0/\lambda}}{[r_0^2 + \rho_0^2 + 2r_0\rho_0 \sin\theta_0 \cos(\gamma_0 - \theta_0)]^{3/2}}\, dr_0 \tag{1}$$

Let ρ and ϕ be the polar coordinates of an area element of the diaphragm outside the orifice area; r the distance from the point r_0 to this elemental area; θ, the angle between r and the normal to this elemental area (see Fig. 1). We obtain

$$\frac{N_{dd}}{N_d} = \frac{E}{8\pi^3}\int_0^{2\pi} d\phi_0 \int_0^{2\pi} d\gamma_0 \int_0^{2\pi} d\phi \int_0^{\pi/2} d\theta_0 \int_{D/2}^{\infty} d\rho \int_0^{D/2} d\rho_0 \int_0^{\infty} \frac{\rho\rho_0 r_0^2 \sin\theta_0 \cos^3\theta_0 e^{-2r_0/\lambda}}{r_0^3 r^3}\, dr_0 \tag{2}$$

After the exponential functions in the integrands are approximated with appropriate parabolic representations (these approximations remain close when D is not much larger than λ), we obtain from Eqs. (1) and (2)

$$N_{id}/N_d \simeq 0.153\,(D/\lambda)\,F_1(\lambda/D) \tag{3}$$

$$N_{dd}/N_d \simeq 0.019\,(D/\lambda)\,F_2(\lambda/D) \tag{4}$$

where $F_1(\lambda/D)$ and $F_2(\lambda/D)$ are given in Fig. 2.

From the hypothesis that the intermolecular-collision effect on the effusion rate is equal to the molecular flux inhibited from hitting the orifice area when closed—namely $(N_{id} - N_{dd})$, we have

$$N/N_F = 1 + [(N_{id} - N_{dd})/N_F] \tag{5}$$

where N_F is the free-molecule effusion rate through the orifice (note that $N_d = N_F$ as a first approximation). A graph of N/N_F as a function of λ/D is shown in Fig. 3, in which are also shown the experimental results[3] which were taken with $p_1/p_2 > 10^3$. It is felt that with refined analysis—e.g., taking into account the contribution to the impinging flux from molecules, emerging from collisions (N_{id}), that are deflected toward the orifice area, the validity of the theory can be extended to lower values of λ/D. The present analysis appears fruitful in illustrating the functional dependency of the effusion-flow rate on the intermolecular collisions.

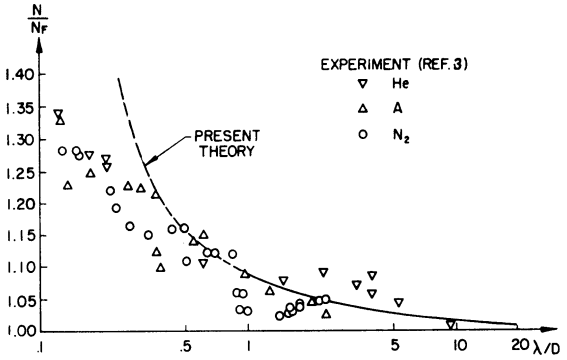

FIG. 3. Effusion rate vs. λ/D.

REFERENCES

[1] Liu, V. C., *On Pitot Pressure in an Almost-Free-Molecule Flow—A Physical Theory for Rarefied-Gas Flows*, Journal of the Aero/Space Sciences, Vol. 25, p. 779, December, 1958.

[2] Liu, V. C., *On the Drag of a Flat Plate at Zero Incidence in Almost-Free-Molecule Flow*, J. Fluid Mech., Vol. 5, p. 481, 1959.

[3] Liepmann, H. W., and Cole, J. D., *Problems in Gaseous Effusion*, Aerodynamics of the Upper Atmosphere, RAND Corporation (Santa Monica, Calif.), R-339, June, 1959.

APPENDIX VIII

ON LAMINAR FREE CONVECTION FLOWS IN CAVITY

(Contributed by V. C. Liu and H. Jew)

(Abstract published in Bull. Am. Phys. Soc. Series II, vol. 5, no. 2, 1960)

C8. On Laminar Free Convection Flows in Cavities.* V. C. LIU AND HOWARD JEW, *University of Michigan.*—A theory is developed for the velocity and temperature fields due to laminar free convection in two-dimensional cavities, closed at the bottom and opening into a reservoir of cool fluid at the top. The outstanding feature of the present problem concerns the effect of confinement and heat conduction at the walls on the laminar free convection flow of a fluid in an external force field. It thus involves the interaction of the velocity and the temperature field. In an earlier study by Lighthill,[1] some estimates of the useful heat transfer and flow parameters for special cases were obtained by approximate methods of solution (of the Karman-Pohlhausen type) to the boundary layer equations. The present paper gives a general solution of the flow by solving the boundary value problem with the Navier-Stokes equations and the equation of heat transfer. A numerical method is developed based on the use of orthogonal polynomials which reduces the solution of the governing equations to the numerical solution of two sets of coupled algebraic equations. The numerical analysis by iteration process is accomplished with an electronic digital computer. Streamlines and isothermals have been plotted for various values of Rayleigh number.

APPENDIX IX

AN EXACT ANALYSIS OF THE STAGNATION PHENOMENON OF LAMINAR FREE-CONVECTION FLOWS IN THERMOSYPHONS

(Contributed by V. C. Liu and H. Jew)

(To appear in Zeitz. fur Angew. Mech. und Math.)

An Exact Analysis of the Stagnation Phenomenon of Laminar Free-Convection Flows in Thermosyphons*)

By Vi-Cheng Liu**) and Howard Jew***)

Es wird eine Methode für die exakte Untersuchung der Geschwindigkeits- und Temperaturverteilung laminarer konvektionsfreier Strömungen in geschlossenen zweidimensionalen Hohlräumen dargestellt. Die Lösung der Gleichungen (der Gleichung von Navier-Stokes und der Gleichung für die Wärmeübertragung) erhält man durch eine Doppelreihen-Entwicklung der Strom- und der Temperaturfunktion nach orthogonalen Polynomen. Die resultierenden Gleichungen für die Entwicklungskoeffizienten werden in zwei gekoppelte Systeme algebraischer Gleichungen umgeformt, und diese werden dann mit einem Rechenautomaten numerisch gelöst. Die angegebene Methode ist z. B. besonders wirksam bei der Behandlung der Staupunkt-Erscheinungen in einem Thermosyphon, welche mit den bekannten Näherungsverfahren der Grenzschichttheorie nicht ausreichend genau behandelt werden können. Die Ergebnisse der Untersuchung werden durch Bilder veranschaulicht.

A method of exact analysis for the velocity and temperature distribution of the laminar free-convection flows in closed two-dimensional cavities is presented. The solution to the governing equations (the Navier-Stokes and the heat transfer) is obtained by the use of double series expansions of the stream and temperature functions into orthogonal polynomials. The resulting equations for the coefficients of expansions are reduced into two sets of coupled algebraic equations which are solved numerically with a computer. The present method is particularly effective in treating problems such as the stagnation phenomena in a thermosyphon which cannot be accurately treated with the existing approximate analysis of the boundary-layer theory. Illustrative result of the analysis are presented in the paper.

В работе излагается метод точного исследования распределения скорости и температуры ламинарных потоков в закрытых двухмерных постоях. Решение уравнений (Навье-Стокса и теплопроводности) находят путем разложения в ряд функций потока и температуры по ортогональным полиномам. Уравнение для коэффициентов разложения сводятся к двум связанным системам алгебраических уравнений, которые решаются численно на вычислительной машине. Изложенный метод применяется, например, при исследовании явления точки торможения в термосифоне, так как изсезтные приблиненные методы теории граничного слоя не дают удовлетворителнього результата.

Результаты исследования сопровождаются рисунками.

1 Introduction

Free-convection flows in open or closed cavities which are generated by the coupling between nonuniform heating and body force effects have been studied frequently of late [1—5], apparently because this particular type of flow constitutes a basic element in many technological applications: e. g., the Clusius thermal diffusion column for separating isotopes, the nuclear reactor, and the Schmidt-Holzwarth [5] thermosyphon cooling scheme for turbine blades. The complete analysis of this interesting flow problem which involves the treatment of the Navier-Stokes equations together with the heat-transfer equation is extremely complicated. Fortunately, much pertinent information concerning the flow can be obtained by an approximate analysis in which the governing equations are simplified by the introduction of the boundary-layer approximations [1]. This simplified analysis gives useful results within the limits of its validity. The boundary-layer approximations are not expected to be valid near the closed ends or the region having flow reversal.

With the geometry of the cavity having large value for the ratio of depth (see Figure 1) over width, a stagnation phenomenon involving flow reversal may develop near a closed end of the cavity. The purpose of the present paper is to study this stagnation phenomenon, which makes the thermosyphonic cooling ineffective, by determining the velocity and temperature distribution without the use of boundary-layer approximations.

---

*) This investigation was supported jointly by the U. S. Air Force Cambridge Research Center and a research grant from the Institute of Science and Technology of The University of Michigan. Generous Computation time allowance from the computer center of the University is gratefully acknowledged.

**) Professor of Aeronautical Engineering.

***) Assistant Research Engineer, Sponsored Research.

2 An Idealized Model

Consider a two-dimensional closed cavity, a cross section of which is shown in Fig. 1. With the prescribed wall-temperature distribution[1]) and the influence of the impressed body force, a layer of hot fluid at the walls, being less dense, is buoyant against the direction of the body force and is replaced by heavier cool fluid moving down the center of the cavity. Thus a circulation pattern, as shown, may develop, provided the depth-width (d/w) ratio is not large enough to cause stagnation, hence flow reversal.

3 The Flow Analysis as a Mathematical Boundary-Value Problem

In formulating the problem, we choose a body force field that contains the main characteristics of that due to the centrifugal acceleration ($\omega^2 \vec{r}$) generated by a rotating body with a constant speed (ω) but not of the CORIOLIS effect[2]). The gravitational force on the fluid, being small compared to the centrifugal force for a high rotating speed, is also neglected. With a moderate temperature difference $(T_0 - T_1)/T_0$, we may treat the fluid as incompressible with negligible viscous heat dissipation and consider its density variation due to nonuniform heating only. The fluid property is otherwise independent of the temperature [6]. Under these assumptions the governing equations for the two-dimensional laminar flows with prescribed body force become

$$u\frac{\partial u}{\partial x} + v\frac{\partial u}{\partial y} = -\frac{1}{\varrho}\frac{\partial p}{\partial x} - \beta\,\omega^2\,x\,(T - T_0) + \frac{\mu}{\varrho}\nabla^2 u \quad \ldots\ldots\ldots \quad (3.1),$$

$$u\frac{\partial v}{\partial x} + v\frac{\partial v}{\partial y} = -\frac{1}{\varrho}\frac{\partial p}{\partial y} - \beta\,\omega^2\,(y_0 + y)\,(T - T_0) + \frac{\mu}{\varrho}\nabla^2 v \quad \ldots\ldots\ldots \quad (3.2),$$

$$\frac{\partial u}{\partial x} + \frac{\partial v}{\partial y} = 0 \quad \ldots\ldots\ldots\ldots\ldots\ldots \quad (3.3),$$

$$u\frac{\partial T}{\partial x} + v\frac{\partial T}{\partial y} = \varkappa\nabla^2 T \quad \ldots\ldots\ldots\ldots\ldots\ldots \quad (3.4).$$

With the elimination of the pressure, p, and the introduction of the dimensionless variables we reduce the Eqs. (3.1)—(3.4) to

$$\Psi_{\xi\xi\xi\xi} + \frac{2}{\alpha^2}\Psi_{\xi\xi\eta\eta} + \frac{1}{\alpha^4}\Psi_{\eta\eta\eta\eta} = Ra\left\{\frac{\xi}{\alpha}\,\Theta_\eta - (\eta_0 + \alpha\,\eta)\,\Theta_\xi\right\} + \frac{1}{\alpha\,Pr}\{(\nabla^2\Psi)_\xi\,\Psi_\eta - (\nabla^2\Psi)_\eta\,\Psi_\xi\} \quad (3.5),$$

$$\Theta_{\xi\xi} + \frac{1}{\alpha^2}\,\Theta_{\eta\eta} = \frac{1}{\alpha}\{\Psi_\eta\,\Theta_\xi - \Psi_\xi\,\Theta_\eta\} \quad \ldots\ldots\ldots\ldots\ldots\ldots \quad (3.6).$$

The associated boundary conditions for the flow field in the region $\xi \geqq 0$ are as follows:

$$\left.\begin{array}{llll}
\Theta(0,0) = 0; & & & \\
\Theta(\xi,1) = 1; & \Theta(\xi,0) = \sin^2\pi\xi & \text{for } 0 \leqq \xi \leqq 1/2; & \\
\Theta(1/2,\eta) = 1; & \Theta_\xi(0,\eta) = 0 & \text{for } 0 \leqq \eta \leqq 1; & \\
\Psi(\xi,0) = 0; & \Psi_\xi(\xi,0) = 0; & \Psi_\eta(\xi,0) = 0; & \\
\Psi(\xi,1) = 0; & \Psi_\xi(\xi,1) = 0; & \Psi_\eta(\xi,1) = 0 \quad \text{for } 0 \leqq \xi \leqq 1/2; & \\
\Psi(0,\eta) = 0; & \Psi_{\xi\xi}(0,\eta) = 0; & \Psi(1/2,\eta) = 0; & \\
\Psi_\xi(1/2,\eta) = 0; & \Psi_\eta(1/2,\eta) = 0 & \text{for } 0 \leqq \eta \leqq 1 &
\end{array}\right\} \quad \ldots \quad (3.7).$$

4 Solution of the Boundary-Value Problem

The appropriate use of orthogonal polynomials for the eigenfunctions in the expansion of the two dependent variables Θ and Ψ, plus suitable integral transforms, may reduce the governing equations to algebraic equations of the expansion coefficients. A similar expansion has been used earlier by POOTS in a simpler free-convection-flow problem [4].

---

[1]) In the open cavity as SCHMIDT-HOLZWARTHS, the side AB is replaced by a free surface of the coolant reservoir. The replacement of the free boundary by a closed surface with prescribed temperature distribution makes the mathematical problem tractable, and yet preserves the main feature of the phenomenon in question.

[2]) CORIOLIS force on the fluid tends to distort the circulation pattern slightly [5].

Let

$$\Theta(\xi,\eta)=\sum_{p=1}^{\infty}\sum_{q=1}^{\infty}A_{p,q}\cos(2p-1)\pi\xi\sin q\pi\eta+\sin^2\pi\xi+(1-\sin^2\pi\xi)\sin\frac{\pi}{2}\eta \quad (4.1),$$

$$\Psi(\xi,\eta)=\sum_{p=1}^{\infty}\sum_{q=1}^{\infty}B_{p,q}X_p(\xi)Y_q(\eta) \quad (4.2),$$

where

$$X_q(\xi)=\frac{\sinh\lambda_p\xi}{\sinh\frac{1}{2}\lambda p}-\frac{\sin\lambda_p\xi}{\sin\frac{1}{2}\lambda_p} \quad (4.3),$$

$$Y_q(\eta)=\cosh\mu_q\eta-\cos\mu_q\eta-\gamma_q(\sinh\mu_q\eta-\sin\mu_q\eta) \quad (4.4).$$

The orthogonal expansions (4.1) and (4.2) satisfy the boundary conditions (3.7) provided the following STURM-LIOUVILLE systems (4.5a) and (4.5b) are satisfied.

$$\left.\begin{aligned}&X_p''''(\xi)=\lambda_p^4X_p(\xi),\\&X_p\left(-\frac{1}{2}\right)=X_p\left(\frac{1}{2}\right)=X_p'\left(-\frac{1}{2}\right)=X_p'\left(\frac{1}{2}\right)=0\end{aligned}\right\} \quad (4.5a),$$

where λ_p satisfies the transcendental expression

$$\coth\frac{1}{2}\lambda_p-\cot\frac{1}{2}\lambda_p=0.$$

$$\left.\begin{aligned}&Y_p''''(\eta)=\mu_q^4Y_q(\eta),\\&Y_q(0)=Y_q(1)=Y_p'(0)=Y_p'(1)=0\end{aligned}\right\} \quad (4.5b),$$

where μ_q satisfies the transcendental expression

$$\cosh\mu_q\cos\mu_q-1=0,$$

$$\gamma_q=(\cosh\mu_q-\cos\mu_q)/(\sinh\mu_q-\sin\mu_q).$$

Note that the functions $X_p(\xi)$, $Y_q(\eta)$, $\cos(2p-1)\pi\xi$ and $\sin q\pi\eta$ form, respectively, orthogonal sets; so it is possible to transform the governing equations into an associated system of algebraic equations after multiplying Eq. (3.5) by $X_m(\xi)\,Y_n(\eta)$, and Eq. (3.6) by $\cos(2m-1)\pi\xi\sin n\pi\eta$ and integrate over the region $0\leqq\xi\leqq1/2$, $0\leqq\eta\leqq1$. Eqs. (4.6) and (4.7) form the infinite set of algebraic equations.

$$\left\{\frac{1}{2}\lambda_m^4+\frac{2}{\alpha^2}D(\lambda_m,\lambda_m)D(\mu_n,\mu_n)+\frac{1}{2\alpha^4}\mu_n^4\right\}B_{m,n}=-\frac{2}{\alpha^2}\sum_{p=1}^{\prime}\sum_{q=1}^{\prime}D(\lambda_p,\lambda_m)D(\mu_q,\mu_n)B_{p,q}$$

$$+\pi Ra\left\{\frac{1}{2\alpha}[F(\lambda_m)-Q(\lambda_m)]E\left(\frac{1}{2};\mu_n\right)-A(2;\lambda_m)\left[\eta_0\left\{C(\mu_n)-A\left(\frac{1}{2};\mu_n\right)\right\}+\alpha\left\{F(\mu_n)-I\left(\frac{1}{2};\mu_n\right)\right\}\right]\right.$$

$$\left.+\sum_{p=1}\sum_{q=1}A_{p,q}\left[\frac{q}{\alpha}V(2p-1;\lambda_m)E(q;\mu_n)+(2p-1)A(2p-1;\lambda_m)\{\eta_0A(q;\mu_n)+\alpha I(q;\mu_n)\}\right]\right\}$$

$$+\frac{1}{\alpha Pr}\left\{\sum_{p=1}\sum_{q=1}B_{p,q}\left[\sum_{r=1}\sum_{s=1}B_{r,s}\left\{\frac{1}{\alpha}K(\lambda_p,\lambda_r,\lambda_m)L(\mu_s,\mu_q,\mu_n)+\frac{1}{\alpha^3}L(\lambda_p,\lambda_r,\lambda_m)H(\mu_q,\mu_s,\mu_n)\right.\right.\right.$$

$$\left.\left.\left.-\frac{1}{\alpha}H(\lambda_p,\lambda_r,\lambda_m)L(\mu_q,\mu_s,\mu_n)-\frac{1}{\alpha^3}L(\lambda_r,\lambda_p,\lambda_m)K(\mu_q,\mu_s,\mu_n)\right\}\right]\right\} \quad (4.6),$$

$$-\frac{\pi^2}{4}\left\{(2m-1)^2+\left(\frac{n}{\alpha}\right)^2\right\}A_{m,n}=\frac{2}{\pi^2}\frac{(2m-1)(-)^m}{(2m-3)(2m+1)}\left\{\frac{1}{n}\left[(-)^n-1\right]+\frac{4n(-)^{n+1}}{(2n-1)(2n+1)}\right\}$$

$$+\frac{2\pi}{\alpha}\left\{\sum_{r=1}\sum_{s=1}B_{r,s}\left\{R(2m-1,2;\lambda_r)\left[B(n;\mu_s)-S\left(\frac{1}{2},n;\mu_s\right)\right]\right.\right.$$

$$\left.-\frac{1}{2}\left[W(2m-1;\lambda_r)-P(2m-1;\lambda_r)\right]R\left(\frac{1}{2},n;\mu_s\right)\right\}$$

$$-\sum_{p=1}\sum_{q=1}A_{p,q}\left[\sum_{r=1}\sum_{s=1}B_{r,s}\{(2p-1)R(2m-1,2p-1;\lambda_r)S(q,n;\mu_s)\right.$$

$$\left.\left.+qG(2m-1,2p-1;\lambda_r)R(q,n;\mu_s)\right\}\right]\Bigg\} \quad \ldots\ldots\ldots\ldots\ldots\ldots\ldots\ldots \quad (4.7).$$

In the integral formulas in the list of symbols, those with λ_p' s refer to $X_p(\xi)$ in the integrand and have limits $\xi = 0$ to $\xi = \frac{1}{2}$. The corresponding formulas with μ_q' s refer to $Y_q(\eta)$ in the integrand and have limits $\eta = 0$ to $\eta = 1$. In the algebraic Eqs. (4.6) and (4.7) relating the coefficients $A_{m,n}$ and $B_{m,n}$, we have, for example, quantities like $R(m, p; \lambda_r)$ and $R(q, n; \mu_s)$ which we define to mean

$$\int_0^{1/2} X_r(\xi)\cos m\pi\xi \sin p\pi\xi\, d\xi \text{ and } \int_0^1 Y_s(\eta)\cos q\pi\eta \sin n\pi\eta\, d\eta,$$

respectively. As the integrands have the same form, we give only $R(m, p; \lambda_r)$ in the list of symbols.

Numerical Iteration of Eqs. (4.6) and (4.7)

The definite integrals appearing in equations (4.6) and (4.7) were computed from thec losed forms for these integrals. The interative IBM 704 computing machine instruction procedure was as follows: Read into memory the integral constants and a set of Ra, Pr, α and η_0 values. From these, compute an initial set of $B_{m,n}$ coefficients using the Eq. (4.6) with terms involving $A_{p,q}$ and $B_{p,q}\,B_{r,s}$ neglected. Using the initial set of $B_{m,n}$ thus obtained, compute an initial set of $A_{m,n}$ coefficients, using Eq. (4.7) with terms involving $A_{p,q}\,B_{r,s}$ neglected. Proceeding from the initial $A_{m,n}$ and $B_{m,n}$ values, compte a second set of $B_{m,n}$ coefficients using the full Eq. (4.6) and the initial $A_{m,n}$ and $B_{m,n}$ values, followed by a second set of $A_{m,n}$ coefficients computed using the full Eq. (4.7) and the initial $A_{m,n}$ and $B_{m,n}$ values. Proceeding from the second set of $A_{m,n}$ and $B_{m,n}$ coefficients, compute a third set of coefficients $A_{m,n}$ and $B_{m,n}$ similarly, and so on, until steady values are obtained.

Results

Fig. 2 shows streamlines and isothermals in the cavity. Fig. 3 shows transverse (across cavity in the ξ-direction) velocity profiles for $\xi = 0.1$, 0.2, and 0.4. Fig. 4 shows axial velocity profiles for $\eta = 0.35$ and 0.36. In Table 1 are shown $A_{p,q}$ and $B_{p,q}$ coefficients. It should be mentioned that NUSSELT numbers (which measure heat transfer) can easily be computed once the $A_{p,q}$ coefficients are known.

Table 1

$A_{p,q}$ and $B_{p,q}$ Coefficients for the Case
$Ra = 10^3$, $\alpha = 10^2$, $Pr = 1.71$, $\eta_0 = 1$

$A_{1,1}$	0.021915630	$B_{1,1}$	0.055326513
$A_{1,2}$	—0.017854899	$B_{1,2}$	-0.013547021
$A_{1,3}$	0.019285883	$B_{1,3}$	0.003974909
$A_{2,1}$	0.009253715	$B_{2,1}$	0.001591794
$A_{2,2}$	—0.000004586	$B_{2,2}$	—0.000778962
$A_{2,3}$	—0.002092713	$B_{2,3}$	—0.000182942
$A_{3,1}$	0.000270965	$B_{3,1}$	0.000239221
$A_{3,2}$	—0.000637357	$B_{3,2}$	—0.000092480
$A_{3,3}$	—0.000952134	$B_{3,3}$	—0.000059894

5 Discussion and Conclusion

The linear iteration process used limits the solution of Eqs. (4.6) and (4.7) for cases with modified RAYLEIGH number up to order 10_5. Beyond this limit, the linear iteration process fails to give proper convergence. The RAYLEIGH number of interest in applications usually runs an order of magnitude higher than 10_5 so that there is need to investigate up to RAYLEIGH number equal to 10_6, above which laminar flow may no longer be possible.

A promising approach to extend the solution to cases with higher RAYLEIGH number is proposed in Appendix I. One of the assets of the present method of analysis is its practically unlimited accuracy which might be of interest when the problem of hydrodynamic stability of the thermosyphonic flow is treated. Its wider scope of adaptability to different prescribed body force fields and boundary conditions is another advantage of the approach. The availability of a medium-capacity digital computer makes the analysis much less formidable than it appears.

Appendix I

Suppose we transpose the left-hand term to the right-hand side of each of Eqs. (4.6) and (4.7). Then these equations may be written as

$$f_{m,n} = 0 \quad \ldots\ldots\ldots\ldots\ldots\ldots \quad (A.1)$$

and

$$g_{m,n} = 0 \quad \ldots\ldots\ldots\ldots\ldots\ldots \quad (A.2).$$

The sum of squares

$$\sum_{m,n} \{f_{m,n}^2 + g_{m,n}^2\} \quad \ldots\ldots\ldots\ldots\ldots\ldots \quad (A.3)$$

is clearly non-negative. By the method of steepest descent [7], minimization of (A.3) gives the zeros of Eqs. (A.1) and (A.2), and hence the zeros of Eqs. (4.6) and (4.7). To start the minimization, good starting $A_{p,q}$ and $B_{p,q}$ values are needed. These can be obtained by solving the linear, the bilinear, and the quadratic terms in $A_{1,1}$ and $B_{1,1}$ of Eqs. (4.6) and (4.7) simultaneously. With $A_{1,1}$ and $B_{1,1}$, we can evaluate the next values $A_{1,1}$ and $B_{1,2}$ similarly, and so on.

References

[1] M. J. LIGHTHILL, Theoretical Considerations on Free Convection in Tubes, Quart. Journ. Mech. and Applied Math. 6 (1953) pp. 398—439.

[2] B. W. MARTIN, Heat Transfer by Free Convection in An Open Thermosyphon Tube, British Journ. Applied Physics 5 (1954) pp. 91—95.

[3] V. C. LIU and H. JEW, On Laminar Free Convection Flows in Cavities, Bull. Am. Phys. Soc. (II) 5 (1960) p. 130.

[4] G. POOTS, Heat Transfer by Laminar Free Convection in Enclosed Plane Gas Layers, Quart. Journ. Mech. and Applied Math. 11 (1958) pp. 257—273.

[5] F. M. LESLIE, Free Convection in the Tilted Open Thermosyphon, J. Fluid Mech. 7 (1959) pp. 115—127.

[6] S. GOLDSTEIN (editor), Modern Developments in Fluid Dynamics, Vol. 2, Oxford 1938, Clarendon Press, p. 607.

[7] R. COURANT, Variational Methods for the Solution of Problems of Equilibrium and Vibrations, Bull. Amer. Math. Soc. 49 (1943) pp. 1—23.

Manuskripteingang: 5. 9. 1961

Anschrift: Prof. V. C. LIU, University of Michigan, Dept. of Aeronautical and Astronautical Engineering, Ann Arbor, Michigan, USA.

Symbols

x, y = cartesian coordinates (see Fig. 1)
u = component of velocity in x-direction
v = component of velocity in y-direction
p = pressure
d = depth of cavity (see Fig. 1)
w = width of cavity (see Fig. 1)
T = absolute temperature
T_0 = uniform temperature of a portion of cavity boundary (see Fig. 1)
T_1 = absolute temperature at $x = 0$, $y = y_0$
μ = viscosity coefficient
β = $\varrho\left[\frac{\partial(1/\varrho)}{\partial T}\right]_p \simeq \frac{1}{T_1}$ coefficient of volume expansion [1]
$\varkappa$ = thermometric conductivity [6]
ν = μ/ϱ kinematic viscosity
α = d/w aspect ratio
ω = rotation speed
ξ = x/w nondimensional distance in x-direction
η = $\alpha\, y/w$ nondimensional distance in y-direction
η_0 = y_0/w nondimensional distance from axis of rotation at $x = y = 0$ to $x = 0$, $y = y_0$
$\frac{T_w - T_1}{T_0 - T_1}$ = $\sin^2 \pi \xi$ prescribed temperature distribution along $\eta = 0$, where T_w is wall temperature along $y = y_0$
Pr = $\nu/\varkappa$ PRANDTL number
Ra = $\beta\, \omega^2\, w^4\, (T_0 - T_1)/\varkappa\, \nu$ modified RAYLEIGH number
$X_p(\xi)$ = eigenfunction of ξ defined by Eq. (4.3)
$Y_q(\eta)$ = eigenfunction of η defined by Eq. (4.4)
λ_p = eigenvalue associated with eigenfunction X_p
μ_q = eigenvalue associated with eigenfunction Y_q
γ_q = coefficient defined by a relation in Eq. (4.5b)
Θ = $\frac{T - T_1}{T_0 - T_1}$ nondimensional temperature defined by Eq. (4.1)

1009 ZAMM 684 VI-Chemg Liu

ψ = nondimensional stream function defined by Eq. (4.2)
$A_{p,q}$ = coefficient defined by Eq. (4.1)
$B_{p,q}$ = coefficient defined by Eq. (4.2)
$A(p;\lambda_n)$ = $\int X_m(\xi) \sin p\pi\xi\, d\xi$ [for Limits of integration see Discussion Following Equation (4.7)]
$B(n;\mu_s)$ = $\int Y_s'(\eta) \sin n\pi\eta\, d\eta$
$C(\lambda_m)$ = $\int X_m(\xi)\, d\xi$
$D(\lambda_p,\lambda_m)$ = $\int X_p''(\xi) X_m(\xi)\, d\xi$
$E(q;\mu_n)$ = $\int Y_n(\eta) \cos q\pi\eta\, d\eta$
$F(\lambda_m)$ = $\int \xi X_m(\xi)\, d\xi$
$G(m,p;\lambda_r)$ = $\int X_r'(\xi) \cos m\pi\xi \cos p\pi\xi\, d\xi$
$H(\lambda_p,\lambda_r,\lambda_m)$ = $\int X_p''(\xi) X_r'(\xi) X_m(\xi)\, d\xi$
$I(q;\mu_n)$ = $\int Y_n(\eta) \sin q\pi\eta\, d\eta$
$K(\lambda_p,\lambda_r,\lambda_m)$ = $\int X_p''(\eta) X_r(\xi) X_m(\xi)\, d\xi$
$L(\lambda_r,\lambda_p,\lambda_m)$ = $\int X_r'(\xi) X_p(\xi) X_m(\xi)\, d\xi$
$P(m;\lambda_r)$ = $\int X_r'(\xi) \cos m\pi\xi \sin^2\pi\xi\, d\xi$
$Q(\lambda_m)$ = $\int \xi X_m(\xi) \sin^2\pi\xi\, d\xi$
$R(m,p;\lambda_r)$ = $\int X_r(\xi) \cos m\pi\xi \sin p\pi\xi\, d\xi$
$S(q,n;\mu_s)$ = $\int Y_s'(\eta) \sin q\pi\eta \sin n\pi\eta\, d\eta$
$T(\lambda_m)$ = $\int X_m(\xi) \sin^2\pi\xi\, d\xi$
$V(p;\lambda_m)$ = $\int \xi X_m(\xi) \cos p\pi\xi\, d\xi$
$W(m;\lambda_r)$ = $\int X_r' \cos m\pi\xi\, d\xi$
$f_{m,n}$ = function defined by Eqs. (A.1) and (4.6)
$g_{m,n}$ = function defined by Eqs. (A.2) and (4.7)

Primed X_p and Y_q denote derivatives with respect to their respective independent variables.

ξ and η, when used as subscripts, denote partial differentiation with respect to these independen variables.

Lower case letters m, n, p, q, r, s, denote indices and parameters which are integers or 1/2 as indicated.

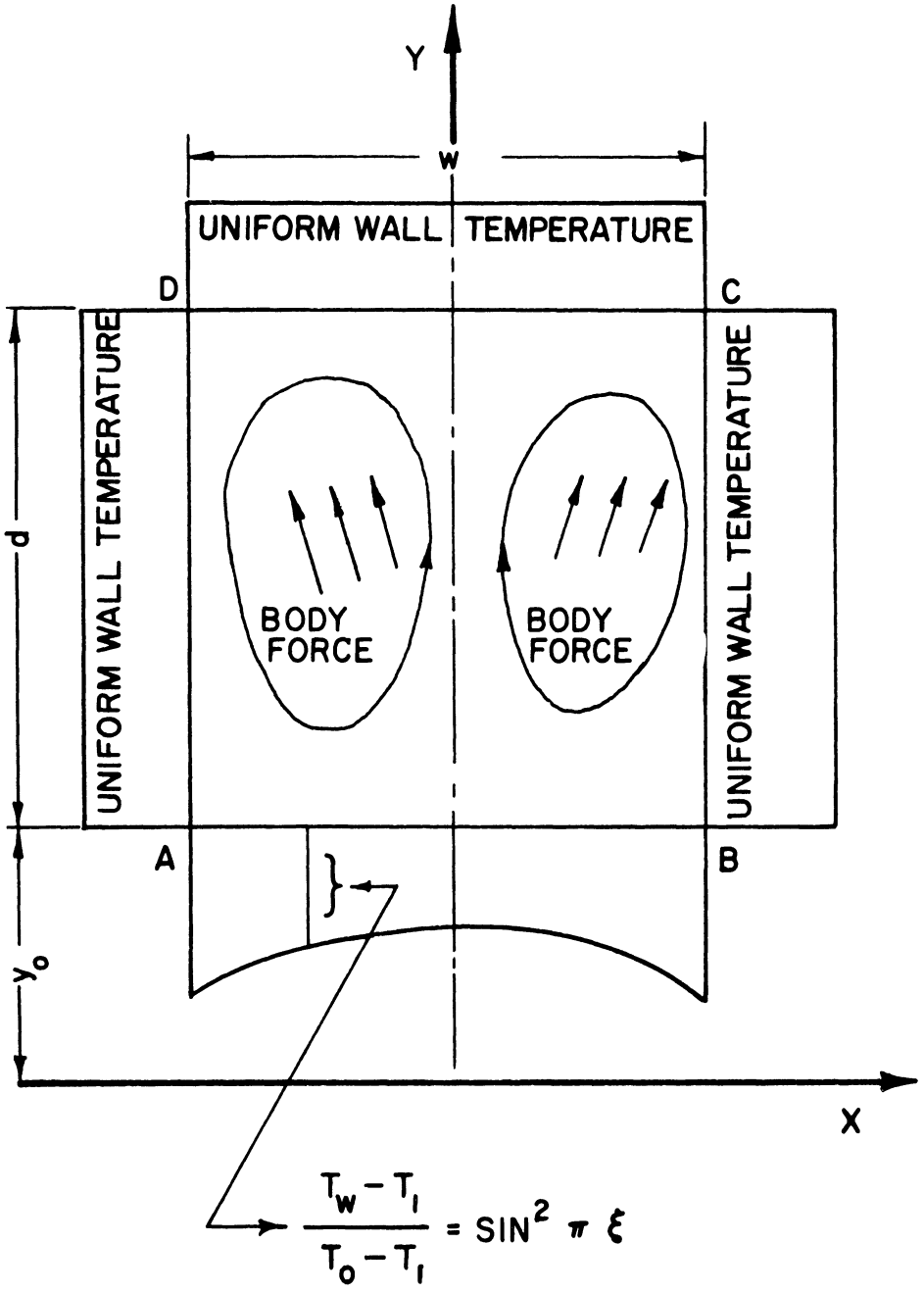

Fig. 1. Two-dimensional cavity section.

Fig. 2. Streamlines and Isothermals in cavity, $Ra = 10^3$, $a = 10^3$, $Pr = 1.71$, $\eta_0 = 1$.
(2a) Streamlines $\psi(\xi, \eta)$ = constant; (2b) Isothermals $\Theta(\xi, \eta)$ = constant.

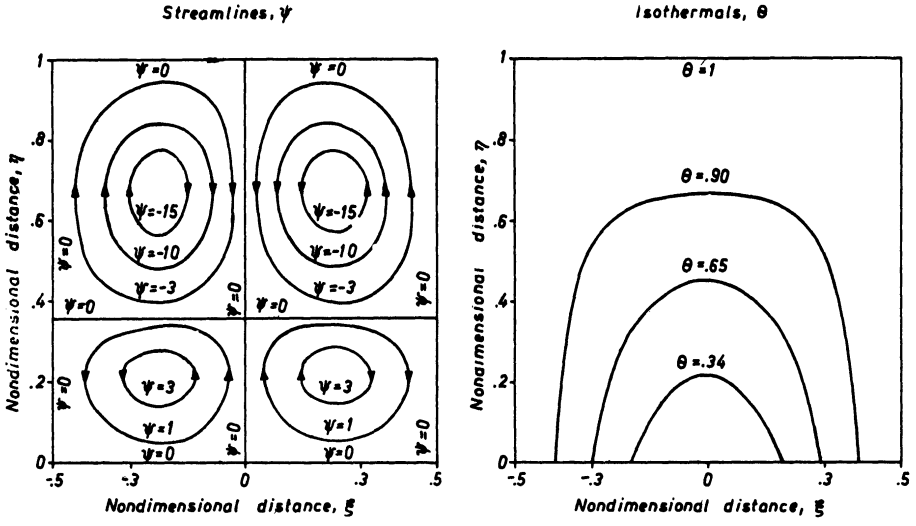

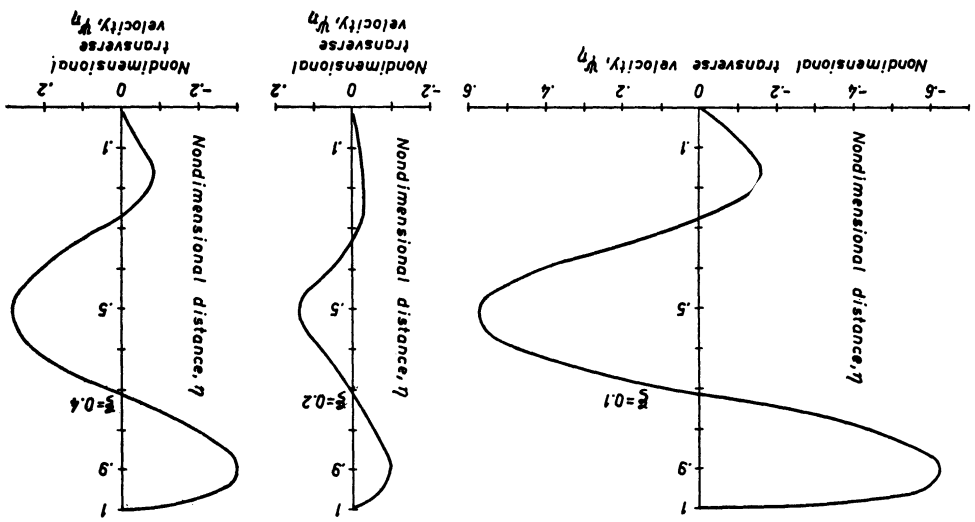

Fig. 3. Transverse velocity profiles, $Ra = 10^3$, $a = 10^3$, $Pr = 1.71$, $\eta_0 = 1$. (3a) ψ_η at $\xi = 0.1$ vs. η; (3b) ψ_η at $\xi = 0.2$ vs. η; (3c) ψ_η at $\xi = 0.4$ vs. η.

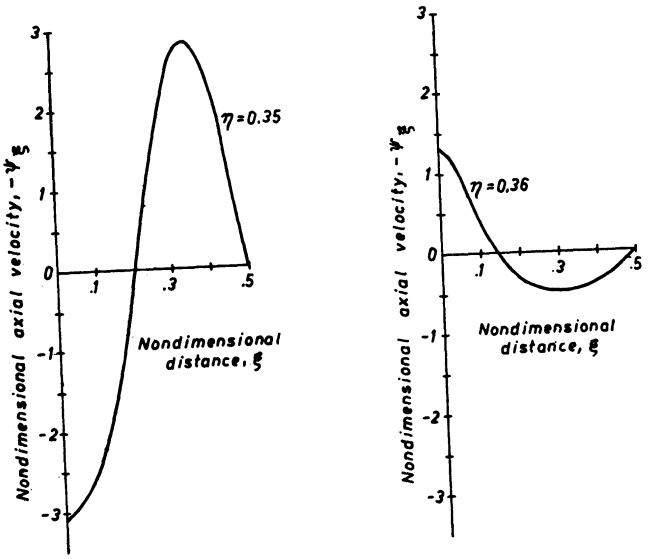

Fig. 4. Axial velocity profiles, $Ra = 10^3$, $a = 10^3$, $Pr = 1.71$, $\eta_0 = 1$. (4a) $-\psi_\xi$ at $\eta = 0.35$ vs. ξ; (4b) $-\psi_\xi$ at $\eta = 0.36$ vs. ξ.

APPENDIX X

RAREFIED GAS DYNAMICAL CONSIDERATIONS IN ROCKET SOUNDING MEASUREMENTS

(Contributed by V. C. Liu)

(An invited paper in Rand Symposium on Aerodynamics of the Upper Atmosphere, 1959; also appears in Rand Report R-339)

RAREFIED-GAS DYNAMICAL CONSIDERATIONS IN THE ROCKET-SOUNDING MEASUREMENTS*

V. C. Liu
Department of Aeronautical and Astronautical Engineering
The University of Michigan, Ann Arbor, Michigan

ABSTRACT

Aerodynamic methods of measuring upper-atmospheric properties by means of sounding rockets are discussed from the rarefied-gas dynamical point of view. On the basis of this discussion, it is proposed that combinations of different aerodynamic methods on the same sounding rocket can and should be designed to acquire additional physical insight into the aerodynamics of rarefied media.

INTRODUCTION

"Rocket-sounding" refers to the experiments of probing the upper atmosphere by means of nearly vertically ascending rockets with the purpose of measuring atmosphere properties, e.g., ambient pressure, density, and temperature. Usually, some form of aerodynamic effects due to the presence of the rocket is registered; these may be the pitot-probe pressure, conical-surface pressure, or the sphere drag. One or more of these quantities, together with the forward speed of the aerodynamic body, can be used to calculate the atmospheric parameters. This general scheme is called the aerodynamic method of upper-atmospheric measurement.

*The support of the Air Force Cambridge Research Center, under Contract No. AF-19(604)-5477, for the work reported here is gratefully acknowledged.

DISCUSSION

The success of an aerodynamic method depends upon, among other things, the availability of a well-established aerodynamic theory which relates the measured aerodynamic effect to the atmospheric parameter of interest. Since the atmosphere forming the flow medium of the aerodynamic theory in question becomes more and more rarefied as the rocket ascends, it is expected that application of the aerodynamics of continuous medium will become less and less valid. At such altitudes where the molecular mean free path λ is not negligibly small compared to a characteristic dimension L of the flow field in question, the concept of rarefied-gas dynamics should be used in treating the flow problems.

Present knowledge concerning dynamics of high-speed flows of rarefied gases is very much limited except for the region of extremely rarefied flows ($\lambda/L \gg 1$) for which the free-molecule hypothesis is applicable (1)*. The validity of the free-molecule concept is confined to cases where the effects of intermolecular collisions between the molecules incident on, and reflected from, a surface element are negligible. With increasing density of the medium, the effects of these collisions become aerodynamically significant. The conventional mathematical treatment of the flow problems in the almost-free-molecule region is based on the principle of perturbation expansion of the Maxwell-Boltzmann equation in powers of L/λ. The calculations along this line of attack are quite formidable and few results of direct aerodynamic interest are available.

Recently, an alternative approach to the problem by means of the free-molecule iteration of the intermolecular collision effects appears to have

---

Numbers in parentheses indicate References at end of paper.

shown some promising results in the analyses of such quantities as the drag of a plate normal to the flow (2), pitot-probe pressure (3), flat-plate drag (4), and sphere drag (5). The significance of these new theories of rarefied-gas flows must be ascertained by comparison with measured results, which are still lacking. Laboratory measurements using facilities such as low-density wind tunnels and ballistic ranges are plagued with experimental difficulties.

With improved rocket technology and better known upper-air properties, rocket-sounding experiments are better able to help in acquiring additional physical insight into the aerodynamics of rarefied media. That this cause has already been served in a limited way can be illustrated by two examples.

Pitot-Probe Pressure

Measurement of the impact pressure given by a pitot probe (see Fig. 1), together with the forward speed of the probe, has been shown as an effective aerodynamic method of determining the ambient density of a stationary and not very rarefied atmosphere (6). At high altitudes where atmospheric air can no longer be considered as a continuous medium pitot-probe pressure must be reformulated, considering the characteristics of the coarse-molecular structure of air as a flow medium. The theory of pitot pressure in extremely rarefied or "free-molecule" flows

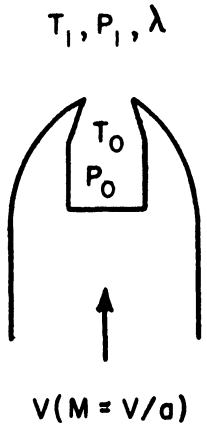

Fig. 1

and moderately rarefied or "almost-free-molecule" flows is illustrated in Fig. 2, along with the pitot-pressure equation for an ideal (continuous) fluid. For comparison, the results of low-density wind-tunnel measurements (7) are shown in the plot. Assuming that the ambient density is the mean density given by the Rocket Panel (8), we may compare the results of the pitot pressure measured on a sounding rocket (6) with those from other sources in Fig. 2. The fact that the cavity temperature T_o of the pitot probe is not available in this particular flight explains the use of finite line segments to represent the uncertainty of the results as indicated. The qualitative check of the rocket-sounding measurements with the theory of almost-free-molecule flows is of interest.

Sphere Drag

Sphere-drag coefficients taken from measurements in ballistic ranges (9) wind tunnels, (10) etc., are plotted as functions of Mach number ($M = V/\sqrt{\gamma RT_1}$) and Reynolds number ($Re = Vd\rho/\mu$) in Fig. 3. If, again, we may assume that the upper-atmospheric density can be represented by the mean density of the Rocket Panel (9), the sphere-drag coefficient can be evaluated from falling-sphere measurements (11). Each of the circular designations represents the mean value of drag coefficients measured in an interval of approximately 20,000 ft of the falling-sphere trajectory. Again, the rocket-sounding measurements show good consistency with results obtained in ballistic ranges and wind tunnels.

The cited examples illustrate that the rocket-sounding measurements, if conducted properly, may serve a dual purpose of both gathering informa-

tion concerning the atmosphere at high altitudes and exploring the basic principles of rarefied-gas flows. The latter purpose appears to have been served in a limited way through indirect interpretations of the restricted amount of free-flight results, even though the experiment had not been designed with this purpose in mind.

Different regions of the atmosphere at various altitudes may serve as typical media of fluid mechanics. Considering the difficulties involved in building workable low-density testing facilities, we feel that it might be less troublesome to perform a rarefied-gas-flow experiment with a sounding rocket or free-falling object than with a low-density wind tunnel or a ballistic range. A proposed experiment with this in mind is to perform the pitot-probe (6) and the falling-sphere (11) measurements on the same rocket. The former is achieved during the ascending flight of the rocket trajectory, while the latter begins with the ejection of the sphere by the rocket near the peak of the flight. By calibrating one method against another, one might expect to learn a great deal about the upper atmosphere and rarefied gas dynamics.

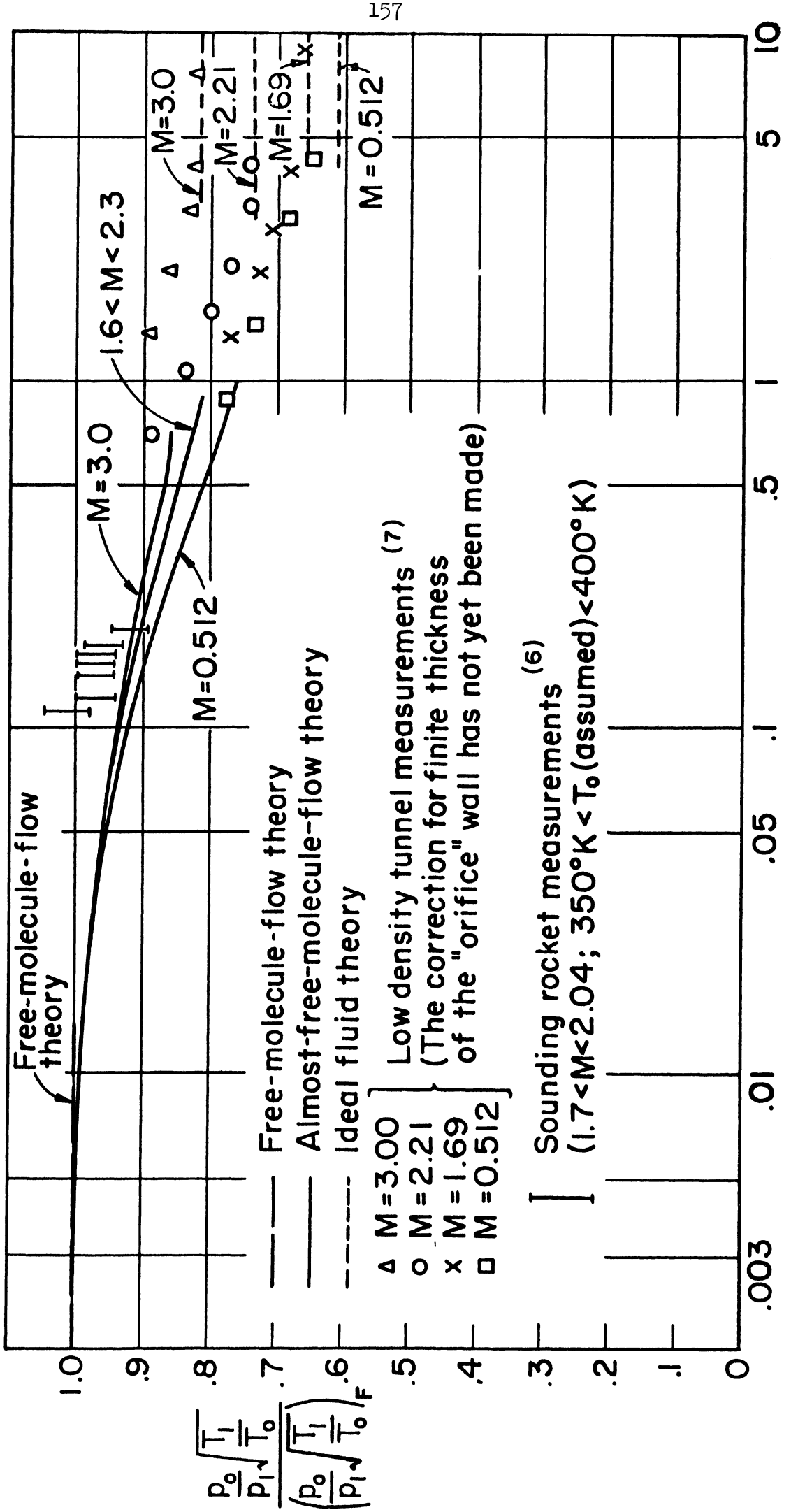

FIG. 2 — PITOT-PROBE PRESSURE

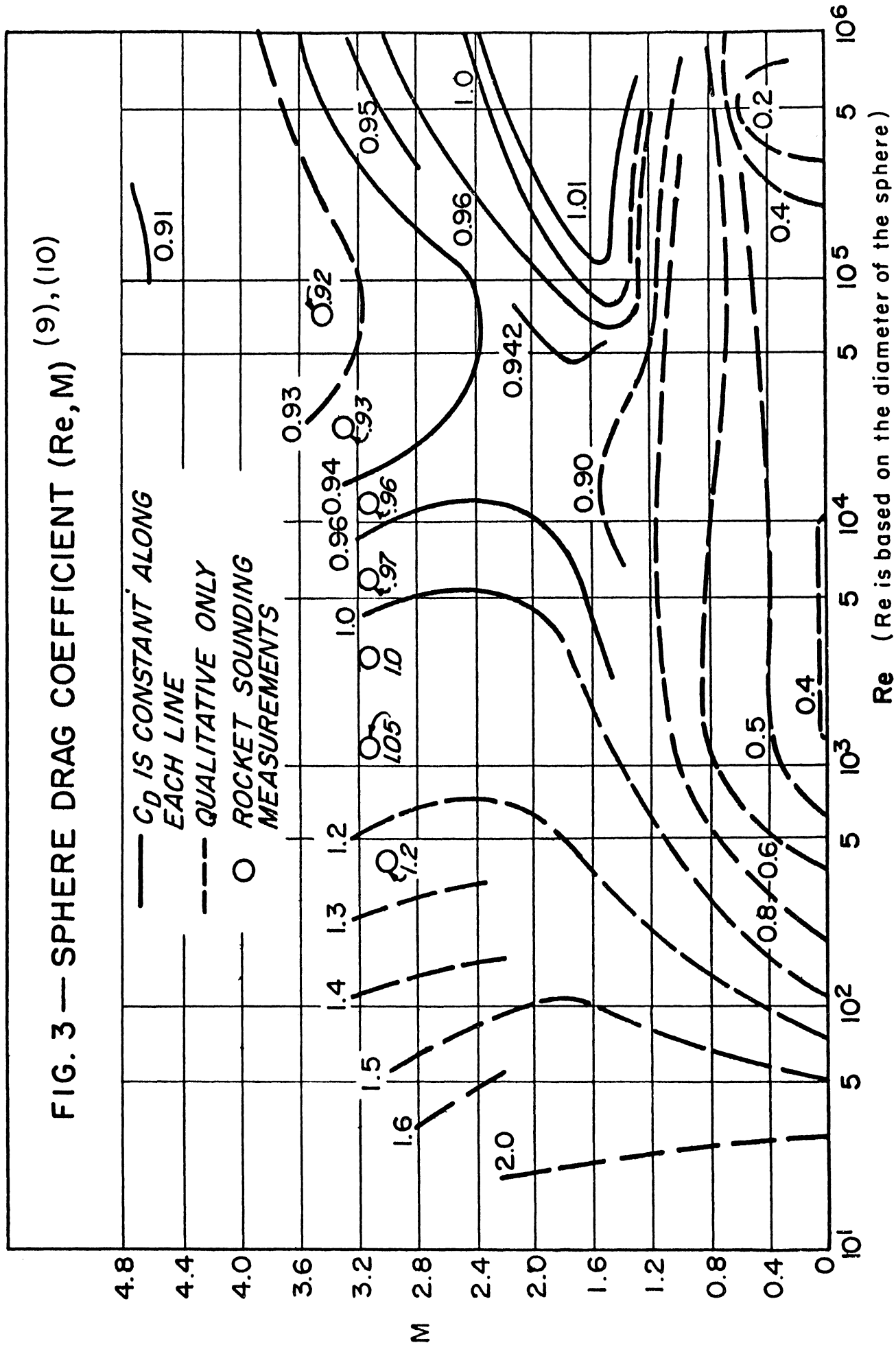
FIG. 3 — SPHERE DRAG COEFFICIENT (Re, M) (9), (10)
C_D IS CONSTANT ALONG EACH LINE
QUALITATIVE ONLY
ROCKET SOUNDING MEASUREMENTS
M
Re (Re is based on the diameter of the sphere)
0.91
0.92
0.93
0.94
0.95
0.96
0.97
1.0
1.01
1.2
1.3
1.4
1.5
1.6
2.0
0.942
0.90
0.5
0.4
0.6
0.8
0.2

REFERENCES

1. Schaaf, S. A., and Chambre, P. L., "Flow of Rarefied Gases"(Fundamentals of Gas Dynamics) Princeton University Press, Princeton,1958.

2. Lunc, M., and Lubonski, J., Bull. Acad. Polon. Sci., 4, No. 1 (1957).

3. Liu, V. C., On Pitot Pressure in an Almost-Free-Molecule Flow—A Physical Theory for Rarefied-Gas Flow, High Altitude Engineering Lab. Research paper No. 18, The University of Michigan, 1957; also J. Aero./ Space Sci., 25, 779 (1958).

4. Liu, V. C., "On the Drag of a Flat Plate at Zero Incidence in an Almost-Free-Molecule Flow," J. Fluid Mech. (in press).

5. Baker, R.M.L., Jr., and Charwat, A. F., Phys. Fluids, 1, 73 (1958).

6. Liu, V. C., J. Geophys. Res., 88, 171 (1956).

7. Sherman, F. S., NACA T.N. No. 2995, Washington, D. C., 1953.

8. Rocket Panel, Phys. Rev., 88, 1027 (1952).

9. May, A., J. Appl. Phys., 28, 910 (1957).

10. Kane, E. D., J. Aeronaut. Sci., 18, 259 (1951).

11. Bartman, F. L., Chaney, L. W., Jones, L. M., and Liu, V. C., J. Appl. Phys., 27, 706 (1956).

APPENDIX XI

ON THE DETERMINATION OF THE EARTH'S ATMOSPHERIC STRUCTURE WITH SOUNDING ROCKETS AND ARTIFICIAL SATELLITES

(Contributed by V. C. Liu)

(An invited paper at the CAI Interplanetary Explorations Symposium in Toronto, October 1961; also appears in Canadian Aeronautical and Space Journal, January 1962)

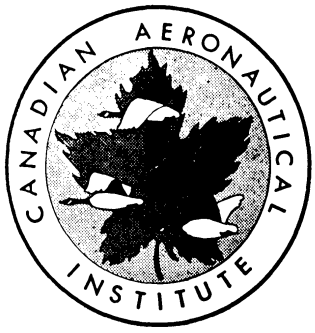

ON THE DETERMINATION OF THE EARTH'S ATMOSPHERIC STRUCTURE WITH SOUNDING ROCKETS AND ARTIFICIAL SATELLITES

by

Professor V. C. Liu

University of Michigan

Reprinted from

CANADIAN AERONAUTICS AND SPACE JOURNAL

Vol. 8, No. 1 : January 1962

ON THE DETERMINATION OF THE EARTH'S ATMOSPHERIC STRUCTURE WITH SOUNDING ROCKETS AND ARTIFICIAL SATELLITES†

by Professor V. C. Liu*

University of Michigan

SUMMARY

The discussion starts with the general description of the physical nature and properties of the earth's atmospheric layers from the tropopause to the exosphere, emphasis being on those atmospheric thermodynamic parameters such as pressure, density, temperature and composition. Significant results of these atmospheric parameters obtained by means of rocket sounding and satellite experiments are reviewed and discussed. Inasmuch as these methods of upper air measurements are usually indirect determinations based on the application of gas dynamic principles, it would be important to see that the assumptions thereby involved are justified from the aerodynamic viewpoint. A critical study is made of the validity and limitations of these gas dynamic methods in the upper air research.

INTRODUCTION

THIS paper is intended as a general survey of the present state of our knowledge concerning the physical nature of the upper atmosphere and an account of the problems which still remain unsolved. In the discussion I shall leave out the atmospheric phenomena occurring in the troposphere. This extends from the ground level to approximately 15 km in altitude. The atmospheric behavior in this region is intimately related to the important and complicated phenomena of weather and can be conveniently treated as a separate branch of atmospheric science – meteorology.

For centuries the upper atmosphere must have appeared, to most people, remote and of little concern. Perhaps the northern lights attracted their admiration, shooting stars were familiar sights on a clear night, and the beautiful display of noctilucent clouds served as the decoration of the tranquil sky. But there were a few who attempted to explain these things, and from these few dedicated men of science, who had no direct means of exploring the upper atmosphere but who used ingenious deduction based on a complex mass of data on meteors and their light intensity distribution, airglow and auroral spectra, radio wave reflections and anomalous sound propagation measurements, we learned much about the upper atmosphere before the start of systematic exploration of the upper atmosphere with sounding rockets and satellites in the last decade.

†Prepared under the upper atmosphere research program in the Dept. of Aeronautical and Astronautical Engineering and supported by the Air Force Cambridge Research Center (Contract No. AF-19-604-5477); read at the CAI Interplanetary Explorations Symposium in Toronto on the 26th October, 1961.

*Dept. of Aeronautical and Astronautical Engineering

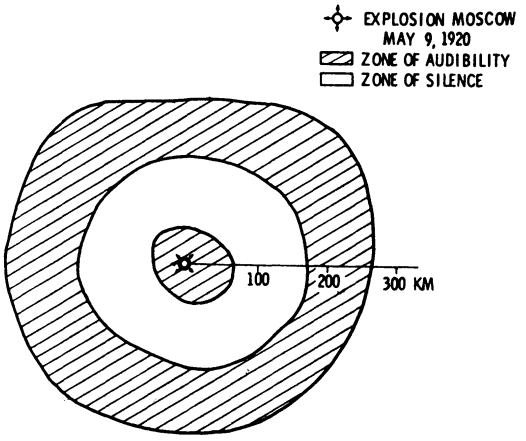

Figure 1
Typical zones of silence and audibility around an explosion

It would be of interest to review briefly some of the clever and fruitful indirect approaches to the atmospheric problem.

Anomalous sound propagation

The anomalous propagation of sound waves was first noted in 1901, when the minute guns fired at Queen Victoria's funeral were heard at several places sixty and more miles distant, but not at some places nearer to the gun site. On many occasions since then, zones of silence around large explosions have been noticed (Figure 1). It is well known that a sound wave travelling over the ground will continually be weakened by being scattered and absorbed by the obstacles in its path and will gradually become inaudible. This accounts for the inner radius of the zone of silence. To explain the anomaly of the recurrence of audibility at distant places, it was rightly supposed by F. J. W. Whipple[1] that there was a wave refraction phenomenon requiring the velocity of sound, which depends on ambient temperature, to increase with altitude somewhere in the upper atmosphere. The sound rays proceeding upwards in an oblique direction are bent downward due to increased velocity of sound waves caused by a gradient of rising temperature in the upper atmosphere. These waves, because of the absence of obstacles, would be less attenuated than the ground waves. The paradox was eventually to disappear in the

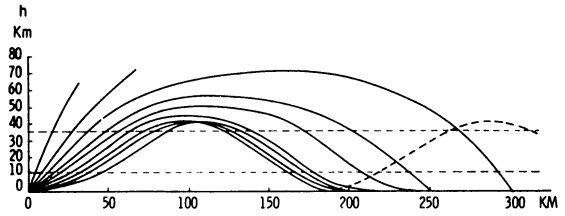

Figure 2
Refraction of sound rays from the upper atmosphere
(after Gutenberg, Zeits. Geophys. 1926)

light of accurate information on the calculated paths of the abnormal rays of sound with a typical temperature distribution in the 30-50 km altitude region (Figure 2).

Observation of meteor drag deceleration

It was on the basis of the ballistic drag theory of meteors and their luminosity that Lindemann and Dobson[2] first definitely concluded that there is an upward increase of temperature in the 30-50 km altitude region. The height velocity and acceleration of a meteor are determined[3] by triangulation from its photographs taken by cameras with special shutters. Luminosity of the meteor trail is measured by comparison with known stars. The ambient density is calculated from these data by means of three fundamental conservation equations of mass, momentum and energy.

The results of these pre-sounding rocket determinations of ambient temperature distribution are shown in Figure 3 and compare remarkably well with those of the recent direct measurements.

THERMODYNAMIC STRUCTURE OF THE ATMOSPHERE FROM DIRECT MEASUREMENTS

Temperature distribution and the atmosphere layers[4]

Meteorological balloon soundings have shown that the ambient temperature, apart from local fluctuations near the ground level, falls steadily with altitude in the troposphere, starting with ground level and rising to a ceiling called tropopause; tropopause varies in height from an altitude less than 10 km in the polar regions to more than 15 km in the equatorial belt. The temperature of the tropopause is about 220°K in the polar regions and about 190°K at the equator.

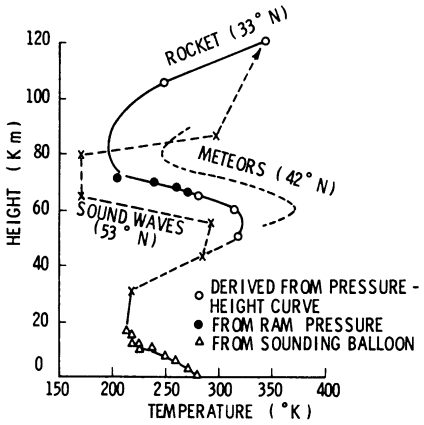

Figure 3
Comparison of temperature distribution in the upper atmosphere
(after Mitra, Compend. Met. 1951)

In the stratosphere (Figure 4) the ambient temperature rises with altitude, first slowly and then at a faster rate to a peak value of about 270°K at an altitude of about 50 km. Above an altitude of about 50 km, the ambient temperature lapses steadily in a layer called mesosphere to a low minimum of about 150°K at approximately 80 km.

The temperature inversion in the altitude region near 50 km is attributed to the absorption characteristics of ozone, a minor constituent of the atmosphere. Solar ultraviolet radiation in the 2000-A region of the spectrum dissociates an infinitesimal proportion of the molecular oxygen into atoms, which combine with

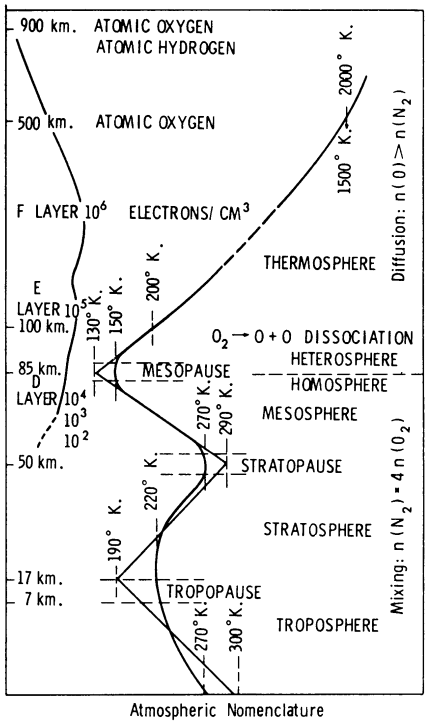

Figure 4
Nomenclature of the upper atmosphere[4]

molecular oxygen to form ozone; the tri-atomic product (O_3) thus obtained is an intense absorber of ultraviolet radiation in the 2500-A wave length region. It is primarily due to the absorption of this energy that the warm layer in the atmosphere near the 50 km region results.

The amount of ozone is very minute; indeed if all the ozone in any vertical column of air were collected at the bottom of the column, at normal temperature and pressure, its thickness would be only about 3 mm as against 8 km for the other constituents. The presence of ozone, which cuts off the solar spectrum at the ultraviolet end, serves as an all important shield for the inhabitants of earth from harmful effects of such rays.

Above the mesopause the ambient temperature mounts again in the layer called thermosphere. The temperature rises very rapidly between 100 km and 200 km, and then less rapidly at higher altitudes. Above 400 km, the temperature is nearly constant with

altitude. The temperature in the thermosphere is essentially governed by heat conduction and absorption of solar energy. Above 400 km, where absorption of energy is negligible, the relatively high heat conductivity annuls the temperature gradient.

It should be noted that the real significance of the temperature at very high altitude is that it is a measure of the mean speeds of the atmospheric molecules and atoms at these levels.

ATMOSPHERIC COMPOSITION

Gravitational effect

If the atmosphere were isothermal and free of turbulent and convective mixing, the number density of its ith constituent at an altitude z, i.e. $n_i(z)$, can be prescribed by the Maxwell-Boltzmann distribution in statistical mechanics:

$$n_i(z) = n_i(z_o)e^{-(z-z_o)/H_i} \tag{1}$$

where H_i denotes the scale height which is equal to kT/m_ig (k = Boltzmann constant, T = temperature, m_i = particle mass of the ith constituent and g = gravitational acceleration).

The total number density of the atmosphere at altitude z can be expressed as the sum of the partial densities of its constituents $n(z) = \Sigma_i n_i(z)$. The concentration ratio of the ith and jth species becomes

$$\left.\frac{n_i}{n_j}\right|_l = \left.\frac{n_i}{n_j}\right|_{z_o} e^{-(z-z_o)\,(H_i^{-1} - H_j^{-1})} \tag{2}$$

The exponential factor in Eq. (2) represents the gravitational separation effect. It must be noted, however, that starting from an arbitrary concentration distribution, the atmosphere takes a long relaxation time constant, which depends on the altitude, to reach the diffusive equilibrium condition (see Eq. (1)); this time constant is in the order of a year's time for helium at an altitude say 100 km[5] and is longer at a lower altitude, and even longer for a heavier gas.

The natural question here is whether the atmosphere has such long periods of uninterrupted quietness, considering the presence of diurnal disturbance due to solar radiation and possibly disturbances from other sources. From observations of meteor trails seen at an altitude region of 80-100 km, it has been noted that distortion and tangle often occur, thus revealing the presence of strong wind shears at such levels. The turbulent mixing must be strong accordingly.

During the last few years, samples of air collected by means of rockets have confirmed that air composition is approximately the same below the thermosphere, except for traces of ozone and water vapor.

Should the whole atmosphere be subjected to perfect mixing up to the highest level and remain isothermal* the mean density at any altitude must be given by

$$\rho(z) = \rho(z_o)\, e^{-(z-z_o)/\bar{H}} \tag{3}$$

where $\bar{H}$ denotes the scale height of the homogeneous atmosphere with a mean molecular mass $\bar{m}$.

*For an atmospheric temperature which varies linearly with altitude z, the equilibrium mean density distribution can be derived without difficulty.

Neither of these two extreme ideal cases of diffusive and homogeneous equilibriums is expected to be valid for the entire altitude region ranging from the ground level to the extreme altitude. At the lower altitude, such as below the mesopause, the relatively intense turbulent and convective mixing appears to assure a homogeneous atmosphere; on the other hand, at high altitudes, the molecular diffusion becomes the predominant influence, hence the atmosphere assumes the state of diffusive equilibrium. It appears that one has the two asymptotic solutions to the problem of the atmosphere diffusive separation. To solve the problem in a more satisfactory manner, one needs the knowledge of convection and turbulence of the upper atmosphere; in recent years our understanding of them has greatly advanced.

For a gross description, it is often assumed that the atmosphere below thermosphere is homogeneous while above it is heterogeneous, since the atmospheric composition is appreciably modified by the enhanced photochemical dissociation of oxygen in the thermosphere.

Now, at this stage, I must point out that so far my discussion concerning the atmospheric composition problem has been limited to the effect of gravity alone. In actuality, there are other effects such as the photochemical and photoelectric effects of the sun.

Solar radiation effect

The electromagnetic spectrum of the sun spans the entire range of wave lengths from gamma rays to radio waves. The sun also spurts out sporadic streams of high energy charged particles. The interaction of the solar radiation, whether corpuscular or electromagnetic, with the atmospheric particles – atomic and molecular, neutral and ionized – produces in different ways the change of atmospheric composition.

It is known that particles may exist in more than one state, and each state has a definite amount of internal energy. These states form a discrete series. The internal energy of an atomic particle is determined solely by the electronic configuration (including the electron spin), while that of a molecular particle may also include energy of internal vibration and of rotation. The minimum energy needed to remove an electron altogether from a particle in its ground state is called ionization energy. The energy necessary to divide a molecular particle (neutral or ionized) into two atomic (or molecular) particles is called dissociation energy. If particles are undergoing transitions from lower to higher energy levels, one way in which the necessary energy W may be acquired is by absorption of light, which must be of frequency W/h where h denotes Planck's constant. Corresponding to the minimum energy required to ionize or dissociate a particle, there is the minimum frequency associated with each of these processes when they are induced by light absorption; but light of any greater frequency may also induce the process, the excess energy going into the kinetic energy of separation of the resulting two particles.

Above about 90 km, molecular oxygen in the atmosphere becomes dissociated to a considerable degree, although nitrogen does not. A consequence of

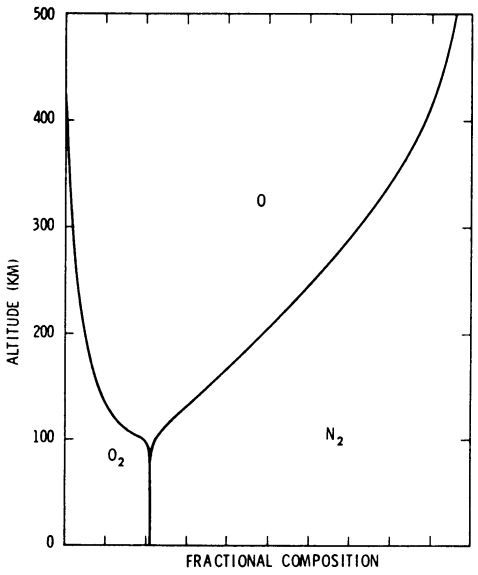

Figure 5
Relative concentration of the major constituents in the upper atmosphere[6]

this dissociation process is the decrease of the mean molecular mass of air in this altitude region due to both the change of mean mass of oxygen particles and the diffusive separation effect. Atomic oxygen, being lighter than molecular nitrogen, increases in relative concentration with altitude, and finally becomes the principal constituent as illustrated in Figure 5. In this figure, the fractional atmospheric composition as a function of altitude is based on the assumption that diffusive separation prevails above 105 km, and the degree of oxygen dissociation at 105 km is 15% as postulated in Reference 6. On account of the low collision frequencies at high altitude, the atomic oxygen cannot recombine as rapidly as molecules are dissociated; the atoms may, however, diffuse downward into the denser gas region to recombine in three-body collision processes. Therefore, the relative concentrations of atomic and molecular oxygen at high altitude are controlled by the rate of diffusion of the two species, as well as the rate of dissociation.

Atmospheric density distribution

The basic relations between pressure, density, and temperature in an atmosphere are the equation of hydrostatic equilibrium

$$dp = -g\,\rho\,dz \tag{3}$$

and the perfect gas law,

$$p = n\,k\,T \tag{4}$$

If the atmosphere has a number density n_i of the ith species, with a particle mass m_i, the total mass density is

$$\rho = \Sigma_i n_i m_i = n\bar{m} \tag{5}$$

where $\bar{m}$ denotes the mean mass per particle. Combining these relations, one obtains from Eq. (3)

$$\frac{dp}{p} = -\frac{dz}{\bar{H}}$$

or

$$p(z) = p(z_o)\exp\left(-\int_{z_o}^{z}\frac{dz}{\bar{H}}\right) \tag{6}$$

where $\bar{H}$ denotes the local scale height $kT/\bar{m}g$.

The equation for the ambient temperature as a function of mass density ρ can also be derived from the above equations,

$$T(z) = \frac{\rho_o}{\rho}\left(\int_{z_o}^{z}\frac{\bar{m}g}{k}\frac{\rho}{\rho_o}\,dz + T_o\right) \tag{7}$$

where subscript o denotes the altitude of initial measurement.

From these relations one may conclude that, with an atmosphere of constant composition, it is possible to determine the variation with altitude of any two of the quantities, pressure, density and temperature, provided that of the third is known accurately. In the measurement of the upper atmosphere by means of rocket sounding, it often happens that ambient density measurements are the most convenient to make.

Pitot pressure method

A pitot tube (sometimes called impact tube) at the nose of a sounding rocket measures the pitot pressure[b] which, together with the forward velocity of the ascending rocket, can be used to determine the ambient density of the atmosphere assuming zero atmospheric wind velocity. The pitot pressure and ambient density relation can be derived from the combined use of Rayleigh's supersonic pitot tube equation in Reference 7 and Eqs. (3) and (4). For the supersonic part of the rocket trajectory, Liu[8] has derived the ambient density equation

$$\rho = \tfrac{1}{4}(4\gamma)^{\gamma/(\gamma-1)}(\gamma+1)^{(\gamma+1)/1-\gamma}\frac{P}{V^2}\left[1-\frac{\gamma-1}{2P}\left(\frac{P_o}{V_o^2}g_o\bar{H}_o-\int_{z_o}^{z}\frac{P}{V^2}g\,dz\right)\right] \tag{8}$$

where γ denotes the ratio of specific heats of air and subscript o refers to the altitude of the initial measurements.

The advantages of the pitot pressure method, as compared with the ambient pressure method and Taylor-Maccoll conical pressure method[9], are the insensitiveness of pitot pressure to the angle of attack and to the increase of viscous effect at higher altitudes.

Falling sphere method

A falling sphere which carries a transient time accelerometer[10], designed to measure the vertical acceleration of the sphere, is a convenient probe to measure the ambient density[11, 12, 13]. From the drag deceleration of the sphere, one can determine the drag

[b] Also called ram pressure.

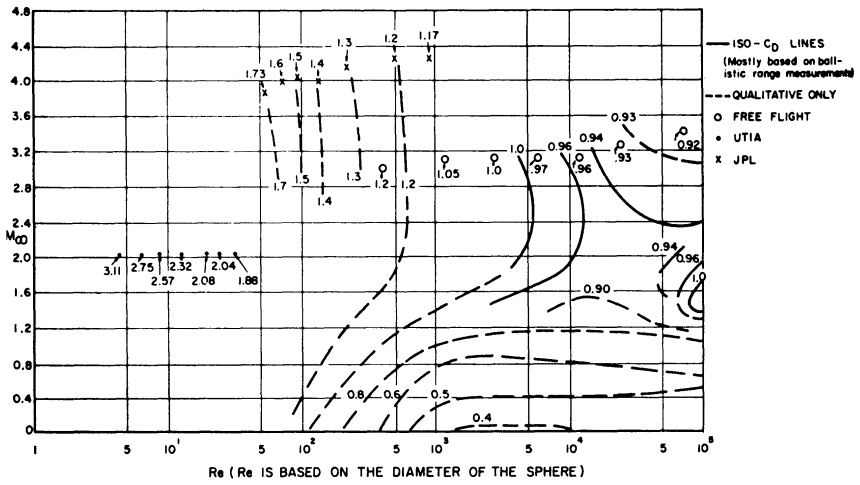

Figure 6
Sphere drag coefficient as a function of Reynolds number and Mach number[14]

force on the sphere from which the ambient density can be calculated, provided the drag coefficient of the sphere at the corresponding Mach number and Reynolds number is known (Figure 6)[14].

Satellite orbital decay method

The air drag of a satellite having an orbit with appreciable ellipticity rises to a sharp maximum at the perigee point (Figure 7) and is almost negligible except in the neighborhood of the perigee. The effect of air drag is to retard the satellite slightly as it passes the perigee; the energy loss causes the elliptic satellite orbit to contract appreciably at the apogee but only slightly at the perigee. By measuring the rate of decrease of its orbital period, the ambient density at altitudes near that of the perigee can be found provided the mass and dimensions of the satellite are known[15]. Since the perigee altitude remains nearly constant each satellite will, during most of its life time, sample the atmosphere at almost the same altitude, and hence provide abundant data at this altitude.

The studies of satellite orbital period decay revealed[16] an irregular variation in the rate at which the orbits of the satellites were shrinking, with a recognizable period of 27 days. It is well known that the sun rotates, relative to the earth, once every 27 or 28 days (the exact value depends on the solar latitude) and gives rise to the 27/28-day periodicities in geomagnetic and aurora display phenomena. The effect of the solar disturbance is explained as due to streams of particles which spurt out from the sun and rotate with it, much like the spray from a revolving water sprinkler, and sweep across the earth at intervals of about 27 or 28 days. The periodicity is not considered infallible because the source of disturbance on the sun may shift in position or intensity, but a tendency towards a 28-day recurrence is usually recognizable.

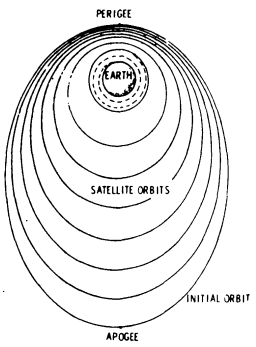

Figure 7
Decay of a satellite orbit

Jacchia compared the rate of decrease of orbital period for Vanguard 1 and the solar radiation on a wave length of 10.7 cm (Figure 8) and showed an interesting correlation between the satellite orbital period decay, which is a measure of the ambient density, and the solar activity.

Results of satellite orbital data have confirmed that the density at high altitude (about 400 km) is much higher near noon than at night. Since high temperatures and high densities tend to go together, the ambient temperature must be higher by day than by night. The diurnal change can be interpreted as due to the difference in heating of the atmosphere by solar radiation.

In conclusion, the upper atmosphere, say above 200 km altitude, must respond vigorously to the changing flux of solar radiation. The ambient density and temperature appear to increase with the solar activity, although the mechanism of solar control over the upper atmosphere is not yet clearly understood.

THE EXOSPHERE AND THE HELIUM PROBLEM

The exosphere can be considered as the fringe of the atmosphere. More precisely it is defined as the region lying above the critical level where a fast neutral particle moving upward has a probability of $1/e$ of escaping from the atmosphere without any collisions. The critical level corresponds approximately to the altitude of 550 km. Between the rare collisions the gas particles in the exosphere behave trajectory-wise as heavy projectiles shot up from the critical level; some may rise far and then drop back to the critical level; others may have sufficient speed to overcome the earth's gravitational attraction and escape into outer space. Light species tend to move faster than heavy species, according to the kinetic theory of gases, and therefore are more likely to escape. The rate of escape increases rapidly with the temperature at the critical level.

According to the kinetic theory of dissipation of gas from terrestrial atmosphere[17, 18], the atmospheric temperature at the critical level may be estimated from

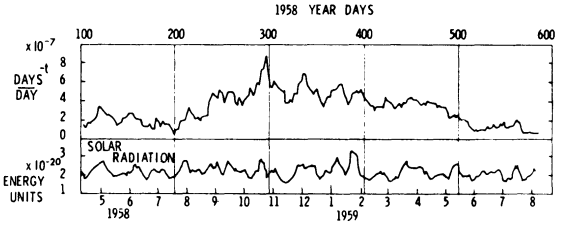

Figure 8
Comparison of the rate of decrease of Vanguard 1 orbital period and the solar 10.7 cm radiation[16]

a given rate of escape of a certain gas, say helium. The helium content of the atmosphere has been estimated, based on some hypothesis of its release from radioactive rocks during the geological time of the earth. The atmospheric temperature at the critical level of the exosphere thus arrived at is at least in the order of 1500°K, which is higher than acceptable from the consideration of heat balance in the thermosphere. It is possible however that helium may not be in equilibrium, with its current generation rate exceeding the escape rate.

GAS DYNAMIC CONSIDERATIONS IN THE MEASUREMENTS OF UPPER ATMOSPHERIC DENSITY

The success of an aerodynamic method of ambient density measurement, which is generally used in rocket and satellite probing of the upper atmosphere, depends upon, among other factors, the availability of a well-established aerodynamic theory, such as Rayleigh's pitot tube equation, that relates the measured aerodynamic effect – the pitot pressure – to the ambient density in question. The extent of rarefaction and plasma state of the upper atmosphere makes it rather unsuitable for treatment as a non-conducting continuum on the basis of which classical aerodynamics is built. Present knowledge concerning dynamics of high speed flows of rarefied gases and plasmas is very limited, except for the region of extremely rarefied flows for which the free-molecule flow theory is applicable.

Pitot pressure method

Rayleigh's supersonic pitot tube equation, on which the pitot pressure method of ambient density measurement is based, is valid, strictly speaking, only for a continuous medium without viscous effect. On the basis of low density wind tunnel results, it has been shown[8] that the limiting altitude of applicability for the pitot pressure method is approximately 80 km. For altitude beyond 80 km, the theory of pitot pressure with consideration of rarefied gas dynamic effect[10] must be used. As to the measurement of ambient density at much higher altitude, where the atmospheric mean-free path is much longer than the diameter of the pitot tube, it would be very tempting to use the free-molecule probe[20]; this however may not be very fruitful in practice because the amount of "out-gasing" from the surface of the vehicle at such low pressure would make the measurement worthless, unless special provision to eliminate the out-gasing effect can be made.

THE SATELLITE ORBITAL DECAY IN AN IONIZED ATMOSPHERE

The presence of appreciable charged particles in the atmosphere complicates the mechanism of the satellite drag which is responsible for the orbital decay of a satellite. It is convenient to treat the satellite drag due to the charged particles separately from that due to the neutral ones; the latter can be fruitfully treated by the classical free-molecule flow theory[21, 22].

The status of our understanding of the interaction between a moving satellite and an ionized atmosphere is very primitive, although much progress has been made in the last few years. It appears that there is yet

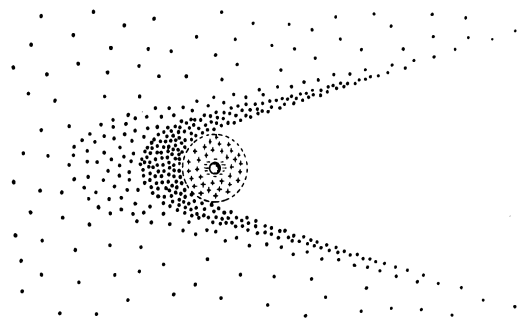

Figure 9
Distribution of charged air particles about a spherical satellite with negative potential
(after Jastrow, Sci. American)

no satisfactory theory of drag of a satellite in an ionized atmosphere, except perhaps some order of magnitude estimate of the drag in question. There are at least three basic physical mechanisms that may contribute to the cause, which are described in the following.

Coulomb drag

A satellite, made of conducting material, will acquire a net electric potential when it is "snow-plowing" in the ionized gas; photons of the ultraviolet light may also liberate electrons from the surface of the satellite leaving a positive charge on it. The charged skin of the satellite would repel other electrons, creating a shell of net positive charge around it (Figure 9). The pursuit to maintain a neutral charged condition is a characteristic property of a plasma state. It has been shown by Jastrow and Pearse[23] that the diameter of the positively charged shell would become the effective diameter of the satellite in collisions with positively charged particles. This increase in effective diameter would correspondingly increase the satellite drag. On the basis of the measured surface potentials of the Russian satellites, it was found[24] that the coulomb drag corresponding to the thermosphere altitude is not more than a few per cent of the total drag. However, at a much higher altitude, e.g. near the Van Allen radiation belt, the satellite collides with high-energy electrons and consequently raises its skin potential to a considerably higher value, thereby resulting in a large coulomb drag.

Induction drag

The presence of free electrons and ions makes the atmosphere a conducting medium. When a conductor, such as a satellite skin, moves through the conducting medium in the presence of the geomagnetic field that has a component normal to the direction of its motion, an electric current is induced in the satellite skin and the satellite experiences an induction drag.

Wave drag

When a dragged satellite moves in an ionized atmosphere with a pervading magnetic field, waves of electromagnetic, hydro-magnetic and electrostatic types may be generated, thereby draining the kinetic energy of the satellite.

CONCLUSION

In conclusion, I hope that my discursive survey of the problem of upper atmosphere and its measurement has generated some interest in aerophysicists, chemists, and mathematicians; as one can see, the field of upper atmospheric physics rests on many techniques of observation and touches many branches of physics, chemistry and mathematics.

REFERENCES

(1) Whipple, F. J. W. – *The High Temperature of the Upper Atmosphere As An Explanation of Zones of Audibility*, NATURE, VOL. 111, 1923.

(2) Lindemann, F. A., and Dobson, G. M. B. – *A Theory of Meteors and the Density and Temperature of the Outer Atmosphere To Which It Leads*, PROC. ROY. SOC. VOL. 102, 1923.

(3) Whipple, F. L. – *Meteors and The Earth's Upper Atmosphere*, REV. MOD. PHYS. VOL. 15, No. 4, OCTOBER, 1943.

(4) Nicolet, M. – *The Properties and Constitution of the Upper Atmosphere*, PHYS. OF THE UPPER ATMOSPHERE, ACAD. PRESS, NEW YORK, 1960.

(5) Epstein, P. S. – *Uber Gasentmischung in der Atmosphäre*, BEITR. GEOPHYS., VOL. 35, 1932.

(6) Johnson, F. S. – *Atmospheric Structure*, ARS PREPRINT No. 2226-61, OCTOBER, 1961.

(7) Liepmann, H. W., and Roshko, A. – *Elements of Gas Dynamics*, JOHN WILEY, NEW YORK, 1956.

(8) Liu, V. C. – *On a Pitot Tube Method of Upper Atmosphere Measurements*, J. GEOPHYS. RES. VOL. 61, JUNE, 1956.

(9) Newell, H. E., Jr. – *High Altitude Rocket Research*, ACAD. PRESS, NEW YORK, 1953.

(10) Jones, L. M. – *Transient Time Accelerometer*, REV. SCI. INST., JUNE, 1956.

(11) Liu, V. C. – *Preliminary Investigation of 'Sphere' method of Ambient Temperature Measurement*, UNIV. OF MICH. ERI ATM. PHENOM. AT HIGH ALT., MEMO 1, AUGUST, 1950.

(12) Liu, V. C. – *On 'Sphere' Method of Ambient Temperature Measurement in the Upper Atmosphere with Wind*, UNIV. OF MICH. ERI ATM. PHENOM. AT HIGH ALT., MEMO 3, JUNE, 1951.

(13) Bartman, F. L., Chaney, L. W., Jones, L. M., and Liu, V. C. – *Upper-Air Density and Temperature by the Falling-Sphere Method*, J. APP. PHYS., VOL. 27, No. 7, JULY, 1956.

(14) Liu, V. C. – *On Aerodynamic Drag of Sphere*, UNIV. OF MICH. SCIENTIFIC REPORT FOR AIR FORCE CAMBRIDGE CENTER (CONTRACT No. AF-19-604-5477), OCTOBER, 1961.

(15) King-Hele, D. G., and Walker, D. M. C. – *Upper-Atmosphere Density During the Years 1957 to 1961, Determined from Satellite Orbits*, R.A.E. REPORT (ENGLAND), MARCH, 1961.

(16) Jacchia, L. G. – *Solar Effects on the Acceleration of Artificial Satellites*, SMITHSONIAN ASTROPHYS. OBS. SPECIAL REPT. No. 29, 1959.

(17) Lennard-Jones, J. E. – *Free Paths in a Non-Uniform Rarefied Gas With an Application to the Escape of Molecules From Isothermal Atmospheres*, TRANS. CAMB. PHIL. SOC., VOL. 22, 1923.

(18) Byutner, E. K. – *The Dissipation of Gas From Planetary Atmosphere*, II SOVIET ASTRONOMY – AJ VOL. 3, 1959.

(19) Liu, V. C. – *On Pitot Pressure in an Almost-Free-Molecule Flow – A Physical Theory For Rarefied-Gas Flows*, J. AERO. SCI., VOL. 25, No. 1, DECEMBER, 1958.

(20) Patterson, G. N. – *Theory of Free-Molecule, Orifice-Type Pressure Probes in Isentropic Flows*, INST. OF AEROPHYS., UNIV. OF TORONTO, REPORT No. 41 (REVISED), 1959.

(21) Lidov, M. L. – *Resistance of an Unorientated Body in Motion in a Rarefied Gas*, IZV. AKAD. NAUK. SSSR, SER. GEOFIZ., No. 12, 1958.

(22) Schaaf, S. A. – *Aerodynamics of Satellites, Aerodynamics of Upper Atmosphere*, COMPILED BY D. J. MASSON, RAND REPORT R-339, JUNE, 1959.

(23) Jastrow, R., and Pearse, C. A. – *Atmospheric Drag on the Satellite*, J. GEOPHYS. RES., VOL. 62, No. 3, SEPTEMBER, 1957.

(24) Sedov, L. I. – *Dynamic Effects in the Motion of Artificial Earth Satellite*, PLANETARY AND SPACE SCI., VOL. 5, No. 3, JULY, 1961.

APPENDIX XII

ON A DISTRIBUTION FUNCTION SATISFYING THE LOCAL H-THEOREM

(Contributed by Paul B. Hays)

(Published in J. A. S. June 1962)

On a Distribution Function Satisfying the Local H-Theorem†

Paul B. Hays
Graduate Student,
Dept. of Aeronautical and Astronautical Engineering,
University of Michigan, Ann Arbor, Mich.
January 25, 1962

THE STATISTICAL DESCRIPTION of a gaseous system utilizes a probability-distribution function in order to describe the behavior of the particles in the six-dimensional phase space. However, each distribution function represents an extremely large number of actual arrangements of the various particles. This fact is used within the Boltzmann H-Theorem to restrict the choice of the distribution function itself. Boltzmann's classical theorem states that a system has the greatest probability of having the distribution function which exhibits the largest number of molecular arrangements. This is stated mathematically as follows:

$$H = \int_x \int_\xi f \log f d\mathbf{x} d\xi = \text{minimum}$$

In the case of a homogeneous system the solution has been shown to be the Maxwell-Boltzmann distribution law, where ρ_0 = density, β = (most probable speed)$^{-2}$, and c = random velocity—viz.,

$$f_0 = \rho_0(\beta/\pi)^{3/2} e^{-\beta c^2}$$

(For a complete description of the H-Theorem and subsequent developments see Ref. 1.)

One may go farther than this and postulate that the H-Theorem is satisfied locally in the physical space as well as throughout the phase space. This hypothesis cannot be proved, nor should it be true in general. However, it has been used fruitfully by Epstein[2] and may lead to useful results if one remembers that it is only a hypothesis. The conclusions reached here should be interpreted critically for this reason, but as we shall show they are consistent with the results of other contemporary analysis.

In order to obtain meaningful results one must apply the local H-Theorem, and must also insist that the macroscopic densities, velocities, stresses, etc., are also satisfied. These last conditions may be imposed as integral constraints in the formal development of the variational statement of the local H-Theorem. One should note that it is these constraints or macroscopic moments which provide the variation from equilibrium and thus generate meaningful results.

In general the problem outlined above can be carried out with any number of moments, however here the number of moment constraints will be restricted to the first thirteen. This is consistent with the truncation used by Grad[3] and will be subject to the same criticism and justification as he mentions in his development. Thus if one is willing to tentatively accept these hypotheses including the local H-Theorem then the distribution function is obtained from the solution of an elementary variational problem with integral constraints:

$$H = \int f \log f d\xi = \text{minimum} \qquad (1)$$

where this statement is subject to the following constraints:

$$\left.\begin{aligned} \rho &= \int f d\xi & P_{ij} &= p\delta_{ij} + p_{ij} = \int c_i c_j f d\xi \\ \rho \mathbf{u} &= \int \xi f d\xi & q_i &= \int c_i (c^2/2) f d\xi \end{aligned}\right\} \qquad (2)$$

where

$$c_i = \xi_i - u_i = \text{random velocity}$$

This set may be restated using the methods of variational calculus.[4] Taking the variation of H and using the method of Lagrangian multipliers on the constraints yields

$$\delta \int f \{\log f + a_0 + b_i \xi_i + d_{ij} c_i c_j + e_i c_i (c^2/2)\} d\xi = 0 \qquad (1a)$$

This contains thirteen Lagrangian functions required to satisfy the thirteen constraints. A solution to this equation is

$$f = \exp\{-(a_0 + b_i \xi_i + d_{ij} c_i c_j + e_i c_i c^2/2)\} \qquad (3)$$

One now applies the condition of small variations from local equilibrium and linearizes the exponential. Thus,

$$f = f_0\{1 - b_i' c_i - d_{ij}' c_i c_j - e_i' c_i c^2/2\} \qquad (3a)$$

The thirteen constraint equations are now evaluated yielding thirteen equations for the unknown Lagrangian functions:

$$\left.\begin{aligned} \rho &= \rho_0 \left(1 - \sum_1^3 \frac{d_{ii}'}{2\beta}\right) \\ b_i &+ (5/4)(e_i/\beta) = 0 \\ P_{ij} &= -d_{ij}' \rho_0 / 4\beta^2 \quad i \neq j \\ P_{ii} &= (\rho_0/2\beta)\{1 - (1/2\beta)(3d_{ii}' + d_{kk}' + d_{ll})'\} \\ q_i &= (5/8)(\rho_0/\beta^2)\{b_i' + (7/4)(e_i'/\beta)\} \end{aligned}\right\} \qquad (4)$$

These invert to yield the Lagrangian functions in terms of the thirteen moments when combined with the equation of state:

$$\left.\begin{aligned} \rho_0 &= \rho & e_i &= -(16\beta^3/5\rho) q_i \\ b_i &= +(4\beta^2/\rho) q_i & d_{ij} &= 4\beta^2/\rho \end{aligned}\right\} \qquad (5)$$

These are combined with the equation of state and substituted into the distribution function to give the final distribution:

$$f = \rho(\beta/\pi)^{3/2} e^{-\beta c^2} \{1 + p_{ij}(c_i c_j / 2pRT) - (q_i c_i / pRT)[1 - (c^2/5RT)]\} \qquad (6)$$

This result is identical with that used by Grad in his development of the thirteen-moment equations based on an expansion in Hermite polynomials.

Thus it has been shown that near equilibrium the local H-Theorem and the thirteen-moment distribution functions are consistent. This cannot be taken to be a justification for the use of either of these. However, it may be of some use in the criticism of both. That is to say, if one can show that one of these is inconsistent with physical reality in some region, then it follows that the other is also inconsistent. Unfortunately, at the present, very little can be said specifically about either and thus one should be very conservative about drawing broad conclusions from such circuitous reasoning.

† This investigation was a part of a broad upper-air research program supported by the U.S.A.F. Cambridge Research Center under Contract No. AF 19(604)-5477 with the University of Michigan.

The author wishes to express his appreciation to Dr. Vi-Cheng Liu for his guidance during this investigation.

REFERENCES

[1] Tolman, R. C., *The Principles of Statistical Mechanics*, Oxford University Press, 1938.

[2] Epstein, P. S., *On the Resistance Experienced by Spheres in Their Motion through Gases*, Physical Review, Vol. 23, No. 6, June 1924.

[3] Grad, H., *On the Kinetic Theory of Rarefied Gases*, Commun. Pure and App. Math., Vol. 4, No. 4, Dec. 1949.

[4] Courant, R., and Hilbert, D., *Methods of Mathematical Physics*, Vol. 1, Interscience Publishers, Inc., New York, 1953.

Reprinted from JOURNAL OF THE AEROSPACE SCIENCES